CROP DISCRIMINATION USING TIME SERIES SENTINEL-1 SAR DATA

MUTASHA BRIAN MULENGA
June,2022

SUPERVISORS:
Dr. Roshanak Darvishzadeh
Dr. Michael Schlund

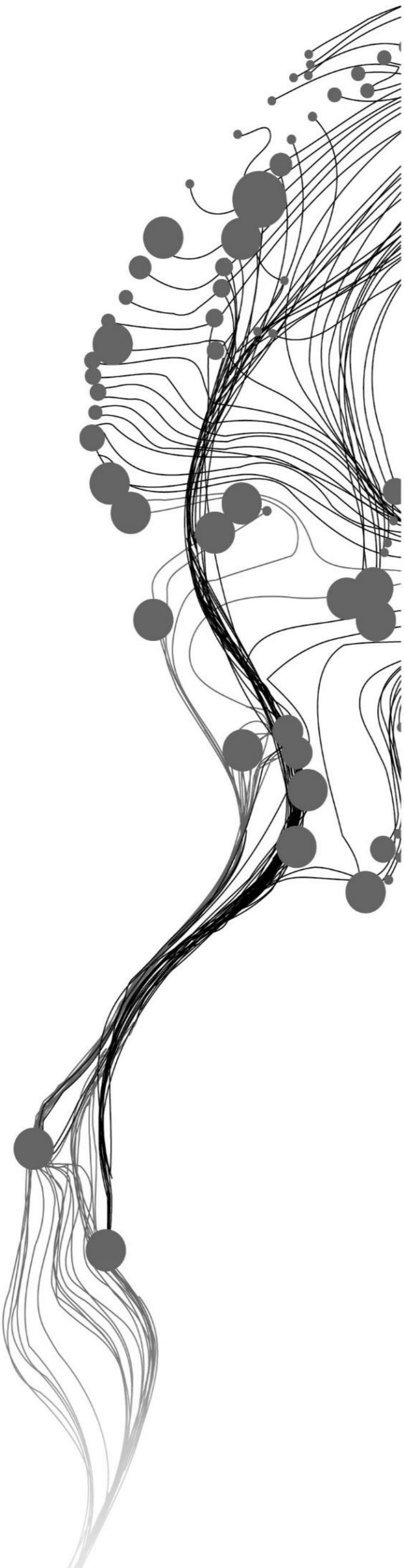

CROP DISCRIMINATION USING TIME SERIES SENTINEL-1 SAR DATA

MUTASHA BRIAN MULENGA
Enschede, The Netherlands, June, 2022

Thesis submitted to the Faculty of Geo-Information Science and Earth Observation of the University of Twente in partial fulfilment of the requirements for the degree of Master of Science in Geo-information Science and Earth Observation.
Specialization: Natural Resources Management

SUPERVISORS:
Dr. Roshanak Darvishzadeh
Dr. Michael Schlund

THESIS ASSESSMENT BOARD:
Prof. Dr. Andy Nelson (Chair)
Dr. Alice Laborte (External Examiner, International Rice Research Institute)

ABSTRACT

Despite efforts to end world hunger and undernourishment, food security and food production are serious concerns in many parts of the world. Accurate and timely information about the agricultural landscape and crop type are therefore important for proper food production management and monitoring. Remote Sensing provides a reliable data source for crop discrimination and large-scale assessment of planted acreage. In this regard, relatively few studies have exclusively focused on crop discrimination using time series Sentinel-1 SAR data. This study examined whether phenological information (SAR metrics) obtained from Sentinel-1 time series and Support Vector Machine (SVM) algorithm, a non-parametric supervised learning technique, would allow to discriminate rice and maize as main crops in the Philippines.

The research utilized secondary dataset made available by the International Rice Research Institute (IRRI) as part of the Pest and Disease Risk Identification and Management (PRIME) project. The reference data included field survey and farmer interview data collected between 17th February to 17th April 2019 on 317 crop fields, from which 31 fields were selected in Pangasinan province, where maize was cultivated in only 12 fields during the 2019 growing season. The Sentinel-1 time series data acquired during the same period and pre-processed by IRRI, were used to extract the temporal mean backscatter for each field at different growth stages. Statistical tests to determine whether there were significant differences between rice and maize growth stages were done using the Mann-Whitney U Test. The discrimination of rice and maize was studied using SVM algorithm, implemented in R environment. The discrimination of crop types in the study area comprised performing the classification at different growth stages as well as the whole growing season.

The results show that differences exist during the crop development phases that could be utilized to discriminate rice from maize. The temporal backscatters during the early crop development stage (crop establishment phase) were not statistically significant in all the three polarizations (VH, VV and VV/VH ratio). Additionally, no significant difference was observed in the VH polarization at the flowering and harvest stages. A significant difference was only observed at the flowering and harvest stages in the VV polarization and VV/VH ratio. The backscatter difference was also significant in the VV/VH ratio polarization only . Another significant difference was seen in the crop duration between rice and maize. It was observed that crop establishment phase had the highest overall accuracy (O.A = 80.6%, Kappa = 0.58). The discrimination of rice and maize at the harvest stage had the lowest overall accuracy (O.A. = 67.7%, Kappa = 0.28). This can be explained by the decline in water content and the gradual drying of the plants at late phenological stages which strongly influence SAR backscatter. Interestingly, the overall accuracy improved when all the growth stages' features were used for crop discrimination (O.A. = 80.6%, Kappa = 0.59). This can be attributed to rich information due to longer time series of data that improved crop classification. The study demonstrates the importance of including all the polarizations (VH and VV and their CR) to increase the information content when discriminating cereal crops. The classification results obtained from running the SVM model at various growth stages show comparable crop type distributions with field observation. In general, maize was cultivated in the northern part of the study area around San Roque and Caturday while rice occupied the southern part during the 2019 growing season.

Keywords: Agriculture, Crop discrimination, SVM, Phenology, Sentinel-1, SAR, Time Series, Philippines, Rice, Maize, Monitoring, Growth Stages.

ACKNOWLEDGEMENTS

I would like to express my sincere thanks to the following individuals and institutions for the contributions made towards the preparation of this work. Firstly, I would like to acknowledge my first supervisor, Dr. Roshanak Darvishzadeh and my second supervisor, Dr. Michael Schlund for the direction, constructive remarks, thought provoking discussion and encouragements rendered during the whole research process. I am deeply indebted for their professional supervision, patience and commitment throughout my thesis study.

I would also like to thank Prof. Dr. Andy Nelson the Chairman of the thesis assessment board for the invaluable suggestions and comments that improved the work. Further gratitude is extended to following for their help and suggestions: Mr. Willem Nieuwenhuis for the assistance rendered during working with the files in Matlab software and Ewelina Dobrowolska of Serco for the guidance to various resources for Machine Learning Algorithms.

I further wish to thank NUFFIC for the OKP scholarship and my employer, Ministry of Lands and Natural Resources for granting study leave that gave me an opportunity to study at the Faculty of ITC, without the assistance and support my studies would have been impossible.

I am profoundly grateful also to my family and friends who supported me in various ways or another. Particularly I would like to extend my gratitude to Cindy Sithole, Mwangala Simate, Blessing Munakamwe, Dora Dadey and the entire ITC-SADC team for their support and time during my wonderful stay in Enschede. Special thanks to Sebastian Wesselman for encouraging me to join the University of Twente. Your efforts have finally yielded good results.

Many thanks also to ITC staff, my teachers and classmates in the Natural Resources Department for being supportive and inspirational in numerous ways and sharing their valuable time for discussion during the entire course of the MSc study. Finally but not the least, I would like to thank my wife Joyce Masinja Mutasha for her constant support and encouragements during my stay in the Netherlands.

- Mutasha Brian Mulenga.

TABLE OF CONTENTS

LIST OF FIGURES

LIST OF TABLES

ACRONYMS

BBCH	: Biologische Bundesanstalt, Bundessortenamt and CHemical industry general scale
CR	: Cross polarisation Ratio
EOS	: End of Season and
ESA	: European Space Agency
FAO	: Food and Agriculture Organisation
GDP	: Gross Domestic Product
GRD	: Ground Range Detected
Ha	: Hectare
IRRI	: International Rice Research Institute
IW	: Interferometric wide swath
Kg	: Kilogram
LOOCV	: Leave-one-out cross-validation
LOS	: Length of Season
LPS	: Land Surface Phenology
ML	: Machine Learning
NDVI	: Normalized Difference Vegetation Index
PRIME	: Pest and Disease Risk Identification and Management Project
RF	: Random Forest
SAR	: Synthetic Aperture Radar
SNAP	: Sentinel Application Platform
SPSS	: Statistical Product and Service Solutions (originally Statistical Package for the Social Sciences)
SOS	: Start of season
SVM	: Support Vector Machines
VH	: Vertical Transmit – Horizontal Receive polarization
VI	: Vegetation Index
VV	: Vertical Transmit – vertical Receive polarization
WGS84	: World Geodetic System 1984

1. INTRODUCTION

1.1. Background

Agriculture is key to the global economy, as its products are essential for human existence (Beckman and Countryman, 2021). The sector produces an estimated average of 23.7 million tons of food daily and provides a source of income for many households (CBD, 2016). However, despite efforts to end world hunger and undernourishment, food security and food production are serious problems in many countries (Sibhatu and Qaim, 2017). The global need for food is critical. Evidence points to an increase in world hunger, with an estimated number of nearly 821 million people affected by chronic food deprivation in 2017 (FAO et al., 2018). Although current estimates suggest slowing down trends, the world is still off track to achieving Zero hunger and more than 840 million people will be affected by hunger by 2030 if recent trends continue (FAO et al., 2020). This is particularly true for the Philippines, a country that is heavily reliant on agriculture (Briones, 2005). Despite the fact that agricultural areas in the Philippines account for 41.7% of the total land area of 30 million hectares, the agriculture sector faces many challenges due to a growing population (Dikitanan et al., 2017). According to the World Food Programme (2021) "its population of 110 million people is becoming increasingly urban"; with a total number of 10.1 million people in the Philippines being undernourished (FAO et al., 2021). This growing population with increased consumption and changing dietary preferences presents one of the key challenges confronting the Philippines' agriculture sector (Dikitanan et al., 2017; Godfray et al., 2010). As a result, a constant difficulty is balancing food availability with the demands of an ever-increasing population (McNairn and Shang, 2016). This outlines the Philippines' need for timely and accurate information on crop production for agriculture monitoring, economic planning, agricultural market management, as well as assessments of food security issues in view of climate variability and extremes.

In recent years, evidence of climate change's effects on the agricultural sector is already severe and widespread; and ensuring food security will be one of humanity's most complex challenges (FAO, 2017), requiring agriculture to develop and evolve to meet these demands. However, when unforeseen disasters strike, the task of forecasting food production becomes even more challenging (McNairn and Shang, 2016), specifically in places where the weather is projected to be unpredictable and more variable due to the increased effects of climate change (Dikitanan et al., 2017). Because of its location in Southeast Asia, the Philippines is particularly vulnerable to natural disasters such as typhoons, floods, and droughts. These natural disasters have a negative economic and environmental impact on the affected areas and the people who live there and therefore limit food production and, in turn, food security (FAO, 2017; Ramos et al., 2016). As a result, forecasting food supply necessitates continuous and frequent updates of information on crop production (McNairn and Shang, 2016).

Crop area extent and crop type maps provide critical information to policymakers for agricultural monitoring (Inglada et al., 2015). The ability to manage the agriculture sector and ensure that it meets the increased pressure primarily depends on the timely information available to inform decision making. The agricultural landscape in the Philippines is expected to expand by 5.2 million hectares by 2025, which can only be accomplished through better agricultural policies that effectively address food security issues (Briones, 2005). The consistent flow of information is critical for various stakeholders and policymakers to identify threats to the agricultural sector's stability, competitiveness, and profitability. Additionally, this information plays an essential role in developing and evaluating policies that are put in place and their implementation to address these challenges (Fisette et al., 2013; McNairn and Shang, 2016) and to prioritise and draw strategies for improved sustainability of the agro-ecosystems in delivering services to societies. For instance, one of the government policies in the Philippines which require accurate and immediate knowledge of potential production is the estimation of shortfalls in crop production and importing the difference in production, especially rice, to control domestic prices (Chen and Mcnairn, 2006). Besides emphasising resilient food production, agriculture policies could also help mitigate climate change and promote the sustainable utilisation of natural resources (D'Andrimont et al., 2021). Weiss et al., (2020) note that "overall, policy-makers and local to regional decision-makers will increasingly need updated spatial information on how agro-ecosystems evolve in order to improve their management." Therefore, the methods for obtaining crop information need continuous improvements to effectively implement policies to ensure sustainable development.

Different methodologies, including total enumeration, have been used to collect information on crop area estimates. Statistics about crop production data can be obtained from various sources, including agricultural agencies. The conventional method of compiling this information relies heavily on ground-based field surveys, which are both time and labour-intensive (Bruzzone et al., 2016; Guarini et al., 2016). Furthermore, when data is required regularly across large areas, cost and technical resources present substantial constraints to obtaining such information (FAO, 2016). Remote Sensing provides a reliable data source that can be frequently used for crop discrimination and large-scale assessment of planted acreage. For many years, multispectral optical Remote Sensing systems have been the foundation for crop identification and monitoring (Chen et al., 2018; Mingwei et al., 2008; Mondal and Jeganathan, 2018; Wang et al., 2015a). Multi-spectral satellite data such as Landsat, RapidEye and Sentinel-2 have commonly been used for crop mapping (Khosravi and Alavipanah, 2019; Kobayashi et al., 2020; Ouzemou et al., 2018). Additionally, multi-temporal imagery has been critical for crop type discrimination as it allows for a more robust classification than single date imagery (Salehi et al., 2017). Previous studies focusing on large scale crop discrimination have used optical sensors such as SPOT vegetation (Khan et al., 2010), PROBA-V (Zhang et al., 2016) and MODIS (Wardlow and Egbert, 2008). However, due to the coarse spatial resolution of these sensors, the classification accuracies tend to decrease due to the heterogeneity in the landscape during the growing season (Atzberger and Rembold, 2013). The reliance of optical data on the cloud-free cover is a major constraint and limits image acquisition at regular intervals, limiting the use of optical data for crop mapping (Van Tricht et al., 2018). This limitation can be addressed by using Spaceborne Synthetic Aperture Radar (SAR) data (Karthikeyan et al., 2020).

SAR sensors provide a reliable and alternative source of valuable information on vegetation cover irrespective of solar illumination and cloudiness. SAR data is an effective and important data source for monitoring crops and other agricultural targets because the quality of SAR images is less affected by atmospheric conditions (Liu et al., 2019). Prior to 2002, before the launch of the ENVISAT-ASAR satellite, most research in radar application was focused on single-band and single-polarisation images for crop mapping (Wang et al., 2015b). However, classification using a single SAR system with a particular configuration, such as a single image at a certain frequency, polarisation, and incidence angle, is considered insufficient to achieve the required classification accuracy, especially in fragmented farm areas (Del Frate et al., 2003; Mashaba-Munghemezulu et al., 2021). With improvements in terms of data and technology, Sentinel-1 time series SAR data provide new opportunities and have been widely applied in agricultural condition monitoring, providing a strong complement and support for crop identification when used in combination with optical data (Wang et al., 2015). However, the majority of current multitemporal crop classification methods based on radar use a stack of images collected during the whole vegetative season in the classification process without considering the crops' phenology (Bargiel, 2017). Hu et al. (2019) observed that the standard image stacking approach might mask some subtle but potentially critical phenological events, despite the fact that time series analysis is a widely used and useful tool for characterising the seasonal dynamics of crops. Li et al., (2020) further demonstrated an improvement of crop type maps' accuracy when information about phenological status was incorporated into the classification scheme. Due to its high spatial and temporal resolution, Sentinel-1 SAR time series offers a great opportunity to map crop types. Many of the previous research has taken advantage of the unique capabilities of SAR time series data for crop discrimination and crop classification, albeit over small areas (Bargiel, 2017; Gella et al., 2021). While the benefits of SAR are well understood, and the Sentinel-1 series of satellites offers an unprecedented opportunity for large-area crop type mapping (Song et al., 2021), its use in national scale agricultural crop inventories is relatively low. Only a few countries use spaceborne SAR to operationally produce national-scale maps of their agricultural landscapes (Dingle Robertson et al., 2020). Dingle Robertson et al. (2020) add that the lack of familiarity with SAR data by many agricultural end-user agencies, and the lack of a "scheme" for implementing an operational SAR-based mapping system, are among the barriers to its operational use. However, a recent study by D'Andrimont et al. (2021) has demonstrated the capability for large scale crop type mapping based on Sentinel-1 (D'Andrimont et al., 2021). Furthermore, Meroni et al., (2021b) utilised Sentinel-1 data to retrieve the phenology of major crop types over Europe. The consistent time series, therefore, provide a reliable data source to detect different growth stages and monitor phenology (Wang et al., 2019).

Plant phenology, the timing of seasonal changes or recurrent biological events in plants offers insights into the ecology and ecosystem processes (Meroni et al., 2021b). This information is critical for crop monitoring and tracking the conditions and progress of crops in the field (Rembold et al., 2019; Sakamoto et al., 2013). However, phenology presents many challenges in mapping cropping patterns and individual crop types because of the spatial and temporal dynamics that substantially change in these agricultural landscapes at short time intervals during the growing seasons (Bargiel, 2017). Crop type maps that are generated using satellite Remote Sensing require robust data acquisition at high spatial and temporal resolutions (Song et al., 2021). Bargiel (2017) argues that current approaches for crop classification based on SAR time series data and utilising only backscatter intensity values do not take into account knowledge of the dynamics of the crops' phenology because they classify a stack of images taken during the whole vegetative season. For instance using multitemporal TerraSAR-X achieved over 90% overall accuracy for classifying six classes (Sonobe et al., 2014a). Although these studies produced impressive results for the classification of certain crop types and demonstrated the high potential for radar-based crop classifications, some of them have difficulty distinguishing between crop types (Bargiel and Herrmann, 2011). Previous research has shown that information about crop phenological stages particularly shooting, ripening, and harvest stages was important for crop monitoring and improved the accuracy of crop type maps (Bargiel, 2017; Li et al., 2020). Schlund and Erasmi, (2020) further demonstrated that phenological information could be extracted from dense Sentinel-1 time series data.

Time series data can be utilised to derive land surface phenology (LSP), the spatio-temporal development of the vegetated land surface, despite many phenological events related to vegetation physiological processes such as flowering and fruiting cannot be directly detected from Remote Sensing (De Beurs and Henebry, 2005; Zeng et al., 2020). Phenological metrics such as the Start of season (SOS), End of Season and Length of Season extracted from fitted curves of time series provide information on management practices and crop types over agriculture landscapes (López-Lozano et al., 2015). According to Meroni et al. (2021) "the estimation of phenological metrics from times-series Remote Sensing data generally consists of three main steps: 1) data cleaning and flagging; 2) data smoothing and time-series data reconstruction and 3) phenological metrics extraction based on the reconstructed time series data". Remote Sensing methods to study changes in crop phenological developments have been proposed in previous studies based on these key steps and a recent review of phenology retrieval outlines the methods and instruments in depth (Zeng et. al., 2020). In general, there are two common approaches for retrieving phenology from remotely sensed data. These include the Vegetation Index (VI) change detection and the threshold-based method. However, the common approach mainly consists of computing spectral vegetation indices with NDVI being widely used (Zhang et al., 2003). Recently the VI category has included the Cross polarisation Ratio (CR) using SAR data which may be applied similarly to NDVI (Veloso et al., 2017a). The threshold can be arbitrarily established as in the fixed method or calculated based on a VI ratio as in the dynamic threshold method (Lloyd, 1990). The phenology metrics extracted by further smoothing the time series data can be transformed into a classification strategy by developing a series of classification features as input in the classifier for further image classification (Mascolo et al., 2016).

Remote Sensing image classification or the process of assigning pixels into meaningful thematic classes can be accomplished in two ways: supervised and unsupervised classification (Tolpekin and Stein, 2013). Application of classification algorithms that result in these discrete categories of crop types based on Remote Sensing measurements can be a complex task due to the dynamic structure of agro-ecosystems in space (Weiss et al., 2020). In supervised classification, knowledge of the area of interest is required where classes are defined in line with what is actually on the ground (ground truth data) during the training process. In unsupervised classification, a clustering algorithm automatically finds and defines a number of classes to form clusters in the feature space (Tolpekin and Stein, 2013). The supervised classification approach is widely used in Remote Sensing where parametric methods such as Minimum-Distance-to-Means and Maximum Likelihood are commonly used algorithms, despite the increasing acceptance of Machine Learning (ML) classifiers (Maxwell et al., 2018). However, amidst the big data era and high-performance computing, Machine Learning classification has become a major focus of the remote-sensing community. Its application has significantly advanced in many areas, including classification problems (Pfeil et al., 2020). Various studies have employed ML techniques for crop type classifications and have generally demonstrated that these techniques provide higher accuracy in comparison to typical parametric classifiers- which assume the normal distribution of the data without acceptance of various inputs of predictor data (Bargiel, 2017) (Maxwell et al., 2018). However, Weiss et al. (2020) note that "the accuracy of crop maps still remains dependent on the performance of the classification methods used to generate them".

Among the relatively mature ML methods, Support Vector Machines (SVMs) and Random Forest (RF) have dominated in the Remote Sensing application, including crop classification, as is evidenced by the wide usage of the technique (Barrett et al., 2014; Dey et al., 2020; Song et al., 2018). A meta-analysis of 251 articles conducted by Sheykhmousa et al. (2020) discovered that 42% and 68% of the papers employed RF and SVMs, respectively, in the implementation of ML classification algorithms and attributed its dominance to the relative ease of implementation of the two classification algorithms as compared to deep learning algorithms. Sheykhmousa et al. (2020) further note that, while Deep Learning methods are capable of retrieving complex patterns and informative features from satellite image data, their hidden layers, or "black box" nature, lead to a loss of interpretability, posing problems in the interpretation of the results. Pfeil et al. (2020) argue that common ML classifiers, such as RF, treat input variables as independent features and are not originally designed for time series analysis because they are sensitive to weather-related shifts during the growing season. Previous research has demonstrated the use of ML techniques with time series data (Mansaray et al., 2021; Ngo et al., 2020). However, the comparison of the two classifiers is somewhat confusing due to the relatively high similarity in performance in terms of classification accuracies between RF and SVMs (Mather and Tso, 2016; Sheykhmousa et al., 2020). Sheykhmousa et al. (2020) further add that although RF and SVMs are well-known and highly ranked ML algorithms, SVM is rarely used to classify SAR images.

The review of the literature reveals that the results of the previous studies are contradictory. Therefore, this research aims to further investigate the performance of SVM classification method when it comes to using SAR time series data by incorporating phenological metrics. Additionally, the majority of these studies in the area utilising SAR have focused on specific crop, rice monitoring (Boschetti et al., 2017; K. Clauss et al., 2018; Kersten Clauss et al., 2018; Nelson et al., 2014; Son et al., 2018). Considering the importance of rice and maize crops for food security in the area, the current study aims to discriminate crop types by exploiting the capabilities of Sentinel-1 SAR time series and ML.

1.2. Conceptual framework

The conceptual diagram shows the link between the problem and the potential use of SAR data in discriminating crop types in the study area (Figure 1.1). The conceptual diagram outlines the geographical boundary of the system and the relationships between elements (boxes) and processes (arrows) within the system. The subsystems that are critical in understanding the temporal backscatter from the various crop types over the growing seasons in the provinces of the Philippines are also indicated. The provinces are characterised by varying agricultural landscapes with differing growing seasons (wet and dry seasons). Further, the diagram shows the effects of certain decisions on the farmer that determine whether a crop field will be cultivated or remain fallow.

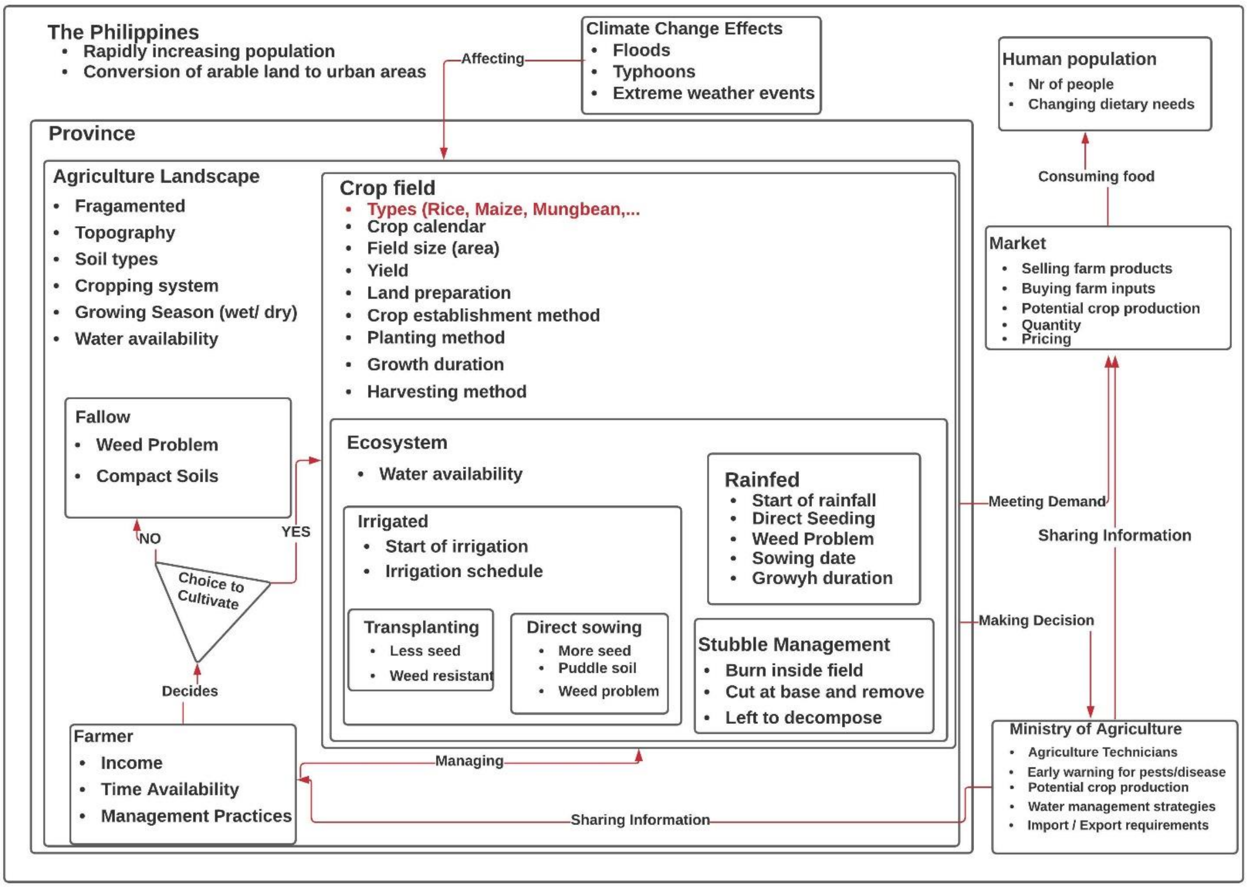

Figure 1. 1 Conceptual diagram linking the problem, the stakeholders and how the systems interact within the study area

1.3. Problem statement

Accurate and timely monitoring of crop types is required to inform policymakers about the agricultural landscape and food production. However, Philippines' agricultural landscape is becoming more fragmented due to the rapidly increasing population. The spatial and temporal dynamics that strongly affect these land cover at short time intervals during the growing seasons further make mapping specific crop types challenging (Bargiel, 2017). Additionally, the inherent characteristics of most farming areas, such as crop rotation and seasonal changes in crop morphology, make the classification of crop types using Remote Sensing technology a difficult task (Dey et al., 2020). Previous research has demonstrated that phenology status provides valuable information and increases the accuracy of crop type maps (Chen et al., 2016; Hua et al., 2019). Furthermore, SAR data is sensitive to crop structure, and the dielectric properties of the target objects make it relevant for crop monitoring (Nelson et al., 2014). The consistent availability of SAR observations makes it ideal data for ML classification (D'Andrimont et al., 2021). However, Gella et al., (2021) argue that " although these classifiers can incorporate multitemporal observations across the growing season as a stack of time series images, their implementation strategy does not allow to leverage phenological information into a classification scheme".

Considering the importance of rice and maize crops as main crops in the Philippines, the current study will examine whether phenological information (metrics) obtained from Sentinel-1 time series SAR data as input into the SVM ML algorithm are able to enhance the crop discrimination.

1.4. Research objectives

1.4.1. Main objective

The main aim of the study is to analyse the potential of SAR temporal backscatter data for crop type discrimination using time series Sentinel-1 imagery.

1.4.2. Specific objectives

The specific objectives of the study are:-

i. To understand the variation of temporal radar backscatter responses (VH, VV and VV/VH ratio) of the various crop types within the growing season;
ii. To determine the best SAR metrics in discriminating crop types in the study area;
iii. To evaluate the performance of SVM in discriminating the studied crop types using various accuracy metrics; and
iv. To identify the distribution of the studied crop types in the study area during the 2019 growing season.

1.5. Research questions and hypothesis

i. How are the crop specific temporal profiles in the study area?

Ho: There is no difference in the temporal backscatter behaviour of the different crop types (rice and maize) in the study area

ii. Which SAR metrics from the Sentinel-1 time series data are relevant for discriminating crop types (rice and maize) in the study area?

Ho: There is no relationship between the SAR metrics extracted from the Sentinel-1 time series data and the specific growth stages of rice and maize in the study area.

iii. How can the SVM classification algorithm leverage phenological information from the time series data?

Ho: Extracted phenological information does not affect the outcome of the classification of time series data.

iv. Which growth stage gives higher accuracy in discriminating rice and maize during the growing seasons?

Ho: There is no significant difference in the overall classification accuracy in discriminating rice and maize at the various growth stages.

v. How can Sentinel-1 time series data be used to map the distribution of rice and maize within the 2019 growing season in the study area.

2. STUDY AREA AND DATA

2.1. Study area and site characteristics

2.1.1. Location

The proposed study will take place in the Republic of the Philippines, which lies between latitudes 21°20' and 4°30' north and longitudes 116°55' and 126°36' east, on the Southeast coast of the mainland of Asia. An archipelago with over 7,640 islands and approximately 30 million ha of land (Dikitanan et al., 2017), the Philippines is divided into three main Island groups, namely Mindanao, Luzon, and the Visayas and is split into 17 regions. Five regions have been selected to develop and test the methodology, namely Pangasinan (Region I), Cagayan (Region II), Iloilo (Region VI), Leyete (Region VIII) and Agusan del Sur (Region XIII) (Figure 3.1.) All the sites are spread across the Philippines and represent the four geographic conditions of the country.

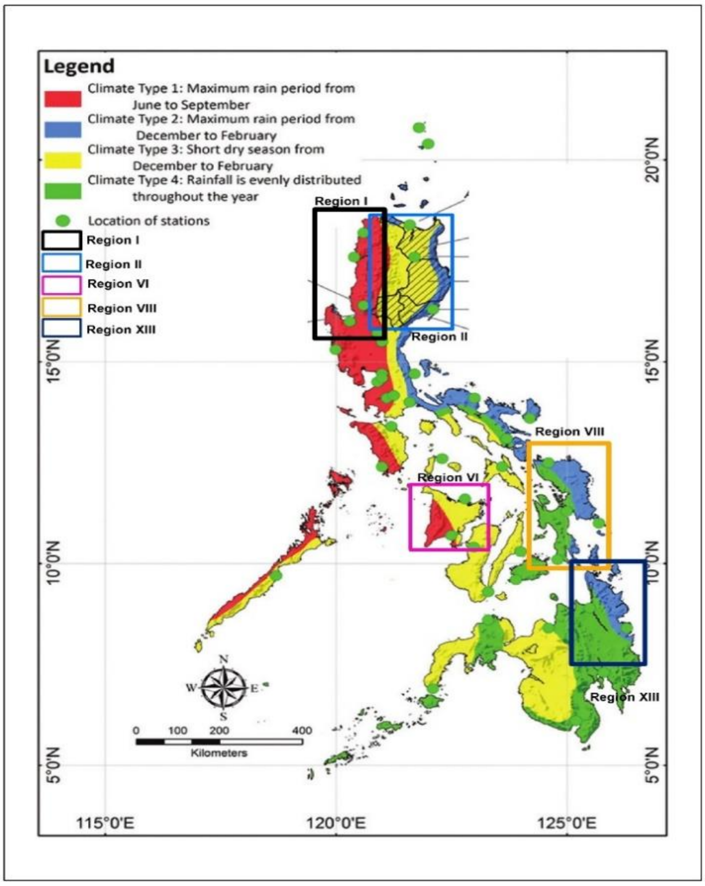

Figure 2. 1 Climate types in the Philippines. Source Basconcillo et. al., 2018, with modification

2.1.2. Climate

The Philippines has a tropical marine climate, with a mean annual temperature between 25°C to 27°C, with two marked seasons; annual dry seasons from December to May, and annual wet seasons from June to December. The climate is classified into four types based on the prevalence of the northwest and southwest monsoons and the distribution of monthly rainfall (Altoveros and Borromeo, 2007). The monthly average rainfall ranges from as low as 120 mm to 270 mm as the highest. The rainfall patterns are grouped into two with clear dry seasons from November to April in the west coast and east coast regions (Moron et al., 2009). The western regions of the country mostly belong to Type 1 climate (see Table 2.1). This type of climate has a distinct summer monsoonal wet and dry season from May to October and November to April.. Climate Type 2 (Table 2.1) comprises regions along or very near the eastern coast with no pronounced dry season but with a clear maximum rain period in December, January and February. This climate cover Catanduanes, Sorsogon, eastern part of Albay, Camarines Norte, Camarines Sur, eastern Quezon, Samar, Leyte and eastern Mindanao, which are not sheltered from the north-eastern monsoon. Climate Type III is an intermediate band between types I and II. It has maximum rainfall from May to October with an unclear but relatively dry season from November to April. Most southern areas belong to type IV, which has evenly distributed rainfall throughout the year (Figure 2.1 and Table 2.1). Figure 2.2 shows the annual variation of monthly mean, maximum and minimum temperature, and the monthly precipitation over a 29 year period in Region I (left) and Region VI (Right).

Table 2. 1 Climate types in the Philippines

Type	Description	Regions/Provinces	Remarks
1	Two pronounced wet and dry seasons; wet during the months of June to November and dry from December to May	Western part of Luzon, Mindanao, Palawan, Panay and Negros	The controlling factor is topography. These regions are shielded from the northeast monsoon and even in good part from the tradewinds by high mountain ranges. They are open only to the southwest monsoon and the cyclonic storms.
2	No dry season with a very pronounced maximum rain period in December, January and February.	Catanduanes, orsogon, eastern part of Albay, Camarines Norte, Camarines Sur, eastern Quezon, Samar, Leyte and eastern Mindanao.	These regions are along or very near the Eastern coast and are not sheltered either from the northeastern monsoon and tradewinds nor from the cyclonic storms.
3	Intermediate type with no pronounced maximum rain period and short dry season lasting from one to three months only.	Western parts of the Cagayan valley, eastern parts of the Mountain region, southern Quezon, Masbate, Romblon, northeastern Panay, eastern Negros, central and southern Cebu, eastern Palawan and northern Mindanao.	These localities are only partly sheltered from the northeastern monsoon and tradewinds and are open to the southwest monsoon or at least to frequent cyclonic storms.
4	Uniformly distributed rainfall	Batanes, northeastern Luzon, southwestern Camarines Norte, western Camarines Sur and Albay, Bondoc peninsula, eastern Mindanao, Marinduque, Western Leyte, northern Cebu, Bohol and most of central, western and southern Mindanao.	These regions are so situated that they receive the moderate effects of the northeast monsoon and tradewinds as well as the southeast monsoon and cyclonic storms.

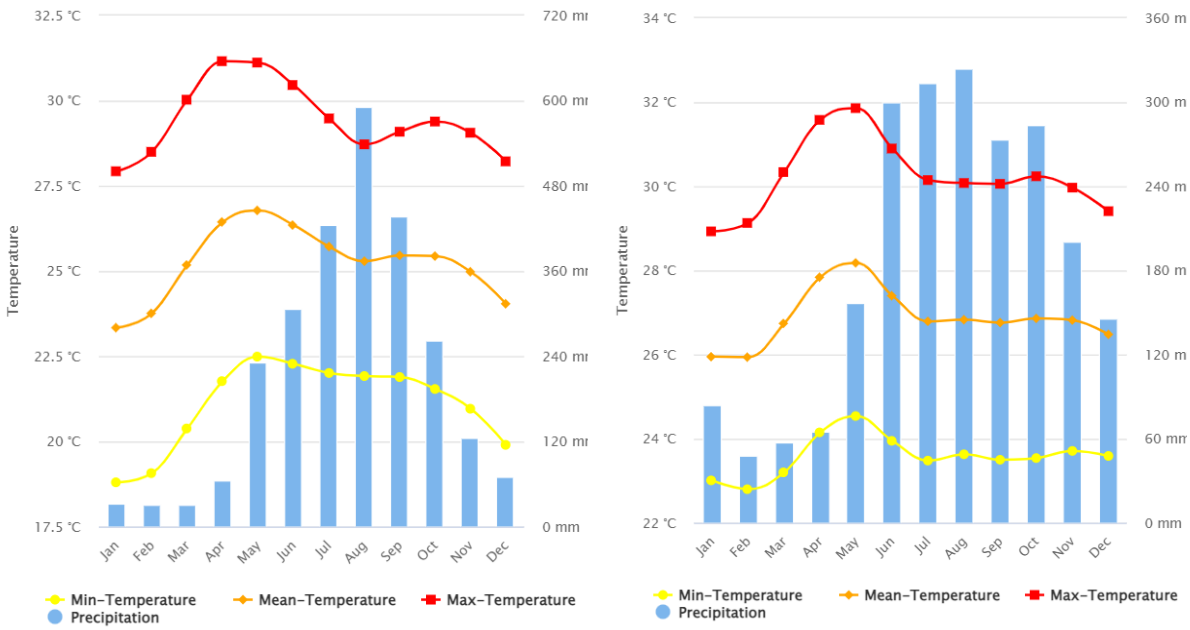

Figure 2. 2 Monthly Climatology of Min-Temperature, Mean-Temperature, Maximum Temperature and Precipitation 1991-2020 in Region I (left) and Region VI (Right). Source climate change knowledge portal: https://climateknowledgeportal.worldbank.org/country/philippines/

2.1.3. Major agricultural systems and their diversity

Agriculture plays a significant role in the Philippines economy, with crop cultivation as the main agricultural enterprise. However, the share of the agriculture sector in the gross domestic product (GDP) has declined from previous years and was just 9% in 2018 (WorldBank, 2020). According to Briones, (2005), "food crops, particularly rice and corn, continue to be the major contributors to agriculture's gross value added and have become major sources of growth."

Although rice is the most important and key staple food in the Philippines (Koide et al., 2013; Stuecker et al., 2018), agricultural diversity exists with major products including maize, coconuts, sugarcane, bananas, pineapples, and mangoes. Several crop-based systems mostly based on rice, maize, sugarcane and coconut can be found in the Philippines (Altoveros and Borromeo, 2007). Despite, rice being grown throughout the year, there is variation in the planting dates due to differences in climate (Table 2.1), with the largest share cultivated during the wet season (Stuecker et al., 2018). The Philippines' rice growing regions are mainly irrigated, although precipitation remains vital in rainfed rice (USDA, 2018). Maize is second to rice as the most cultivated crop with one-fifth of the Philippines dependent on it as a stable grain, especially in areas and periods of rice scarcity. Major agricultural systems include lowland irrigated farming, rainfed farming and upland farming. Roughly 70% of the total rice area is under irrigation, while 30% is rain-fed and upland. In the upland, farming systems are oriented towards subsistence framing (Legaspi et al., 2021). Irrigated farm areas mainly grow rice and sugarcane, whereas rainfed areas are planted with coconut, corn and cassava. Generally, in irrigated areas, the cropping sequence rice-rice is practised mainly for rice, though other crops such as mungbean, the most important legume in the Philippines, have been raised after two rice cropping (Altoveros and Borromeo, 2007).

The sites in this research are based on a previous project, Risk Identification and Management (PRIME) were selected in a way that the four climate types in the Philippines are represented. In Lyete, rice-rice system is mostly used with most farmers practising transplanting during the crop establishment which commences in May, both east and west (Nelson et al., 2014). The areas in Agusan del Sur are mainly classified as irrigated lowland as they rely on irrigation facilities in Rosario and Veruela for a regular supply of water for rice production (Varela et al., 2013). The cultivated fields especially rice areas in Pangasinan province are more fragmented during the dry season as the water supply is from the rain and borehole (Asilo et al., 2014). In Iloilo, the agricultural landscape is mainly rice paddy, although other crops such as maize can be found or grown as a second crop (Dela Torre et al., 2021). Two major ecosystems exist with mainly irrigated and rain-fed rice located in the central and eastern part of the province. In Cagayan province, rice is the most important crop, cultivated both through irrigated and rainfed conditions. About 78% of the province's total rice area is irrigated, while 22% is rainfed and can be grown twice a year during the wet and dry seasons (Nelson et al., 2015).

2.2. Data

2.2.1. Field survey data

This study benefited from an existing dataset made available by the International Rice Research Institute (IRRI) as part of the Pest and Disease Risk Identification and Management (PRIME) project. The reference data include field survey and farmer interview data collected between 17th February to 17th April, 2019 on 323 crop fields in 5 provinces of Agusan del Sur, Cagayan, Iloilo, Leyte and Pangasinan, introduced earlier. The field data covered a period between 2017 – 2019. Figure 2.3 shows the distribution of the field sample in the selected province of the Pangasinan in the Philippines. The farmer interviews correspond to three growing seasons, the current season (when the data was collected during the dry season of 2019) and the two seasons before that (wet and dry 2018). The main focus of the current study was to discriminate between the major crop types that is rice and maize cultivated during the 2019 growing period. However, after a thorough exploratory analysis of the provided survey data, it was revealed that only Pangasinan had enough samples for the target crops and was selected for further analysis. Table 2.2 shows the distribution of crop types and field status in the study area during the time of the survey. The average field size was 1.25 hectares (Ha), with the smallest being 0.4 Ha and the largest 3.4 Ha.

Table 2. 2 Distribution of field samples during the 2019 dry season in Pangasinan province

Crop type/Field status	***No.***
Rice	19
Maize	12
Others	9
Fallow	32
Total	***72***

Various information were collected during farmer interviews, including the cultivated crops, crop establishment method, crop calendar (land preparation, crop establishment date, flowering and harvesting data), and irrigation schedule. The geographical location of the field and the size were also collected which was used as input in the backscatter extraction.

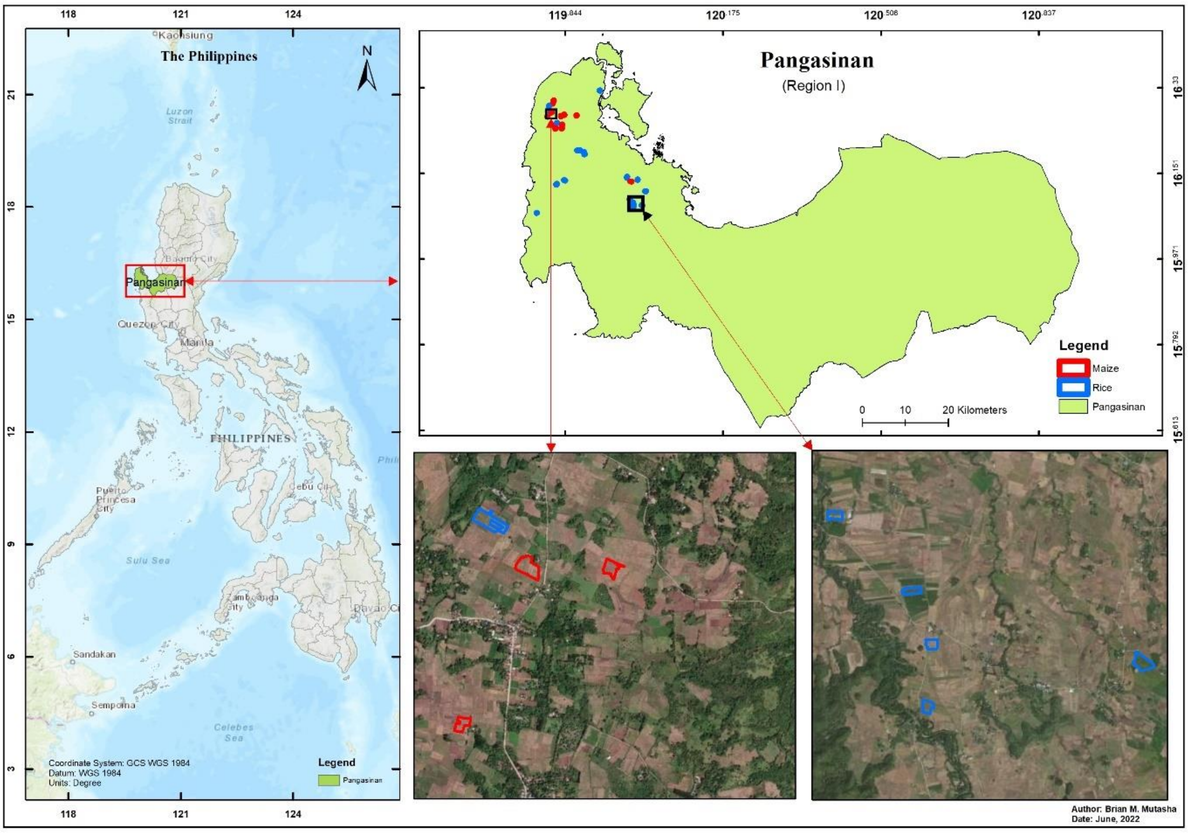

Figure 2. 3 The location of the study area showing Pangasinan province in the Philippines and the distribution of field samples in the province. Service layer credits: source: Esri, GeoEye, USDA and USGS

2.2.2. Sentinel-1 SAR data

Sentinel-1 SAR datasets downloaded from the European Space Agency (ESA's) Copernicus Hub, were used in the study. Sentinel-1 operates at 5.404 Ghz (central frequency), which corresponds to 5.6 cm wavelength (D'Andrimont et al., 2021). SAR time series images from Sentinel-1A with a 12-day revisit time covering the 2019 growing season were used (Table 2.4). The interferometric wide swath (IW) mode with dual polarimetry was used for this study.

One SAR satellite image covered the study area. Altogether, 17 Sentinel-1A images covering the region were acquired from 9/09/2018 – 20/03/2019 (Table 2.4). The images are freely available from ESA and the Ground Range Detected (GRD) data format was selected. The GRD products are processed from focussed SAR data that has been detected, multi-looked, and projected to the ground range using the WGS84 Earth ellipsoid model (ESA, 2013). The GRD products, although lack the phase information they have been used for various agricultural applications, whereas it can be assumed that the backscatter information alone is adequate for the crop classification purpose (Bargiel, 2017; Son et al., 2018; Tufail et al., 2021; Veloso et al., 2017b). Table 2.4 shows the images that were used in the current research and the metadata of the selected SAR images are indicated in Table 2.3.

Table 2. 3 Metadata of the selected SAR images to be used in the study

Attribute	**Sentinel-1**
Polarization	Dual Polarimetry (VH, VV)
Orbit Direction	Descending
Band (Central Frequency)	C-band (5.405GHz)
Azimuth and Range Resolution	22m by 20 m
Pixel spacing	10 m by 10 m
Sensing Mode	Interferometric Wide Swath (IW) mode
Incidence angle	30^{o} to 46^{o}
Number of Scenes	282
Observation period	9/09/2018 – 20/03/2019

Table 2. 4 Acquisition of Sentinel-1 images during the 2019 dry season in Pangasinan Province

<table>
<tr><th rowspan="2">S-1A acquisitions</th><th colspan="2">Tracks/Orbit</th></tr>
<tr><th colspan="2">T105</th></tr>
<tr><th>VH+VV (descending mode)</th><th rowspan="2">Month</th><th>Pangasinan (Region I)</th></tr>
<tr><th>Season</th><th>Day</th></tr>
<tr><td>2019S1</td><td>September</td><td>9;21</td></tr>
<tr><td rowspan="6">2019 Season 1 (2019S1)</td><td>October</td><td>3;15;27</td></tr>
<tr><td>November</td><td>8;20</td></tr>
<tr><td>December</td><td>2;14;26</td></tr>
<tr><td>January</td><td>7;19;31</td></tr>
<tr><td>February</td><td>12;24</td></tr>
<tr><td>March</td><td>8;20</td></tr>
</table>

3. METHODS

The methodology for discriminating crop types in the study area is outlined in the flowchart (Figure 3.1) following a similar approach by Fikriyah et al., (2019). The major steps including data collection and pre-processing were performed by earlier projects. The pre-processing was performed by IRRI and temporal mean backscatter computation for each field sample for different growing stages was done by the NRS Department of the Faculty of Geo-Information Science and Earth Observation at the University of Twente. The focus was to extract phenological information (SAR metrics) from sentinel-1 SAR time series data, identification of target crop types and evaluation of results. The dataset used in the study are summarised in (Tables 2.3 and 2.6) and include Sentinel-1 data and Field survey data.

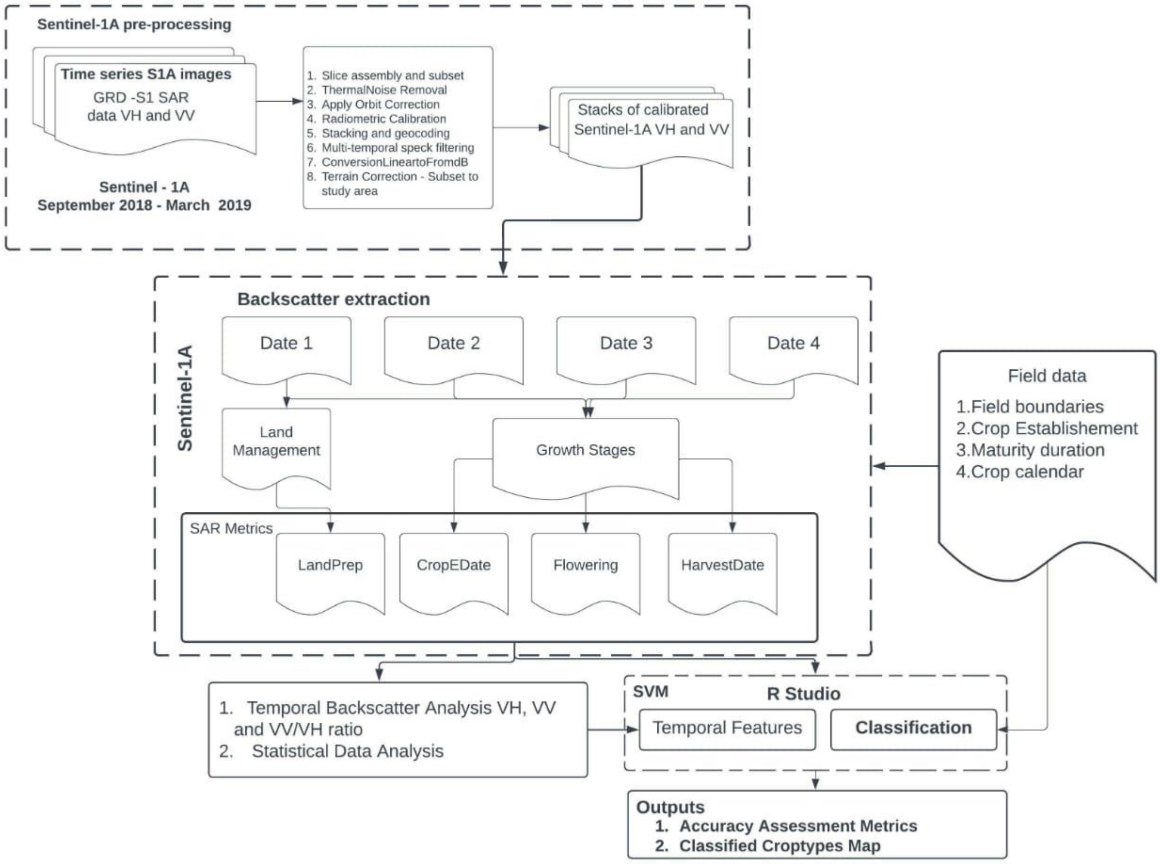

Figure 3. 1 Methodological flowchart of the crop type classification process

3.1. Extraction of SAR metrics and analysis of multi-temporal profiles

SAR metrics are additional parameters that are generated from multi-temporal SAR data (Santoro and Wegmüller, 2014), with acknowledged potential in crop discrimination. The proposed crop discrimination was based on features related to the phenology of the studied crops. Previous research has demonstrated that phenological features are valuable and improve the accuracy of crop type maps (Chen et al., 2016; Li et al., 2020). Phenological information as reported by the farmers during the field surveys were used to extract the backscatter at different growth stages for each field. The study analysed the extracted mean backscatter of rice and maize and their temporal variation. These metrics are based on the growth and development of the studied crops during the growing season

The mean backscatter (in VH, VV and VV/VH ratio) was extracted for each crop type at field-level. Four dates corresponding to Land management practice (LandPrep) and crop growth stages relating to crop establishment date (CropEDate), Flowering and Harvest (HarvestDate) were identified based on field survey data. The crop establishment date relates to the transplanting date for transplanted rice or sowing/broadcasting date for direct-seeded rice, and sowing for maize (non-rice crops). HarvestDate was the harvesting date for both rice and non-rice crops, while flowering is the flowering date for rice. However, for maize only two stages (CropEDate and HarvestDate) were recorded in the survey information. Thus the LandPrep for maize was assumed to be the backscatter at the date after the previous harvest in that field but before the reported CropEDate. The flowering phase for maize was also inferred from the growth development of the crop and was taken to be around 76 days after CropEDate (for varieties taking 120-144 days maturity duration). For shorter duration varieties (less than 60 days), flowering was taken to be at 36 days. The HarvestDate for both crop types was, however, considered as the image before the reported harvest date in the field survey data. This was to ensure that the analysed backscatter represented the actual crops before the harvest took place.

The SAR metrics considered in this study were the minimum backscatter at CropEDate, maximum backscatter at the Flowering stage and the backscatter at HarvestDate. The features were extracted from both polarizations (VH and VV) and their ratio (VV/VH). Due to varying management practices occurring in the study area, the selected growth stages also varied significantly. For instance, the crop establishment dates of maize range from 15th October 2018 – 12th February 2019 due to different sowing dates. This further resulted in different flowering or harvesting dates. Additionally, for rice, due to different crop establishment methods, transplanted or direct-seeded rice, the heading and maturity were also different for rice growth. The corresponding time series backscatter for each cultivated field for both crops was different on one satellite image date. This scenario hindered the utilization of the backscatter directly. Therefore, the mean backscatter was extracted for each growth stage and used as an input feature in the SVM algorithm. As only four stages were considered in extracting these metrics, smoothing of the original time series using Savitzky-Golay filtering (Chen et al., 2004) and other filters such as double logistic functions before extracting main phenological events were not necessary. Table 3.1 summarises the extracted features at each stage. A similar trend was also observed in the rice growth-related features.

3.1.1. Backscatter difference

Due to the farming characteristic of rice cultivation, the obvious changes of the plant during the growing season correspond considerably to the radar backscatter coefficient compared to other non-rice crops such as maize. From the extracted backscatter for rice and maize, it was observed that the maximum backscatter was at the flowering stage for both crops the minimum backscatter was noticed at the crop establishment stage in both polarization. According to Chang et al. (2021), "the backscatter difference between maximum and minimum values of the time series data during the rice growing season of rice is greater than that of other non-rice crops." Therefore, the backscatter difference (BackDiff) in VH, VV and the VV/VH ratio was further examined for rice and maize.

3.1.2. Crop duration

The time interval from sowing/transplant dates to maturity of crops is another important SAR metric which can be used to characterise the growth of crops (Chang et al., 2021). However, as the complete time series was not considered, the crop duration from the field interview was used in the analysis. The growth period of crops, that is the duration taken for the crops to mature, is an important feature (Nguyen et al., 2016). Each crop has its own characteristic growth period. In this study, the growth period (Maturity_days) was estimated as the difference between HarvestDate and the CropEDate. For rice the mean duration for crop maturity was 93 days (92.79) with minimum and maximum being 62 and 120 days, respectively. The average duration for Maize growth cycle was 110 days (109.92) with a maximum duration being 144 days and a minimum of 59 days.

Table 3. 1 Extracted features at different growth stages and the additional variable used in the SVM classification

Stage	VH	VV	VV/VH Ratio
Land Preparation	LandPrepVH	LandPrepVV	LandPrepCR
Crop Establishment	CropEDateVH	CropEDateVV	CropEDateCR
Flowering	FloweringVH	FloweringVV	FloweringCR
Harvesting Date	HarvDateVH	HarvDateVV	HarvDateCR
Additional features			
Backscatter Difference	BackDiffVH	BackDiffVV	BackDiffCR
Maturity_days* - Crop duration in days estimated from field survey information			

3.2. Statistical analysis

The study site represented varied geographic areas characterised by different climates and cropping practices. Given the spatial-temporal characteristics in these sites, a preliminary exploratory statistical data analysis was carried out to understand the temporal behaviour of the backscatter in relation to the different crop types. Statistical tests to determine whether there were significant differences between rice growth stages and maize during the 2019 growing season was done using the Mann-Whitney U Test. (Gardener, 2012) This statistical test is performed when the data is not normally distributed (non-parametric or skewed) which was the case for the current study. The statistical analysis was performed in IBM SPSS statistical analysis software package version 28.0.1.0 (142).

3.3. Support Vector Machines

The Support Vector Machines (SVM) algorithm developed based on the statistical learning theory is one of the most effective kernel-based classification methods in various machine learning techniques (Mountrakis et al., 2011). SVM is a supervised non-parametric algorithm that overcomes the shortcomings of traditional classifiers such as Maximum Likelihood classifiers, as it is insensitive to the underlying distribution of the input data (Löw et al., 2013; Sheykhmousa et al., 2020). Many advantages have been outlined in support of SVM in the field of Remote Sensing, including its good performance with limited training datasets and producing high classification accuracies (Mantero et al., 2005; Pal and Foody, 2010).

The SVM in its simplest original form, is a linear binary classifier. According to Son et al., (2018), "this algorithm projects training samples in the input space into a high-dimensional space using a kernel function in which the classes can be separable". The SVM training algorithm determines an optimal hyperplane to separate the dataset into discrete classes based on the distribution of the training dataset in feature space (Jia et al., 2012). As shown in Figure 3.2, SVMs use a subset of the training data set close in the feature space to the optimal decision boundary (hyperplane) as support vectors to maximise the margin (Foody and Mathur, 2004; Mather and Tso, 2016). However, in practice basic linear decision boundaries cannot often guarantee a high accuracy as different classes overlap, making the linear separability difficult (Mountrakis et al., 2011; Sheykhmousa et al., 2020). An example of the SVM linearly separable data is shown in Figure 3.2. To address the limitation of linear SVM, Cortes and Vapnik, (1995) introduced an extended SVM using kernel functions (Figure 3.3). A detailed description of the theoretical development can be found in Burges, (1998). An assessment of SVM for landcover classification as well as the mathematical formulation of the algorithm is provided in Huang et al. (2002). Several kernel models exist to build different SVMs and the radial basis function (RBF) and polynomials are commonly utilised kernels for remotely sensed image analysis (Mountrakis et al., 2011).

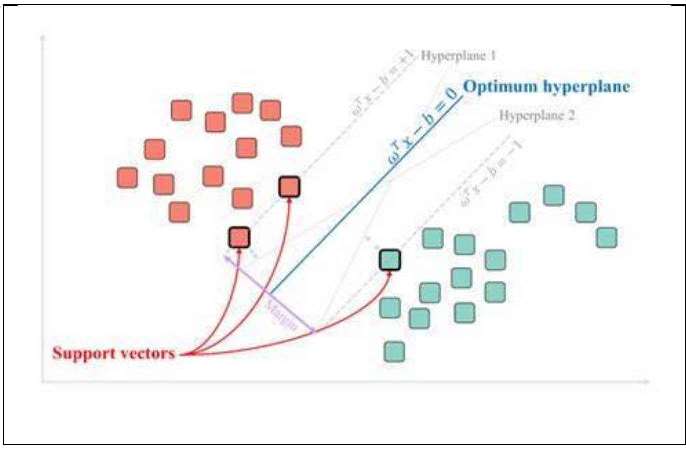

Figure 3. 2 SVM example of linearly separable data

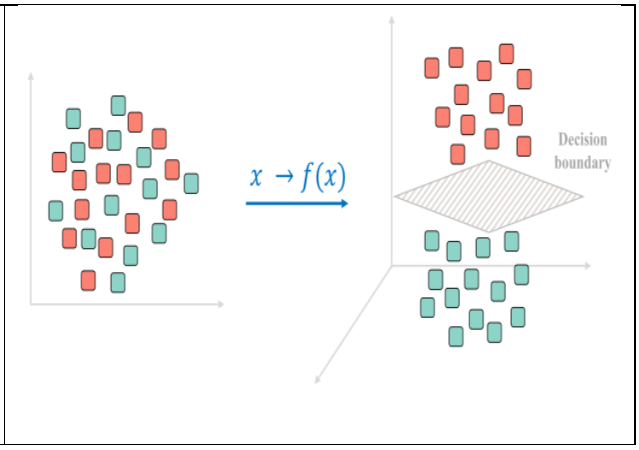

Figure 3. 3 SVM example of nonlinearly separable data with kernel trick (Source: Sheykhmousa et al. 2020)

Various studies have used the SVM for the classification of remotely sensed data (Foody and Mathur, 2004; Son et al., 2018). In this study, the radial basis function kernel was used for the classification of the SAR time series data as previous research has demonstrated to achieve accurate results (Huang et al., 2002; Jia et al., 2012; Pal and Mather, 2005). Further parameters to be set when using SVM include the kernel specific parameter and the cost or penalty parameter. The cost and kernel specific parameter for the RBF was initially selected randomly and the performance was re-valuated using a grid search to identify the best pair parameter to train the model (Mantovani et al., 2015). The training data selection for parameter tuning was based on the leave-one-out cross-validation approach. (Ramezan et al., 2019). The final values used in the model for the SVM classification for the different approaches were fixed with Cost = 128 and gamma = 0.102 for comparability of the results.

3.3.1. SVM Classification

The discrimination of rice and maize was implemented in R using the support vector machine (SVM) algorithm. Model building, tuning and accuracy assessment were performed using R version 4.2.0, an open-source language and statistical computing software. SVM is a supervised learning technique considered superior among machine learning (ML) algorithms. The creation of the algorithm based on SVM (Cortes & Vapnik, 1995: Vapnik, 1998), several add-on packages within R were used. Specifically, the SVM uses "kernlab" package for support vector machines and "e1071" that provides various functions required by the caret package for machine learning algorithms. The classification code was written and performed in

Rstudio using various packages and libraries. The process was implemented using the identified growth stages in VH, VV and VV/VH ratio. The classification approaches implemented comprised performing the classification at early and later development of the crops during the growing season. The significant features based on the results of the Mann-Whitney U-test were used to train the model as inputs as the first approach.

3.4. Sampling procedure

Samples in Remote Sensing serve two purposes as training data and test data for training the model and performing validation of the model respectively. The selection of training samples is an important factor and one must consider the spatial resolution of the data to obtain reliable classification results (Lu and Weng, 2007). Congalton, (1991) states that "a balance between what is statistical sound and what is practically attainable must be found." A variety of sample selection methods both statistical and non-statistical are commonly used in Remote Sensing. Due to the limited number of samples (31 for both crop types) cross-validation using Leave-one-out (LOOCV) approach was used (Kearns & Ron, 1999). This is a resampling method used to repeatedly draw samples from a training set by splitting the set into two parts. A general rule of thumb is that the samples used for classification should not be used for evaluation or assessment of accuracy. As the name implies, in LOOCV only a single observation is used as a test set (validation). Unlike using a separate sample of comparable size, which further limits sample size, this method yields an unbiased estimate of the classification accuracy. Therefore, instead of the reference samples being split into two sets: training and validation data, for each cycle, 30 measurements were used to build the model (training), and the remaining single observation was used for testing.

3.5. Accuracy assessment and evaluation of model performance

Accuracy assessment or validation forms a critical part of most mapping projects based on Remote Sensing data (Congalton, 2001). In order to assess the accuracy of the classification results of the SVM model, a confusion matrix (error matrix or contingency matrix) a commonly used technique to evaluate classification results (Congalton and Green, 2019), was established. The matrix was based on the results from each iteration and used in the research to evaluate the model's performance (c.f. 3.4).

The confusion matrix was further used to compute a variety of mapping accuracy metrics including user's and producer's accuracies (UA and PA) and the overall accuracy. The kappa coefficient, another discrete multivariate measure of map accuracy that takes into account the degree of accuracy resulting from assigning labels at random was also computed to test if classification results have different levels of accuracy (Congalton, 1991; Tolpekin and Stein, 2013). Kappa coefficient was used as a measure of agreement between the model predictions and the field observation.

4. RESULTS

This section outlines the main findings of the current study to evaluate the proposed methodology. The results of SAR metric determination and accuracy assessment are presented, including the findings obtained from the field survey information, temporal signature analysis of the studied crops as well as the statistical tests for the discrimination of rice and maize in the study area.

4.1. Statistical Analysis

4.1.1. Histogram analysis

As indicated earlier, rice is the major crop cultivated in the Philippines. The total number of samples from the selected fields were 31, where maize was cultivated in only 12 fields during the 2019 growing season. The histograms for the crop development phases and the corresponding average backscatter were utilized for the various crops to illustrate the statistical temporal behaviour of the different events. The histograms provide the backscattering time series distribution of the crop type classes during the 2019 dry season. Figures 4.1 and 4.2 show the histogram of rice and maize fields at various growth stages. The histograms for all stages do not exhibit a Gaussian-like distribution. The graphs illustrate the distribution of the studied crops at the identified stages as reported by the farmer. The graphs are shown in VH polarization only as similar distribution was observed in the other polarizations. The purpose was to explore whether the growth stages for this class can be distinguished using parametric tests. As can be seen from the figures, the graphs are not normally distributed and parametric tests are not appropriate.

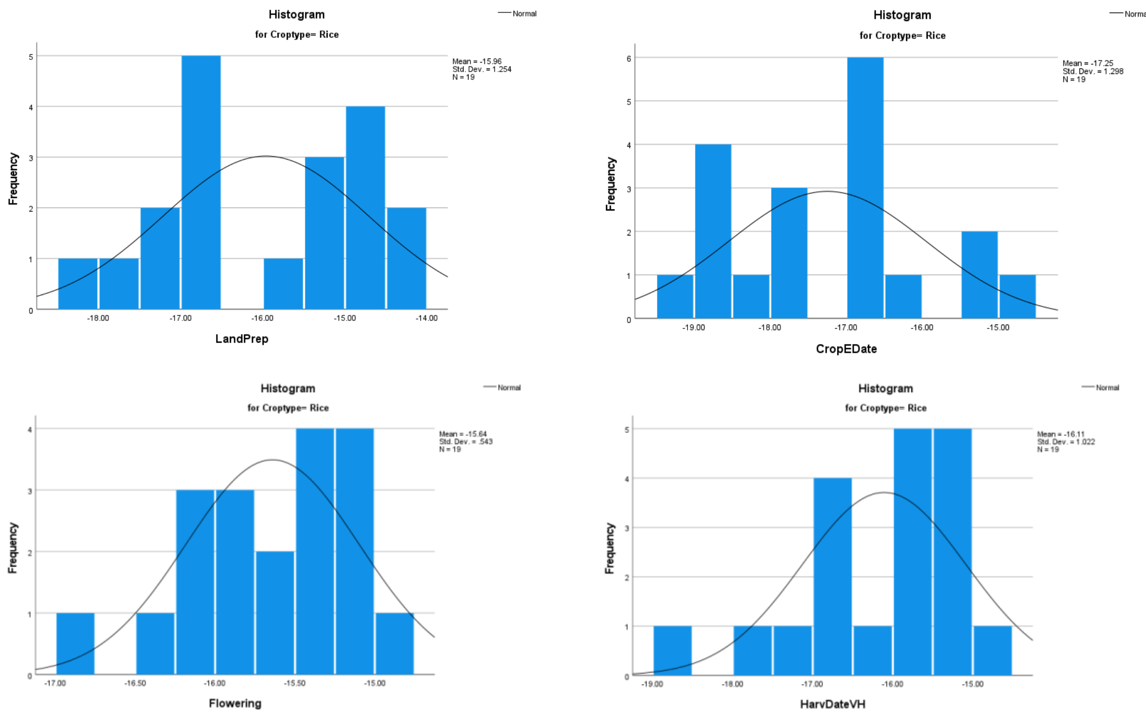

Figure 4.1. Histograms illustrating the distribution of rice at different growth stages in VH channel.

Based on the backscatter distributions some samples were identified as potential outliers. Farmers could not have recalled the actual date the event took place. For rice at flowering and harvest stages, one could be treated as a possible outlier (Figure 4.1). The flowering for maize is estimated from the crop development while land preparation is taken as a date before crop establishment as these stages were not reported by the farmers.

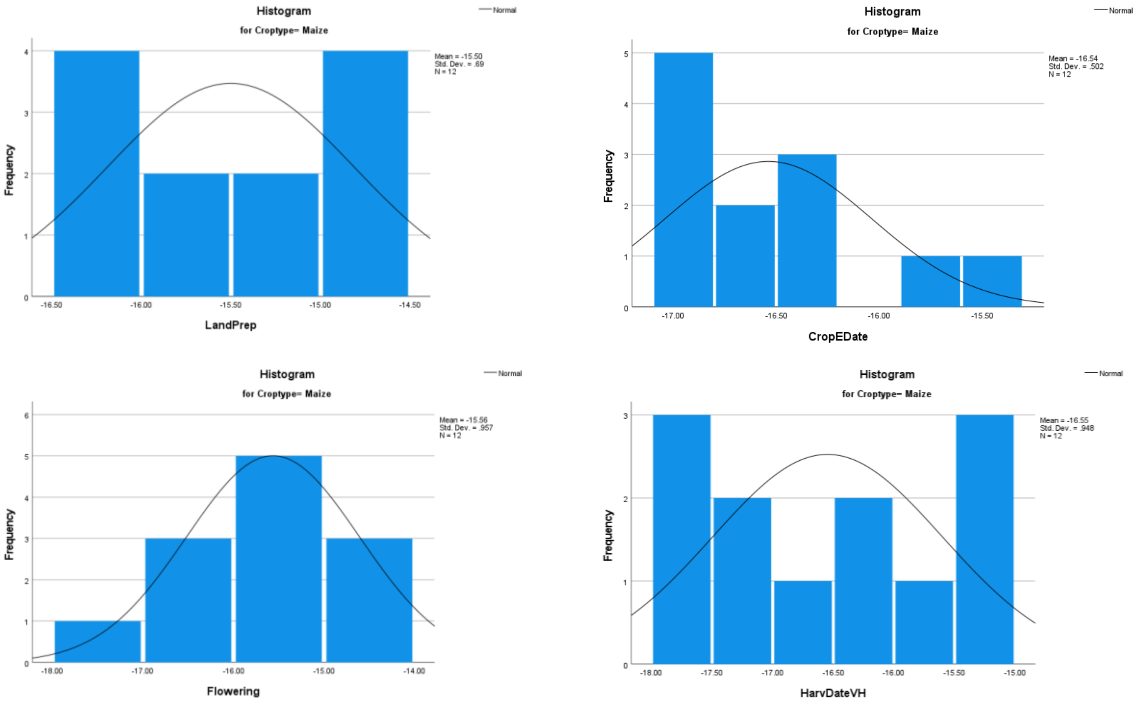

Figure 4. 2. Histograms illustrating the distribution of maize at different growth stages in VH channel

4.1.2. Significance tests (Mann-Whitney U-Test)

Statistical tests to determine whether there were significant differences between rice growth stages and maize during the 2019 growing season was done using the Mann-Whitney U Test. This statistical test is performed when the data is not normally distributed (non-parametric or skewed) and is based on the rank of the data. The data is summarized using the median or range as the t-test (parametric) is not appropriate in this case (see Figures 4.1 and 4.2). The p-values for the Mann-Whitney U Test results are summarised in Table 4.1. As can be seen from the table, a significant difference (p-value < .05) was only observed at the flowering and harvest phase in the VV polarization and VV/VH ratio. At VH no significant difference was found in any of the stages. The same phenomena was also observed in the overlap between the box-whisker plots at the various growth stage (Figure 4.12). The backscatter difference (Table 4.2) was also significant at the VV/VH ratio only (p-value .008). Other significant difference was seen in the crop duration between rice and maize (p-value = .018).

Table 4. 1 p-values from Mann-Whitney U-test between rice (n=19) and maize (n=12)(grouping variable: crop type) at the various growth stages during the 2019 dry season

	VH	VV	VV/VH
LandPrep	.372	.871	.292
CropEDate	.133	.543	.256
Flowering	.570	**.007**	**.043**
HarvestDate	.209	**.039**	**<.001**

Table 4. 2 p-values from Mann-Whitney U-test between rice (n=19) and maize (n=12)(grouping variable: crop type) using the Backscatter Difference (BackDiff) during the 2019 dry season

	VH	VV	VV/VH
BackDiff	.199	.071	**.008**

Figure 4. 3 p-values from Mann-Whitney U-test between rice (n=19) and maize (n=12)(grouping variable: crop type) using the Crop duration (Maturity_days) during the 2019 dry season

	p-value
Crop duration	.018

4.2. Variation of temporal radar backscatter profiles

To understand the variation of temporal radar backscatter responses of the studied crops (rice and maize), the backscatter intensities of the two crops were examined at each growth stage in the different polarizations (VH, VV and VV/VH ratio) during the growing season.

As can be seen from the temporal profiles, the variations in the backscatter provide pertinent information on the developments of the crops (Figures 4.4 and 4.5). The temporal signatures are plotted from the crop establishment date which is the second image acquisition (12 days) after land preparation stage. For both crop types, the plots indicate that the backscatter in parallel polarization (VV) at all phenological stages and their temporal variation are larger compared to the cross polarization channel (VH). Generally, the backscatter values for maize is larger than that of rice in both the VH and VV channel. A continuous increase in the radar backscatter after the crop establishment stage was observed in the VH polarization, which reached the maximum at the flowering stage before it started decreasing (Figure 4.4). A similar pattern was observed in the VV channel for the maize class, however, there was a lot of variation in the temporal backscatter in VV for the rice crop type (Figure 4.4).

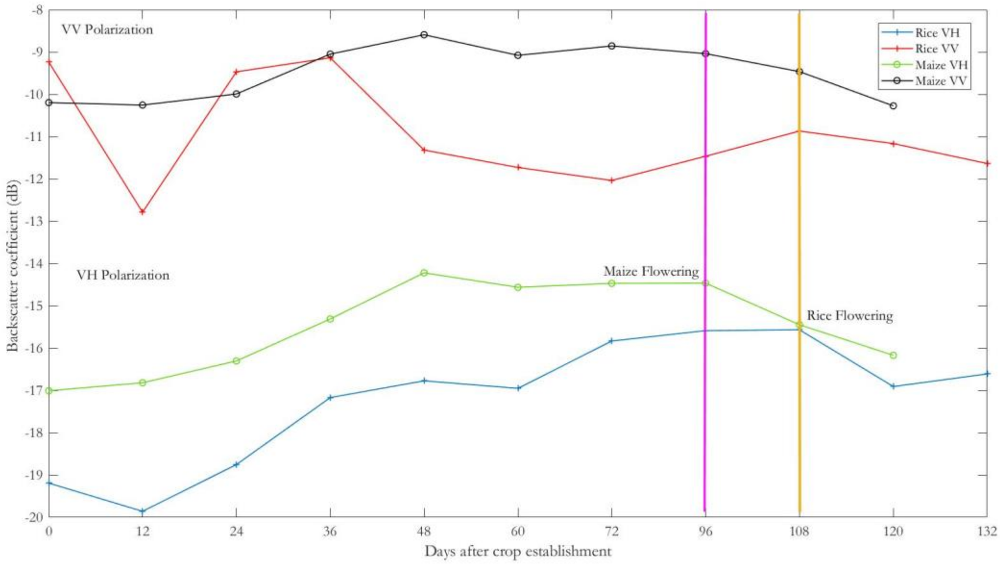

Figure 4. 4. Temporal backscatter of rice and maize in VH and VV from crop establishment to harvest at the end of the time series. Vertical lines indicate the flowering stages purple (maize) and brown (rice).

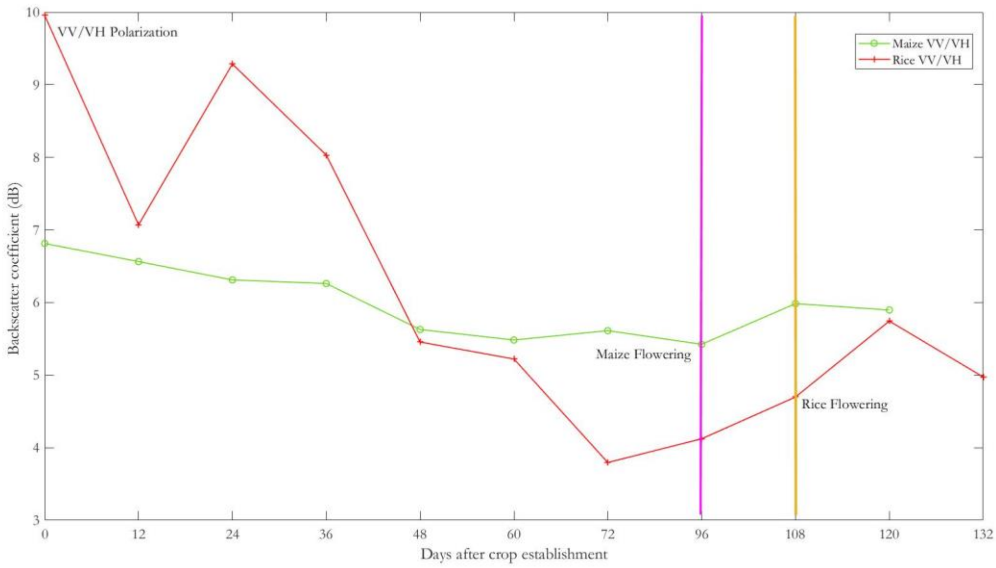

Figure 4. 5. Temporal backscatter of rice and maize in VV/VH from crop establishment to harvest at the end of the time series. Vertical lines indicate the flowering stages purple (maize) and brown (rice).

In the VV/VH ratio, Figure 4.5, a decreasing trend in the backscatter for maize and rice was observed from crop establishment to the harvest phase. Further examination was performed to understand the variation of temporal radar backscatter responses of a single crop (maize) in different fields. The variation in the backscatter intensity during the entire growing season (in VH, VV and VV/VH ratio) is shown in Figures 4.6 – 4.8. As can be observed, a lot of variation also exists within the same crop type in different fields.

Notice the differences in the crop duration that resulted in different harvest dates in the study area. In all the fields an increasing trend in the backscatter values was observed from the crop establishment in both the VH and VV channel (Figures 4.6 and 4.7). In the VV/VH a decreasing trend was noticed in some fields, reaching a minimum at 84 days, before the backscatter started increasing again. However, in other fields no clear pattern was observed in the VV/VH ratio.

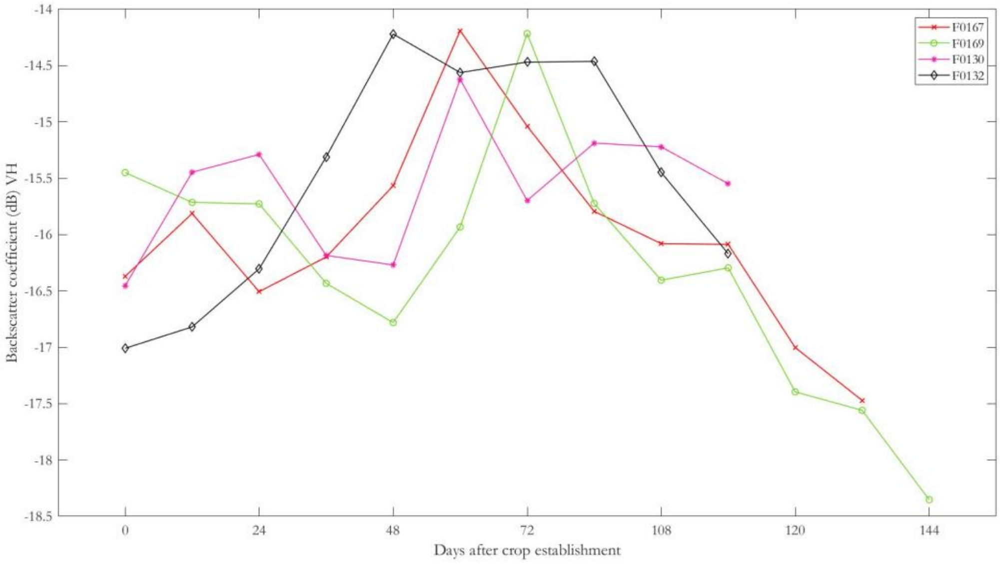

Figure 4. 6. Temporal backscatter of maize in VH for four different fields from crop establishment to harvest at the end of the time series

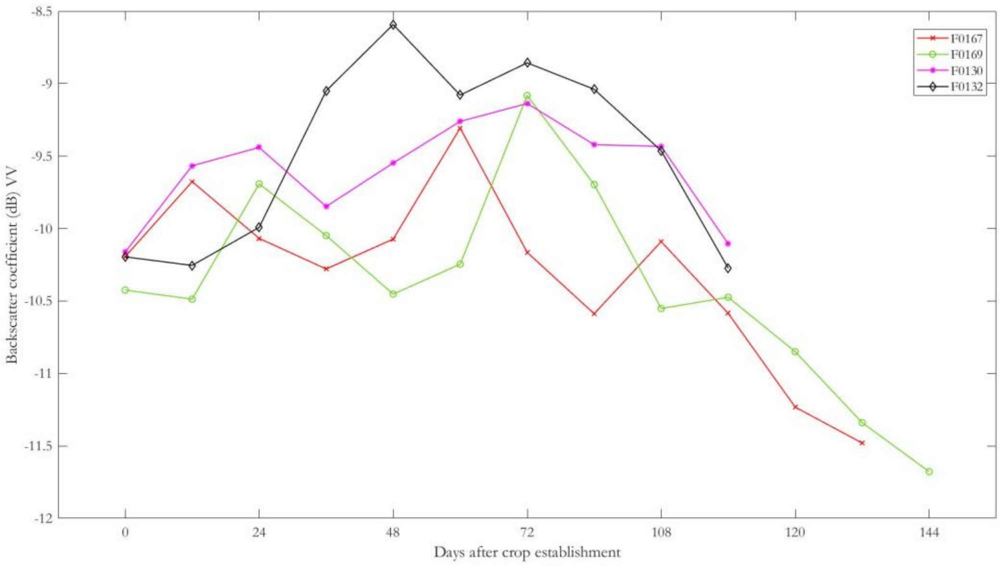

Figure 4. 7. Temporal backscatter of maize in VV for four different fields from crop establishment to harvest at the end of the time series.

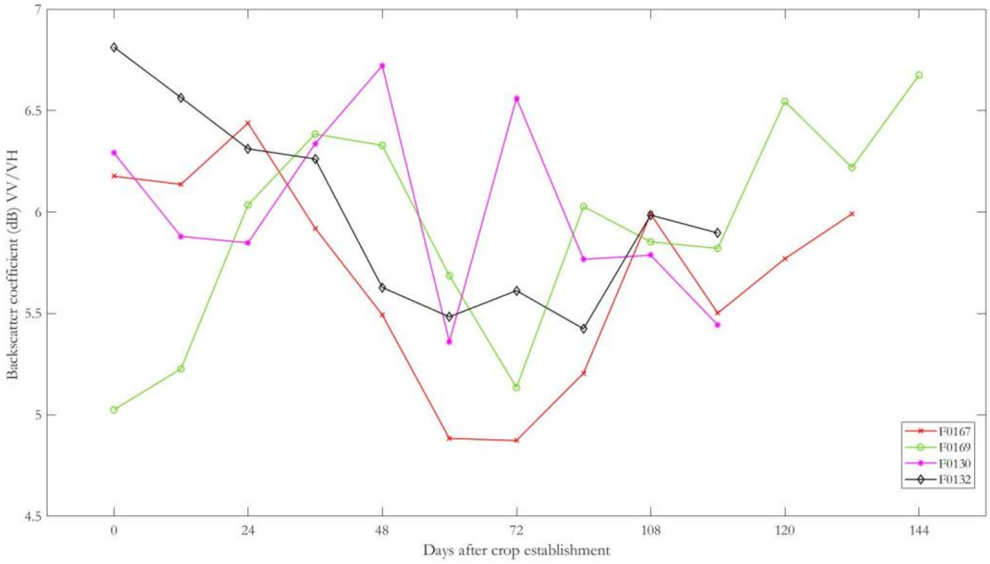

Figure 4. 8. Temporal backscatter of maize in VV/VH for four different fields from crop establishment to harvest at the end of the time series.

4.3. Multi-temporal SAR metrics

The extracted SAR metrics from the backscatter intensities for rice and maize were plotted at the identified growth stages during the 2019 growing season as shown in the following figures (Figures 4.8-4.10). The temporal radar backscatter of the identified four stages follows the expected temporal signature of the complete time series for both crops. As can be noticed from Figures 4.8-4.10, the mean backscatter values vary at each growth stage for the two crops in the different polarizations and follow a similar pattern to that of the complete time series (Figures 4.3 and 4.4). The temporal profile of rice and maize are very similar in the VH channel (Figure 4.8). Additionally, the signature for maize in both VH and VV channel show a similar pattern during the growing period (Figures 4.8 and 4.9). However, a peculiar temporal behaviour in VV is observed for the rice crop that shows a decreasing trend in the backscatter coefficient from the cropEDate to Harvest.

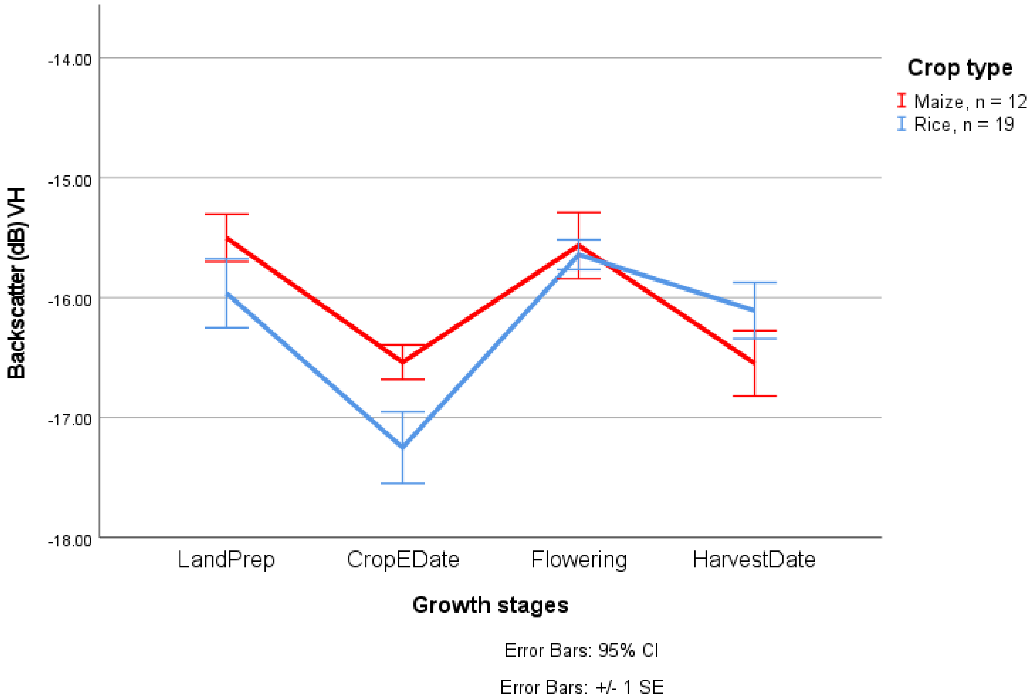

Figure 4. 9. Temporal backscatter of rice and maize during the dry season of 2019 in VH polarization with Error bars representing +/- 1 Standard Error

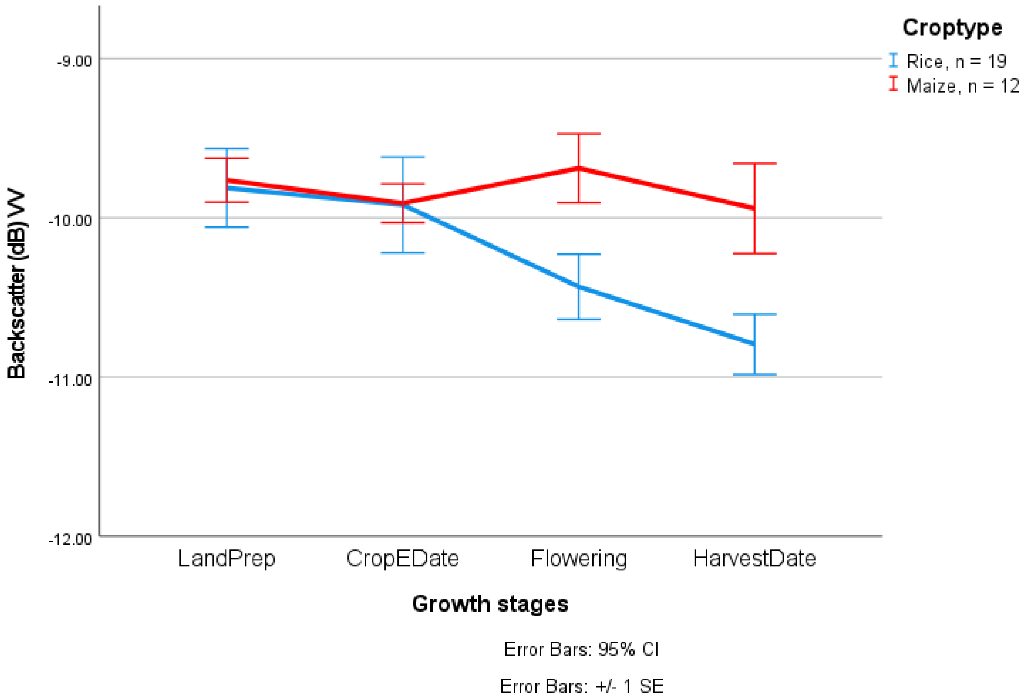

Figure 4. 10. Temporal backscatter of rice and maize during the dry season of 2019 in VV polarization with Error bars representing +/- 1 Standard Error

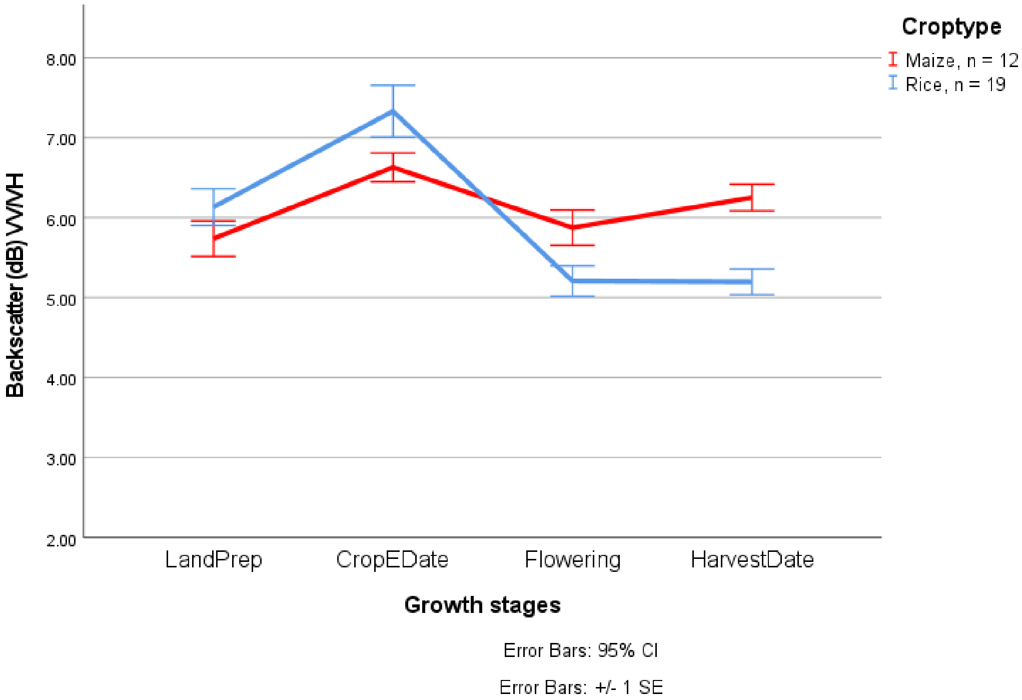

Figure 4. 11. Temporal backscatter Temporal backscatter of rice and maize at various crop growth stages in VV/VH during the dry season of 2019. The error bars at 95% CI indicate the variation at each growth stage.er of rice and maize at various crop growth stages in VV/VH during the dry season of 2019. The error bars at 95% CI indicate the variation at each growth stage.

To understand the variation of the temporal radar backscatter responses (in VH, VV and VV/VH ratio), the backscatter time series for the different development phases were further analysed using box-whisker plots (Figure 4.12). Note the variation in the scale in each polarization (Figure 4.12) and the overlap (in the median) at VH polarization which relate to the results of the statistical tests (as Mann-Whitney U-test uses the rank order (median)). This explains why none of the results in the VH channel and also at CropEDate in all the polarizations are significant (Figure 4.12a).

VH in 2019 dry season

a)

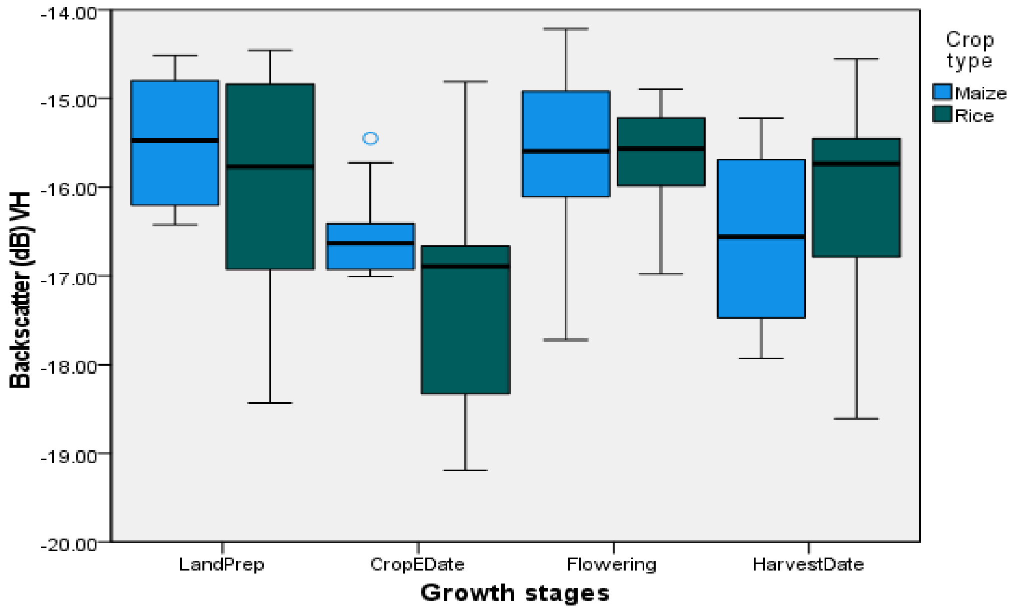

VV in 2019 dry season

b)

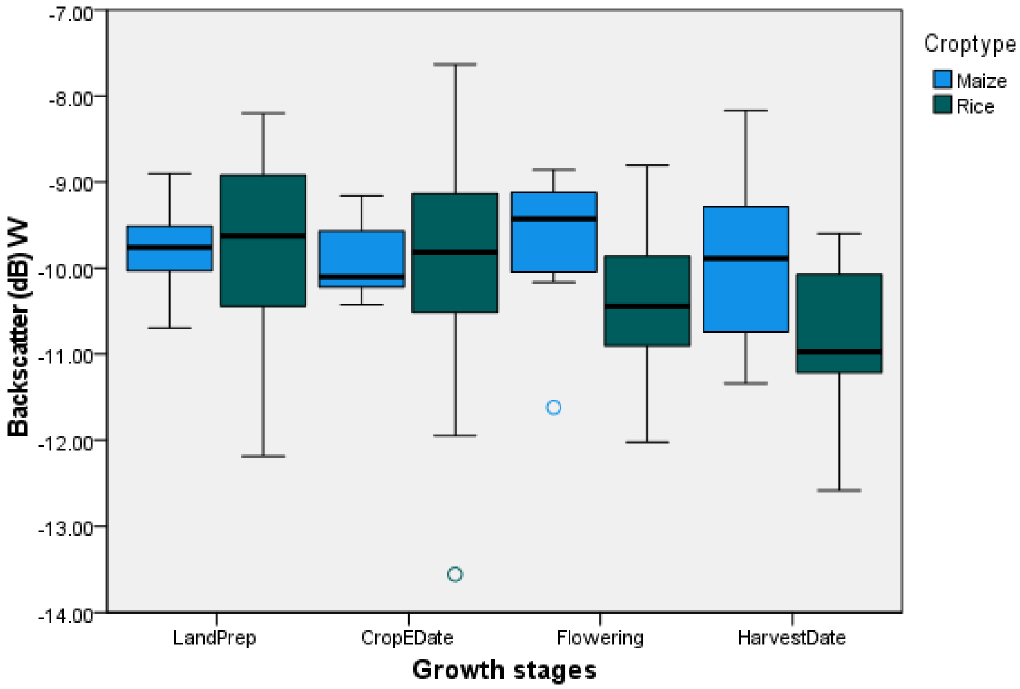

Figure 4. 12. Box-whisker plots showing the variation of the temporal backscatter coefficient at the crop development phases in VH (a), VV (b) and the VV/VH ratio (c) during the 2019 dry season. The plots are grouped per crop type maize (blue) n= 12, and rice (dark green) n=19. The variation in backscatter at each stage can be clearly seen. The coloured circles represent the outliers, the thick horizontal black line in the box is the median, the lower half of the box is the 25th percentile and the upper part of the box is the 75th percentile, and the extent of the lines represents the minimum and maximum backscatter values.

VV/VH ratio in 2019 dry season

c)

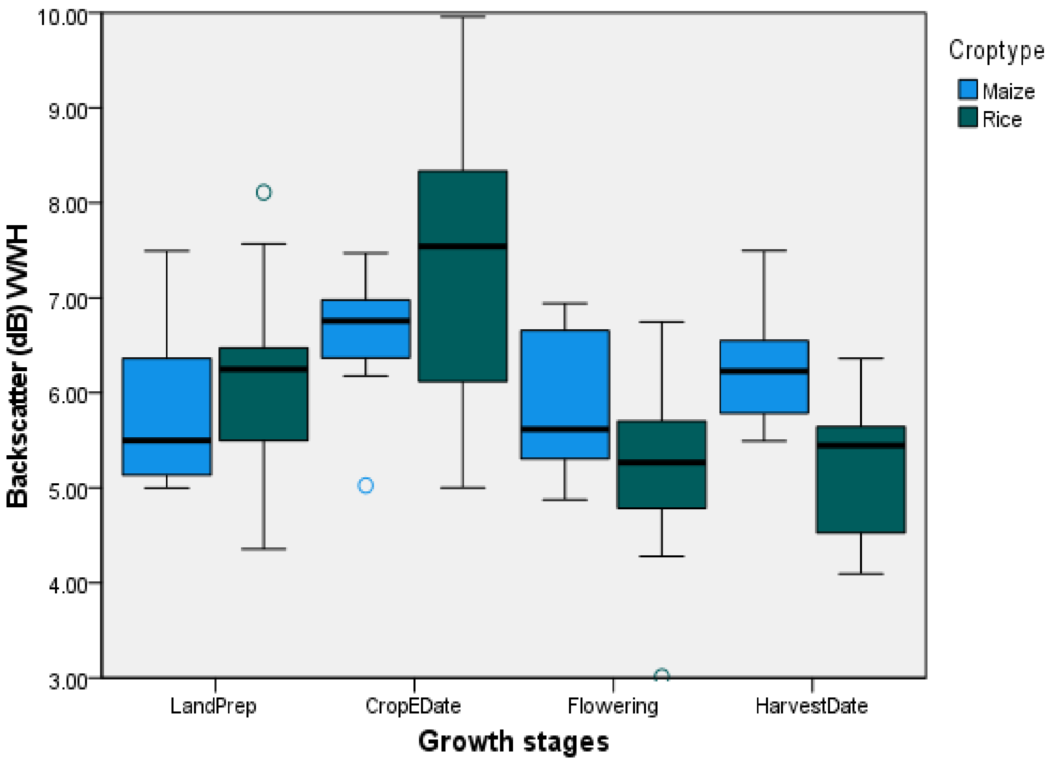

Figure 4.12. Box-whisker plots showing the variation of the temporal backscatter coefficient at the crop development phases in VH (a), VV (b) and the VV/VH ratio (c) during the 2019 dry season. The plots are grouped per croptype maize (blue) n= 12, and rice (dark green) n=19. The variation in backscatter at each stage can be clearly seen. The coloured circles represent the outliers, the thick horizontal black line in the box is the median, the lower half of the box is the 25th percentile and the upper part of the box is the 75th percentile, and the extent of the lines represents the minimum and maximum backscatter values.

4.4. Accuracy assessment and evaluation of model performance

The accuracy of the classification results obtained were evaluated using Leave-one-out cross-validation method. The most common measures of assessing the accuracy was performed as shown in the confusion matrix. The error matrix shows the standard accuracy metric that are used to carry out the evaluation of the algorithm performance and the classification results. The following tables (Tables 4.4 - 4.8) show the error matrices compiled from the overall results of the model using the indicated approach.

4.4.1. SVM classification using significant features

Table 4.3 shows the error matrix compiled when only significant features (Table 4.1) were used based on the results of the Mann-Whitney U-Test. That is the backscatter at the flowering stage in VV, cross ratio (FloweringVV and FloweringCR), harvest date in VV and VV/VVH (HarvDateVV and HarvDateCR) as well as the Backscatter Difference in VV/VH ratio (BackDiffCR). As can be noted, the results show an overall accuracy of 83.9% and Kappa = 0.66. Misclassification was also observed to be minimal, with errors of omission of 25% and 11% for maize and rice, respectively (Table 4.3). The misclassification errors, both omission and commission, were lower for the rice class compared to maize. Additionally, the user and producer accuracy for rice are also higher than maize (Table 4.4).

Table 4. 3 Error Matrix of SVM algorithm for rice and maize using significant features as input in the model (in VV and VV/VH ratio) as predictors

	Reference classes				
Predicted (Classification Results)	Maize	Rice	Total	Error of Commission (%)	User Accuracy (%)
Maize	9	2	11	18	82
Rice	3	17	20	15	85
Total	12	19	31		
Error of Omission	25	11			
Producer Accuracy	75	89			

Overall Accuracy 83.9% , Kappa 65.5% (Substantial)

4.4.2. SVM classification all features

When all the features (sixteen features) are used in the model (Table 4.4) a decline of 3.3% is observed in the overall accuracy compared to using only significant features (Table 4.4) with Kappa reaching 0.59. The user and producer accuracies for both classes are comparable with few errors of commission and omission observed when using this approach.

Table 4. 4 Error Matrix of SVM model when using all sixteen variables (in VH, VV and VV/VH ratio)

	Reference classes				
Predicted (Classification Results)	Maize	Rice	Total	Error of Commission (%)	User Accuracy (%)
Maize	9	3	12	25	75
Rice	3	16	19	16	84
Total	12	19	31		
Error of Omission	25	16			
Producer Accuracy	75	84			

Overall Accuracy 80.6%, Kappa 59% (Moderate)

4.4.3. SVM classification at Crop Establishment Date

Table 4.5 shows the classification results at crop establishment stage. The obtained overall accuracy was 80.6% and Kappa = 0.58. At this stage a lot of maize fields (33%) were omitted and classified as rice.

Table 4. 5 Error Matrix for using features at CropEdate (in VH, VV and VV/VH ratio) as predictors

	Reference classes				
Predicted (Classification Results)	Maize	Rice	Total	Error of Commission (%)	User Accuracy (%)
Maize	8	2	10	20	80
Rice	4	17	21	19	81
Total	12	19	31		
Error of Omission	33	11			

Producer Accuracy	67	89

Overall Accuracy 80.6%, Kappa 57.9%

On the contrary, the rice class had low misclassification errors, with errors of omission and commission of 11% and 19%, respectively (Table 4.5). The user accuracy for both maize and rice (80% and 81% respectively) were comparable. Table 4.5 indicates that maize had a lower producer accuracy (PA=67%) at CropEDate than rice with a PA of 89%.

4.4.4. SVM classification at Flowering

At the flowering stage, a lot of misclassification (50% omission) was observed in discriminating the maize class (Table 4.6). It can be noted in the table that the off diagonal cells (in maize) is large at this stage, indicating poor classification results. Recall that this stage was not reported by the farmers but estimated based on the growth development of maize, thus there could be errors in estimating this stage. A higher producer accuracy (PA=89%) was seen in rice, however, the user accuracy for both classes are similar (Table 4.6). Although the obtained overall accuracy was reasonable (74.2%), the computed Kappa (Kappa = 0.42) was lower compared to the previous approaches (Tables 4.4, 4.5 and 4.6)

Table 4. 6 Error Matrix for using features at the Flowering stage (in VH, VV and VV/VH ratio) as predictors

	Reference classes				
Predicted (Classification Results)	Maize	Rice	Total	Error of Commission (%)	User Accuracy (%)
Maize	6	2	8	25	75
Rice	6	17	23	26	74
Total	12	19	31		
Error of Omission	50	11			
Producer Accuracy	50	89			

Overall Accuracy 74.2%, Kappa 42.1%

4.4.5. SVM classification at Harvest Date

The final approach assessed the performance of the model and classification results at the harvest date in the VH, VV and the VV/VH ratio (Table 4.7). Similar to the flowering stage (Table 4.6), misclassification was more in the maize class compared to rice (Overall Accuracy = 67.7%, Kappa=0.28). However, a slight decline in the producer accuracy and user accuracy was noticed at the harvest date for both classes (Table 4.7).

Table 4. 7 Error Matrix for using features at the HarvestDate (in VH, VV and VV/VH ratio) as predictors

	Reference classes				
Predicted (Classification Results)	Maize	Rice	Total	Error of Commission (%)	User Accuracy (%)
Maize	5	3	8	37	63
Rice	7	16	23	30	70
Total	12	19	31		
Error of Omission	58	16			
Producer Accuracy	42	84			

Overall Accuracy 67.7%, Kappa 28% (Fair)

4.5. Distribution of rice and maize during the growing season

The calibrated and evaluated SVM model was used to map the distribution of the target crop types in the study area during the 2019 growing season. Figures 4.13 – 4.16 show the distribution of rice and maize for selected polygons at different growth stages.

4.5.1. Crop distribution using significant features

Figure 4.13 shows the distribution of crops based on SVM classification using significant features from the results of the statistical tests (Mann-Whitney U-test). It can be observed from the field observations (left) that the crop types are clustered in one area for both crops. The classification results (right) show that the rice fields around San Roque and Catuday (found around maize fields) were misclassified as maize. A similar observation is made in the south-east around Alaminos where the maize field was classified as rice (Figure 4.13). Overall, the accuracy is acceptable (see Table 4.4).

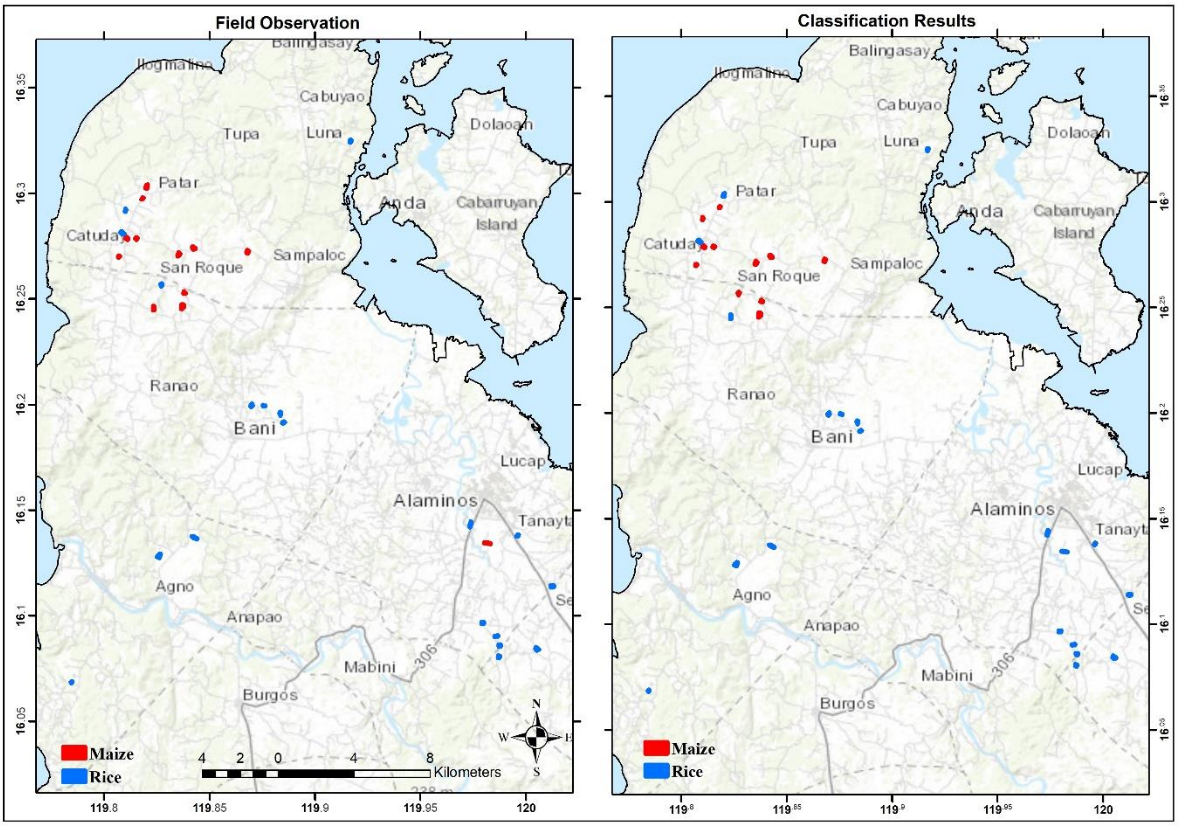

Figure 4. 13. Map showing the field observation in Pangasinan (left) and SVM classification results (right) using only significant features (5) based on Mann-Whitney U-test results

4.5.2. Distribution of crops based on SVM classification using all features

The distributions of crops in the study area based on the results of the SVM classification when all the features were used as input in the model are shown in Figure 4.14. The map zooms in on the two clusters. A similar pattern was observed when the crop duration (Maturity_days) feature was excluded from the model (using 15 features).

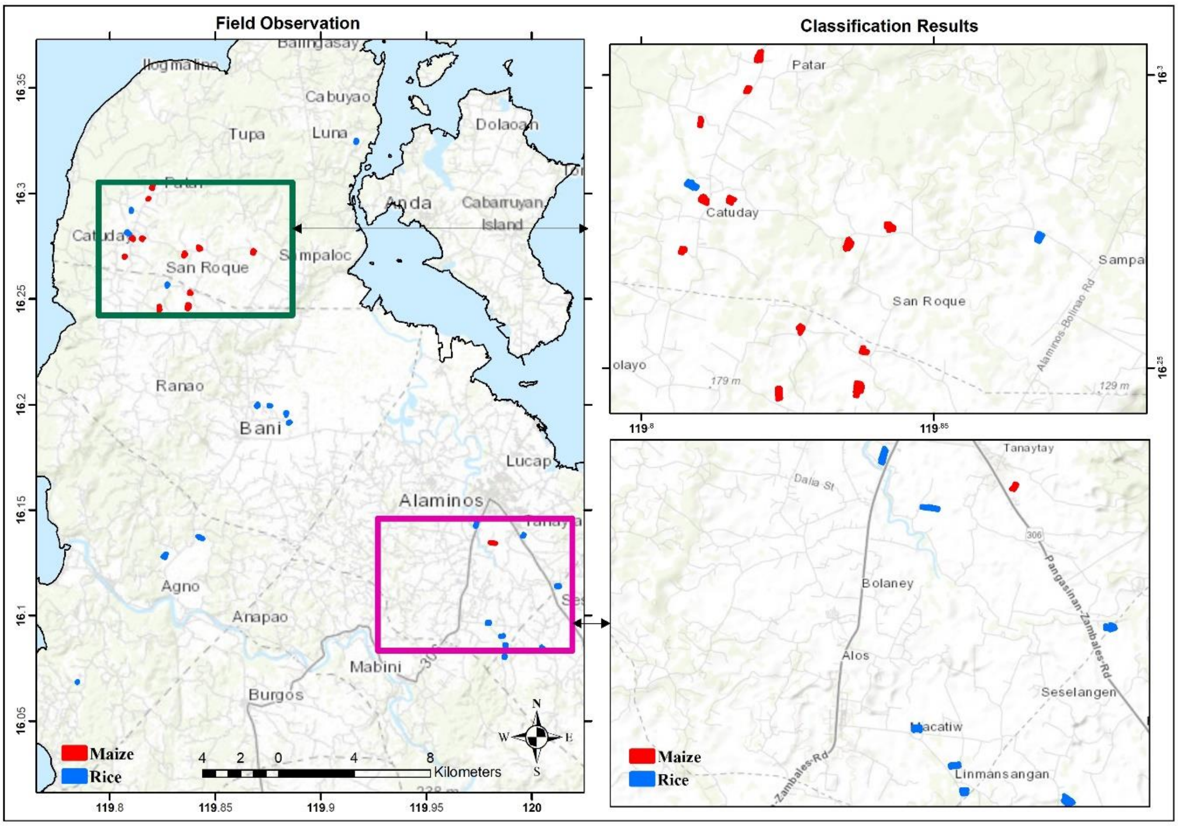

Figure 4. 14. Map showing the field observation of crop types in Pangasinan (left) and the SVM classification results using all (16) features (right) in VH, VV and VV/VH ratio as input to the model.

4.5.3. Distribution of crops based on SVM classification using all features

The map (Figure 4.15) shows field observation and the distribution of crop types based on the SVM classification results at CropEDate. The map shows that the discrimination of crops at this stage was affected by misclassification. More maize fields (four) were classified as rice fields compared to two fields of rice that were misclassified.

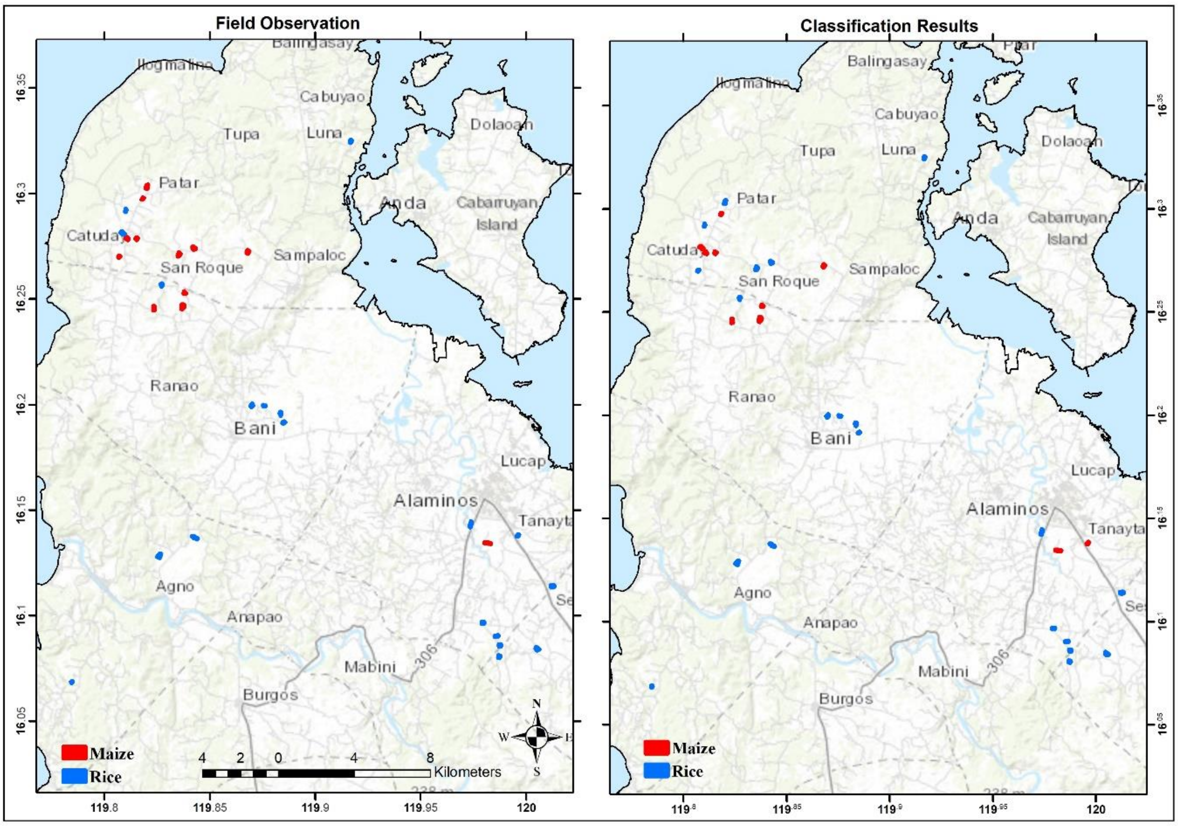

Figure 4. 15. Map showing the field observation of crop types in Pangasinan (left) and SVM classification results (right) using the features from CropEDate (in VH, VV and VV/VH ratio).

4.5.4. Distribution of crop types Flowering

The distributions of crops in the study area based on the results of the SVM classification when the features at a later stage of crop development (Flowering) were used as input in the model is shown in Figure 4.16. A comparison of the two maps shows that a lot of misclassification occurred at this stage. Fifty percent of the maize fields (six) were misclassified. A similar pattern was observed when the features at HarvestDate were used in the model. At HarvestDate 58% (7) maize fields were misclassified as rice, see Appendix II.

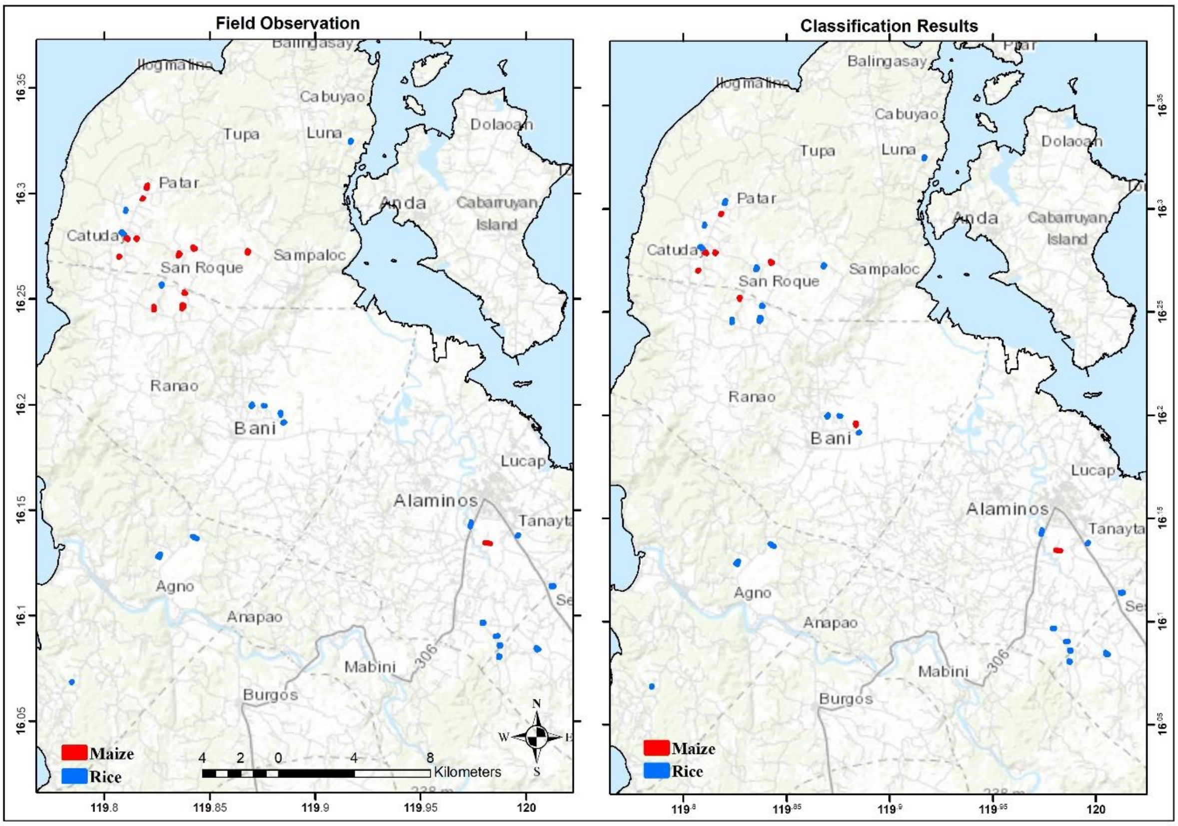

Figure 4. 16. Map showing the field observation of crop types in Pangasinan (left) and SVM classification results using features from the Flowering stage (right) in VH, VV and VV/VH ratio

5. DISCUSSION

5.1. Variation of temporal radar backscatter responses (VH, VV and VV/VH ratio) of rice and maize within the growing season

The backscatter coefficients of rice and maize in the study area were observed to increase after crop establishment, which can be attributed to change in structure and the consequent increase in the biomass, leading to canopy closure. Generally, the radar backscatter response from the vegetation is mainly influenced by the shape, size and orientation of plants and leaves as well as the soil moisture and water content of the vegetation (Pandži et al., 2020). Therefore, the backscattering intensity observed during the growing cycle and at each growth stage is as a result of different scattering mechanisms that occur due to changes in the structure, geometry and dielectric properties of the crops. The farming characteristic of rice cultivation and the characteristic nature of the radar backscatter plays a key role in discriminating rice fields from other landcover classes such as maize. Before sowing or transplanting (in the case of transplanted rice), the soil's surface roughness and moisture content affect the backscattering power as the fields are either cultivated (rough surface) or uncultivated. The higher backscatter intensity in the VH and VV at land preparation can be interpreted as the reflection from the bare soils. The recorded backscatter at this stage, -15.96 dB and -15.5 dB for rice and maize, respectively occurs prior to sowing. The rougher the surface the stronger the backscatter (Umutoniwase and Lee, 2021). Additionally, the backscatter values increases with an increased moisture content in both soils and vegetation. The moisture content of farmland areas is affected not only by rainfall and irrigation, but also by temperature and evaporation (Ma et al., 2021). In the study area, the monthly rainfall is high in August and continues to decline until March. The temperatures start to increase following reduced rainfall reaching maximum temperature in May (Figure 3.2). These changes, coupled with increased evaporation during the dry season, significantly affect the penetration of the microwave signal into the medium. The fluctuations in the time series can be interpreted as due to the influence of rainfall on the radar backscatter.

5.1.1. Rice

Rice is cultivated in flooded fields, and the backscatter is at its lowest value due to specular reflection from the standing water (Chen and McNairn, 2006). Thus the low backscatter in both the VH and VV indicates the planting period (or transplanting) where the rice fields are completely submerged in water resulting in specular reflection. As the plant grows through each growth stage, the backscatter increases from -17.25 dB at CropEDate as a result of volume scattering until the plant reaches a maximum dB of -15.64 at flowering (reproductive stage) where the backscatter saturates in the VH channel. Prior to harvesting, the rice crop backscatter decreases due to ripening of the crop which leads to reduced water content in the plant, reaching -16.11 dB at Harvest Date. This characteristic difference in backscatter at the VH can be used to distinguish rice from maize. A similar observation was made by (Nguyen-Thanh et al., 2021). Kushwaha et al. (2022) also noted that the sensitivity of the SAR data depends on the polarization of the image. The cross polarization (VH) is more sensitive to volume scattering which is influenced by the change in the canopy and dielectric properties. Each polarization thus represents effectively the change in the seasonal backscatter signature that is consistent with the growth development phases of the crops. However, a peculiar temporal behaviour in the VV channel was observed in the results, which showed a continuous decreasing trend from the crop establishment phase to the harvest date. This observation was also noticed by Phan et al. (2021). Unlike what is reported in most studies (Kushwaha et al., 2022; Selvaraj et al., 2019; Wei et al., 2019), where the C-band backscatter is characterised by a continuous increase from the transplanting/sowing phase to the heading stage. The inconsistency in the VV trend can be attributed to several factors, including management practices (direct-seeded/transplanted rice), planting density (with seedrate from 59-120kg/ha) and supplement irrigation. The VV is sensitive to both surface and volume scattering. In addition, the VH and VV contain double-bounce scattering indicating vegetation and soil interaction (Veloso et al., 2017). It can be noticed from the results that large error bars at the land preparation phase as well as harvest dates are observed, suggesting large variations at these development phases (Figures 4.9 and 4.10). Figure 5.1 shows the backscatter mechanisms in relation to the rice growth phases.

The temporal variation of the VV/VH ratio has similar behaviour to VH and VV, as it is dependent on the backscatter value from these polarizations. It was observed that the value of VV/VH increased due to the inundation of the fields with water. A sudden decrease in the backscatter value can be attributed to rainfall/ irrigation during the growing period, as most fields experienced supplement irrigation (Figure 4.11).

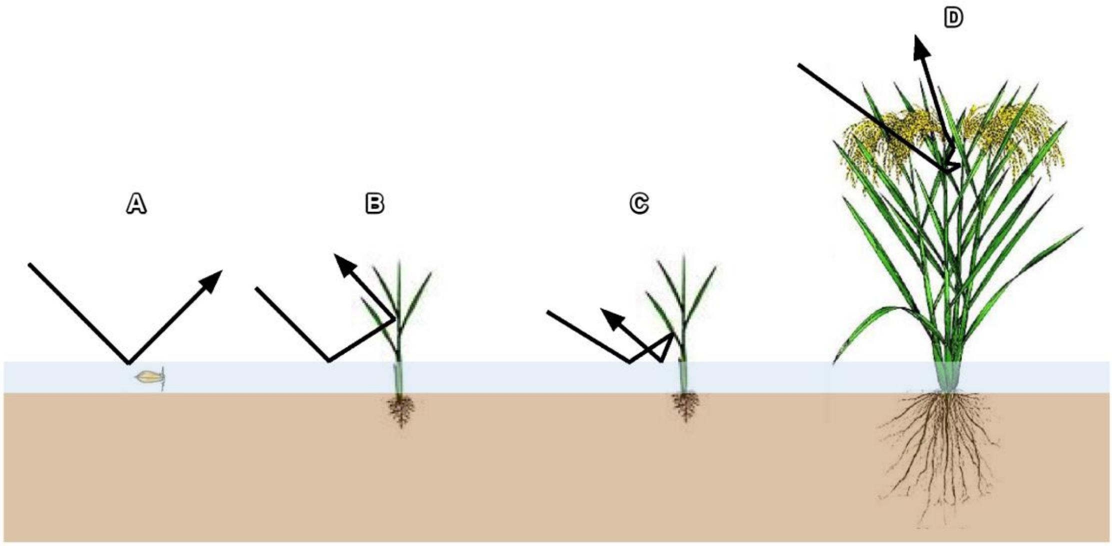

Figure 5. 1 Backscatter mechanisms in relation to rice crop growth stages (a – specular reflection, b, c – double-bounce and d-volume scattering). Source: (Clauss et al., 2018)

5.1.2. Maize

For maize, usually, five different development stages of the plant can be identified (Figure 5.2). The development period comprise mainly of vegetative and reproductive stages. The plant exhibits a variety of phenological stages during its growth stages, with its height as one of the measurements that represent the plant's growth rate (Abdikan et al., 2018). The temporal variation of maize in both VH and VV backscatter is almost similar with the VH being lower by 5.56 dB from the VV backscatter. As can be seen from the temporal profile, the VH backscatter of maize steadily increases after the crop establishment date. The backscatter increases steadily from -16.54 dB at CropEDate to a maximum of -15.56 dB at the Flowering stage. This can be attributed to the increase in volumetric scattering due to the accumulation of biomass as a result of new leaves being formed (emergence of the maize) and subsequently unfolding of leaves (Khabbazan et al., 2019). At the early stages, the crop establishment date of the maize crop, the radar backscatter values at VH and VV are dominated by surface soil moisture at the sowing date. The high backscatter values in both VH and VV at the land preparation stage are due to less moisture in the soil, as soil moisture greatly influences the fluctuations of the backscatter in the VH and VV. Surface roughness, in addition to soil moisture, plays a major influence and affects the return signals of the radar backscatter.

It can be observed from the results that maize has a much higher backscatter than rice (Figures 4.4, 4.9 and 4.10). The growth stages of the maize plant are above the temporal profile of the rice plant except for the harvest date. This can be attributed to the morphology of the maize stalk, which does not tiller and the farming characteristics of rice where fields are flooded (Nguyen-Thanh et al., 2021). In the VV backscatter, the temporal variation of maize is similar to the VH backscatter with the VH being lower by 5.56 dB from the VV backscatter. As expected the backscatter increase steadily from CropEDate to a maximum at the flowering stage before reaching low values at HarvestDate. The increase in the VH and VV backscatter results in a steady decrease in the VV/VH ratio from CropEDate to flowering as a result of the differential attenuation in the VV and VH (Phan et al., 2021). The minor increase in the VV backscatter is interpreted as due to the increase in double-bounce scattering between the vertical stalk and the soil during stem elongation (Khabbazan et al., 2019). The VH and VV backscatter reaches the maximum at flowering; during this stage, there is no more increase in the biomass as the maize develops grains and the radar backscatter saturates as a result of the tasselling stage. An abrupt decrease in the backscatter is then observed at the harvest date.

At VV/VH a similar pattern is observed in both crops with increasing backscatter from LandPrep reaching a maximum at CropEDate when the backscatter starts to decrease again until at the flowering stage. In maize, the backscatter starts to increase again from the flowering stage while in the rice crop a stable trend is observed in the VV/VH ratio after the flowering stage until reaching the HarvestDate (Figure 4.5). Figure 5.2 shows the growth stages of maize from plant emergence to harvesting.

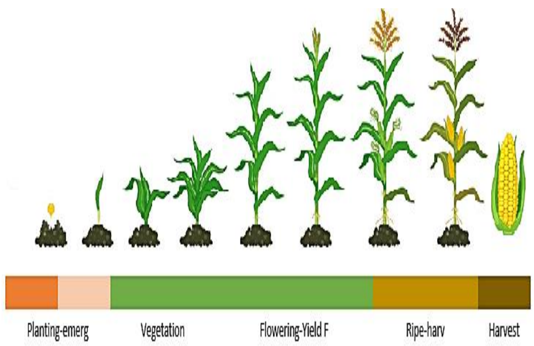

Figure 5. 2 Growth stages of maize

In terms of understanding the temporal variation of the radar backscatter responses (in VH, VV and VV/VH ratio) and answering the research question one, the results indicate that the radar backscatter is susceptible to changes in crop structure. Therefore**,** average backscatter (dB) values are appropriate to monitor and detect the growth stages of rice and maize and subsequently discriminate them at various stages. This observation is consistent with the one made by Aobpaet, (2022) when monitoring the growth stages of crops using Sentinel-1 SAR data. The results show that the VH and VV/VH are suitable for discriminating between rice and maize and could identify the different growth stages. This can be attributed to the sensitivity of the VH and VV/VH to variation in vegetation dynamics. In addition, the backscattering coefficient in the VH polarization accurately distinguishes the phenological stages of the studied crop types (rice and maize). This result agrees with previous studies (Gao et al., 2013; Umutoniwase and Lee, 2021) which also found that the VH is more sensitive to biological parameters and can be used to identify almost all phenological stages.

5.2. Significance tests

The significance tests (Mann-Whitney U-test) indicate that in the dry season, rice was not significantly different from maize at the four stages in the VH polarization. Similar results were also obtained at the land preparation and crop establishment stage in the VV and VV/VH ratio. A significant difference (p-value <.05) was only observed in the VV polarization and VV/VH ratio at the flowering and harvest stage. In the reviewed literature, most studies (Nasirzadehdizaji et al., 2019; Pandžić et al., 2020; Veloso et. al., 2017) focused mainly on monitoring the phenology and growth dynamics of rice and maize using Sentinel-1 SAR parameters. Very few studies, if not none, have addressed the statistical analysis of the two crops to determine the difference in the backscatter in the different polarizations. However, despite the unsatisfactory results in the VH, previous studies have demonstrated the advantages of the cross-polarized (VH) backscatter in monitoring vegetation phenology (Schlund et al., 2017; Yang et al., 2021). Wang et al. (2022) found that the VH channel was more sensitive to maize growth, especially at the early stages than the VV polarization. A study by Abdikan et al., (2018) found high correlation coefficients in the early stages of maize development between SAR backscatter and the plant height as opposed to later growth stages.

One possible explanation for the results at crop establishment is that at this stage, the radar backscatter coefficients in both VH and VV polarization is that of wet soil. Although almost 60% of the rice fields were transplanted rice, the rice plant at this stage is small, coming from the nursery with a small canopy. Therefore, with regard to the VH channel and the crop establishment stage in VV and VV/VH ratio, the first Null hypothesis (1. Ho) was accepted; this could indicate it is difficult to discriminate these crops at this stage. On the contrary, significant results were observed in the VV and VV/VH ratio at the flowering and harvest stages. This could be attributed to the morphology of the maize. The VV for rice showed a downward trend in the time series due to the vertical structure as a result of tillering, which could explain the difference. The backscatter difference was also significant in the VV/VH only. Based on these results, (1.Ho) was rejected and concluded that there was a significant difference in the temporal backscatter behaviour of the two crop types; rice and maize could be discriminated at flowering and harvest stages.

5.3. Extracted SAR metrics

The SAR metrics in VH, VV and VV/VH ratio accurately discriminated between rice and maize at the various growth stages. The backscattering intensity and the temporal profiles in VH and VV/VH ratio capture the different growth stages of rice and maize. Therefore, the extracted SAR metrics correspond to the different phenological stages of the crops. This observation is in line with the findings by Khabbazan et al. (2019) who showed that morphological and biomass changes related to crop growth during the growing season have an influence on the backscattering signal. Results from the significance tests indicate that the flowering stage and the harvest date (in VV and VV/VH) and the backscatter difference in the cross polarization ratio are relevant in discriminating rice from maize in the study area. Therefore, the second Null hypothesis (2. Ho) was rejected; this could mean that the SAR metrics are associated with crop development. However, for the VV polarization for rice growth, a decreasing trend in the time series was observed. This finding is in agreement with the study by Phan et al. (2021) who attributed this peculiarity to differences in cultural practices. Similar results were also observed in the maize time series (Wang et al., 2022) who concluded that the vertical polarization wave is easily affected in the VV due to the vertical structure of the maize plant.

5.4. Accurcy assessment and evaluation of SVM model performance

The discrimination results showed that the overall accuracy of the SVM model using only significant features in VV and VV/VH was acceptable (OA = 83.9%, Kappa = 0.66). The sensitivity of the microwave signals to the geometrical characteristics and dielectric properties of crops provides information suitable to monitor and subsequently discriminate crops at various growth stages. As can been noticed, this was the highest classification result achieved by the SVM model. The performance of the specific growth stages to discriminate between the two crops was determined by the P.A. and O.A. (Chang et. al., 2021).

Comparing the results of crop discrimination at early stages (crop establishment) and later stages (flowering and harvest), Table 5.1, it can be observed that crop establishment had the highest overall accuracy (O.A = 80.6%, Kappa = 0.58). The produce and user accuracy achieved over 80% and 70% , respectively at both the early and late stages of growth. Therefore, the third Null hypothesis (3.Ho), was rejected; this could mean that the extracted phenological information had an influence on the outcome of the classification. This result may come from the fact that the sensitivity of the radar backscatter to variation of vegetation dynamics at different stages. Nasirzadehdizaji et. al., (2019) when analysing the sensitivity of multi-temporal Sentinel-1 SAR parameters to crop height and canopy coverage, observed that at early stages of maize development, the SAR backscatter is more sensitive to crop height compared to later stages. A similar observation was made by Abdikan et al. (2018) who attributed this phenomenon of maize growth to reduced SAR penetration as a result of canopy closure. In relation to rice growth similar findings were made by Kushwaha et al. (2022). This can be observed in the obtained P.A. and U.A. for rice (Table 5.1).

Table 5. 1 Summary of crop discrimination accuracy of the proposed SAR metrics. The P.A, U.A. and O.A. represent the producer accuracy, user accuracy and the overall accuracy, respectively.

No.	Stage/Approach	Rice		Maize		O.A. (%)	Kappa
		P.A. (%)	U.A. (%)	P.A. (%)	U.A. (%)		
1.	Significant features only	89	85	75	82	83.9	0.66
2.	All features	84	84	75	75	80.6	0.59
3.	Crop Establishment Date	89	81	67	80	80.6	0.58
4.	Flowering	89	74	50	75	74.2	0.42
5.	Harvest Date	84	70	42	63	67.7	0.28

The discrimination of rice and maize at the harvest stage had the lowest overall accuracy (O.A. = 67.7%, Kappa = 0.28). This can be explained by the poor sensitivity of SAR backscatter coefficients to crop biophysical parameters at late phenological stages due to a decline in water content in both the soil and vegetation and the gradual drying of the plants as demonstrated by previous studies (Abdikan et al., 2018; Khabbazan et al. 2019; Pandžić et. al. 2020). These studies demonstrated that estimating the harvesting date is challenging.

Interestingly, the overall accuracy improved when all the features were used for crop discrimination (O.A. = 80.6%, Kappa = 0.59).This can be attributed to rich information content due to longer time series of data that improve crop classification (Tuvdendorj et al., 2022). Chakhar et al. (2021) and Wang et. al. (2022) observed that the integration of both cross-polarization (VH) and co-polarization (VV) in agriculture applications enables the extraction of additional information about crop characteristics. Therefore, the fourth Null hypothesis (4.Ho) was rejected; different overall classification accuracy exists at the different growth stages.

5.5. Mapping the distribution of crop types in the study area

Mapping of the distribution of crop types in the study area was based on the discrimination of crop types following the implemented approach (Table 5.1). Due to the limited number of samples (31 samples) for developing and validating the model, the leave-one-out cross-validation approach was used to train and test the SVM model (Kearns & Ron, 1999), with a total number of iterations equal to the sample size (31). Unlike using a separate sample of comparable size which further limits sample size, this method yields an unbiased estimate of the classification accuracy. The maps (Figure 4.13 – 4.16) show the distribution of the crop types in the study area during the 2019 growing season based on the SVM model validation and field observation. The tuning parameter chosen was critical because it determines whether the model underfits or overfits the data (Gareth et al., 2013). The tuning of the hyperparameter for the SVM model could result in overfitting or underfitting of the model, and these affect the classification outcome. The limited sample size used were few to make a conclusive statistical analysis.

5.6. SAR satellite images, field survey data and ancillary data

This study used time series Sentinel-1 Synthetic Aperture Radar (SAR) data as the major data source information on the phenological status and development of rice and maize in the study area. SAR data is increasingly being used for crop monitoring and accurate agriculture management. Due to its unique advantages, the time series SAR data is less affected by weather conditions and the penetration capability into the vegetation canopy enables to obtaining structural information about natural targets. This characteristic provides various unique opportunity to monitor agricultural crops at high temporal and spatial resolutions. As the agricultural landscapes are very dynamic and marked by significant variation at short time intervals throughout the growing season (Bargiel, 2017), Sentinel-1 images were ideal and adequate to monitor changes at different stages. In addition, SAR is sensitive to the structural and dielectric properties of the target surface, which has proven ability in crop monitoring, including phenology estimation and crop-type mapping. However, as the fields in the study area were at different phenological stages on the same SAR image acquisition date due to different cultural practices (sowing and transplanting date) this presented challenges in the extraction of backscatter. The reported growth stages by the farmers did not coincide exactly with the time of SAR image acquisition, therefore the few extracted SAR backscatter coincided with the reported growth stages. Additionally, for maize only two stages were reported by the farmers. In future field survey data should be collected (or fields selected) synchronously to important crop phenological stages and satellite pass dates in the study area. This should ensure that ground data covers important phenological stages based on the Biologische Bundesanstalt, Bundessortenamt and CHemical industry (BBCH) general scale (Meier et al., 2009).

This study benefited from an existing dataset made available by the International Rice Research Institute (IRRI) as part of the Pest and Disease Risk Identification and Management (PRIME) project. The provided field survey data was considered limited for the selected area of focus. Although various information were collected during farmer interviews, the presented data were considered to be inadequate for the current study. Firstly the total number of samples that had the crops of interest, rice and maize, were limited. As rice is the major crop cultivated in the study area, there were more samples compared to the other crops. Therefore, the selected fields were only 31, whereas maize was only cultivated in 12 fields during the 2019 growing season. In addition, there could be some unconscious bias/errors in reporting the dates by the farmers. It could be possible that some farmers may have forgotten the exact dates when the events took place or reported incorrect information by mistake.

Despite the limitation being overcome with the use of cross-validation, the distribution of the data presented challenges in filtering outliers. Few samples at different growth stages were considered outliers (Figure 4.12). However, due to limited samples, these were also considered in the subsequent analysis as SVM is considered to be robust to outliers. Additionally, as the initial focus of the data collection was on the identification of pests and disease risks, it was observed that more focus was placed on rice. In this regard, various growth stages and other management information were available for rice compared to maize. For instance, only crop establishment and harvest dates were recorded for maize.

The returned signal towards the satellite antenna is influenced by dielectric properties. In the study area, monthly climatology data showing the annual variation of monthly mean, maximum and minimum temperature, and the monthly precipitation over a 29 year period was used to get a general overview of the effects of temperature and rainfall on the backscatter. However, in future studies, daily temperature and rainfall data could be incorporated to fully understand the variation in the temporal backscatter of the different crops.

5.7. Limitations and Recommendations

5.7.1. Limitations

The study has demonstrated the potential of using Sentinel-1 time series SAR data to discriminate between rice and maize at different phenological stages. During the current study however, some limitations highlighted below were observed that could constrain the extent to which the findings could be generalized outside the study circumstances.

Limitation of Sample size – The sample size of both rice and maize was limited, 31 observations altogether. Although validation methodology such as Leave-one-out cross-validation was used to overcome the limitation of the sample size, a normally distributed sample size is required to filter out any outliers. In future, there is a need to have more samples that could be used as an independent site (with similar conditions) to check the performance of the model before the algorithm can be generalised to other areas.

Extraction of growth stages and land management practices – In the provided survey data, the focus was placed on rice which had various growth stages and land management practices reported. The land preparation dates, harvest dates and growth stages, including crop establishment dates and flowering dates, were reported. On the contrary, for maize, only crop establishment and harvest dates were reported. The flowering stage for maize was therefore inferred from the crop development while the land preparation was taken as the date before crop establishment. This could have introduced some errors.

Limitation of field survey data and Remote Sensing – The reported dates of the field event and the acquisition of the images were not exactly the same. In most cases, the dates were considered after the event had taken place. For instance, crop established date for some fields could not occur on the exact image and therefore the image after was considered for extraction of backscatter. In future, field survey information should be collected (or fields selected) synchronously to important crop phenological stages and satellite pass dates in the study area. This should ensure that ground data covers important phenological stages based on the BBCH general scale.

5.7.2. Recommendations

Based on the findings of the research, the following recommendations are proposed for future work regarding the discrimination of crop types using time series SAR data.

1. Considering the importance of maize for food security in the study area, further work should aim to increase the sample size to further refine the methodology.
2. The future field survey focusing on crop discrimination should ensure that consistent growth development stages are obtained for crops.
3. The classification was performed at the field-level, however, future work should consider analysing crop discrimination accuracies outside the field or parcel boundaries

6. CONCLUSION

The current study evaluated the performance of one of the commonly used nonparametric classifier (SVM) using SAR time series data and the incorporation of relevant phenological information in discriminating crop types in the study area. This research has demonstrated the potential of SAR time series in discriminating rice from maize at different growth development phases. It was established that the crop types (rice and maize) could be accurately classified at early (crop establishment phase) and at later growth stages (flowering and harvest). Reasonable accuracies were obtained at both stages, although many misclassifications occurred at later stages, flowering and harvest stages. The study defined relevant growth stages for detecting the discrimination between rice and maize crops in the study area. Although, the statistical test (significance tests) showed that some stages were not significant, e.g. crop establishment in both VH and VV as well as their ratio, the introduction of these features improved the classification accuracies of the model. This confirms that the integration of both polarizations provides extra information content that accurately captures the differences that exist during the growth stages. Therefore, this study analysed the contribution of phenological information to the improvement of crop discrimination. Unlike using a stack of images taken during the whole vegetation season, we leveraged phenological information at different stages of crop development into the classification scheme. The SVM model at different growth stages showed promising results. The main finding from this research is that the average backscatter (dB) values are appropriate to monitor and detect the growth stages of rice and maize and subsequently discriminate the two crops at various stages. However, there is a need to repeat the method with a larger sample size to make a conclusive analysis and generalization of results to other areas.

The specific conclusions of the study based on the research questions are highlighted below:-

i. **How are the crop-specific temporal profiles in the study area?**

These results showed that there were significant differences in the temporal backscatter between rice and maize at flowering and harvest stages in the VV and VV/VH channels. The significance test results from the Mann-Whitney U-test showed p-values of .007 and .043 in the VV and VV/VH polarization, respectively at the flowering stage. At harvest the results show p-values of .039 in VV channel and $<.001$in the VV/VH. However, no significant difference (p-value $<.05$) was observed at the early stages of crop development in all polarizations.

ii. **Which SAR metrics from the Sentinel-1 time series data are relevant for discriminating crop types (rice and maize) in the study area?**

The SAR metrics in VH, VV and VV/VH ratio accurately discriminated between rice and maize at the various growth stages. At the crop establishment date (minimum backscatter), the classification accuracy of 80.6% and Kappa = 0.58 was obtained. However, in later stages of crop growth despite acceptable accuracy achieved at flowering (OA = 74.2%, Kappa = 0.42) and harvest stage (OA = 67.7%, Kappa = 0.28), 50% of the maize were misclassified. When using SAR metrics with significant results from the Mann-Whitney U-test, overall accuracy of 83.9% and Kappa = 0.66 was obtained. Similar results were also achieved when all the SAR metrics where used, including crop duration (OA = 80.6% and Kappa = 0.59). However, the implication of the last two options is that the discrimination of crops has to be performed later in the growth cycle which is not appropriate for management purposes.

iii. **How can the SVM classification algorithm leverage phenological information from the time series data?**

The fields in the study area were at different phenological stages on the same SAR image acquisition date due to different sowing and management practices. This offers an opportunity to discriminate crop types at various stages. However, instead of using a stack of the images taken during the whole growing season, phenological information at different growth stages (SAR metrics) were extracted and used as input into the model.

iv. Which growth stage gives higher accuracy in discriminating crop types in the different growing seasons?

The discrimination of crop types at the crop establishment stage yielded highest overall accuracy (OA = 80.6%, Kappa = 0.58) compared to later stages of the growth cycle (flowering OA = 74.2%, Kappa = 0.42 and harvesting stage OA = 67.7%, Kappa = 0.28).

v. **How can Sentinel-1 time series data be used to map the distribution of the crop types within the 2019 growing season in the study area?**

The developed SVM model was used to classify the crop types and map the distribution at the field-level. The distribution was based on the different growth stages. It was observed from the produced maps that the crop types were clustered in specific areas. This could be attributed to the availability of irrigation facilities or rainfall for rainfed rice and maize.

7. LIST OF REFERENCES

Abdikan, S., Sekertekin, A., Ustunern, M., Balik Sanli, F., Nasirzadehdizaji, R., 2018. Backscatter analysis using multi-temporal Sentinel-1 SAR data for Crop growth of Maize in Konya Basin, Turkey. Int. Arch. Photogramm. Remote Sens. Spat. Inf. Sci. - ISPRS Arch. 42, 9–13. https://doi.org/10.5194/isprs-archives-XLII-3-9-2018

Altoveros, N.C., Borromeo, T.H., 2007. Country Report on the State of Plant Genetic Resources for Food and Agriculture of the Philippines (1997-2006) 1–71.

Aobpaet, A., 2022. Monitoring of crop growth stages using Sentinel-1 synthetic aperture radar data. Agric. Nat. Resour. 56. https://doi.org/10.34044/j.anres.2022.56.2.09

Asilo, S., de Bie, K., Skidmore, A., Nelson, A., Barbieri, M., Maunahan, A., 2014. Complementarity of two rice mapping approaches: Characterizing strata mapped by hypertemporal MODIS and rice paddy identification using multitemporal SAR. Remote Sens. 6, 12789–12814. https://doi.org/10.3390/rs61212789

Atzberger, C., Rembold, F., 2013. Mapping the spatial distribution of winter crops at sub-pixel level using AVHRR NDVI time series and neural nets. Remote Sens. 5, 1335–1354. https://doi.org/10.3390/rs5031335

Bargiel, D., 2017. A new method for crop classification combining time series of radar images and crop phenology information. Remote Sens. Environ. 198, 369–383. https://doi.org/10.1016/j.rse.2017.06.022

Bargiel, D., Herrmann, S., 2011. Multi-temporal land-cover classification of agricultural areas in two European regions with high resolution spotlight TerraSAR-X data. Remote Sens. 3, 859–877. https://doi.org/10.3390/rs3050859

Barrett, B., Nitze, I., Green, S., Cawkwell, F., 2014. Assessment of multi-temporal, multi-sensor radar and ancillary spatial data for grasslands monitoring in Ireland using machine learning approaches. Remote Sens. Environ. 152, 109–124. https://doi.org/10.1016/j.rse.2014.05.018

Beckman, J., Countryman, A.M., 2021. The Importance of Agriculture in the Economy: Impacts from COVID-19. Am. J. Agric. Econ. 103, 1595–1611. https://doi.org/10.1111/ajae.12212

Boschetti, M., Busetto, L., Manfron, G., Laborte, A., Asilo, S., Pazhanivelan, S., Nelson, A., 2017. PhenoRice: A method for automatic extraction of spatio-temporal information on rice crops using satellite data time series. Remote Sens. Environ. 194, 347–365. https://doi.org/10.1016/j.rse.2017.03.029

Briones, N.D., 2005. Environmental Sustainability Issues in Nicaragua. Asian J. Agric. Dev. 2, 67–78.

Bruzzone, L., Liu, S., Bovolo, F., Du, P., 2016. Change detection in multitemporal hyperspectral images. Remote Sens. Digit. Image Process. 20, 63–88. https://doi.org/10.1007/978-3-319-47037-5_4

Burges, C.J.C., 1998. A tutorial on support vector machines for pattern recognition. Data Min. Knowl. 2, 121–167.

Chakhar, A., Hernández-López, D., Ballesteros, R., Moreno, M.A., 2021. Improving the accuracy of multiple algorithms for crop classification by integrating sentinel-1 observations with sentinel-2 data. Remote Sens. 13, 1–21. https://doi.org/10.3390/rs13020243

Chang, L., Chen, Y.T., Wang, J.H., Chang, Y.L., 2021. Rice-field mapping with sentinel-1a sar time-series data. Remote Sens. 13, 1–25. https://doi.org/10.3390/rs13010103

Chen, C., Mcnairn, H., 2006. A neural network integrated approach for rice crop monitoring. Int. J. Remote Sens. 27, 1367–1393. https://doi.org/10.1080/01431160500421507

Chen, C.F., Son, N.T., Chen, C.R., Chang, L.Y., Chiang, S.H., 2016. Rice crop mapping using Sentinel-1A phenological metrics. Int. Arch. Photogramm. Remote Sens. Spat. Inf. Sci. - ISPRS Arch. 41, 863–865. https://doi.org/10.5194/isprsarchives-XLI-B8-863-2016

Chen, J., Jönsson, P., Tamura, M., Gu, Z., Matsushita, B., Eklundh, L., 2004. A simple method for reconstructing a high-quality NDVI time-series data set based on the Savitzky-Golay filter. Remote Sens. Environ. 91, 332–344. https://doi.org/10.1016/j.rse.2004.03.014

Chen, Y., Lu, D., Moran, E., Batistella, M., Dutra, L.V., Sanches, I.D.A., da Silva, R.F.B., Huang, J., Luiz, A.J.B., de Oliveira, M.A.F., 2018. Mapping croplands, cropping patterns, and crop types using MODIS time-series data. Int. J. Appl. Earth Obs. Geoinf. 69, 133–147. https://doi.org/10.1016/j.jag.2018.03.005

Clauss, K., Ottinger, M., Kuenzer, C., 2018. Mapping rice areas with Sentinel-1 time series and superpixel segmentation. Int. J. Remote Sens. 39, 1399–1420. https://doi.org/10.1080/01431161.2017.1404162

Clauss, Kersten, Ottinger, M., Leinenkugel, P., Kuenzer, C., 2018. Estimating rice production in the Mekong Delta, Vietnam, utilizing time series of Sentinel-1 SAR data. Int. J. Appl. Earth Obs. Geoinf. 73, 574–585. https://doi.org/10.1016/j.jag.2018.07.022

Congalton, R.G., 2001. Accuracy assessment and validation of remotely sensed and other spatial information. Int. J. Wildl. Fire 10, 321–328. https://doi.org/10.1071/wf01031

Congalton, R.G., 1991. A review of assessing the accuracy of classifications of remotely sensed data. Remote Sens. Environ. 37, 35–46. https://doi.org/10.1016/0034-4257(91)90048-B

Congalton, R.G., Green, K., 2019. Assessing the accuracy of remotely sensed data: principles and practices. CRC press.

Cortes, C., Vapnik, V., 1995. Support-vector networks. Mach. Learn. 20, 273–297. https://doi.org/10.1007/BF00994018

D'Andrimont, R., Verhegghen, A., Lemoine, G., Kempeneers, P., Meroni, M., van der Velde, M., 2021. From parcel to continental scale – A first European crop type map based on Sentinel-1 and LUCAS Copernicus in-situ observations. Remote Sens. Environ. 266. https://doi.org/10.1016/j.rse.2021.112708

De Beurs, K.M., Henebry, G.M., 2005. Land surface phenology and temperature variation in the International Geosphere-Biosphere Program high-latitude transects. Glob. Chang. Biol. 11, 779–790. https://doi.org/10.1111/j.1365-2486.2005.00949.x

Del Frate, F., Schiavon, G., Solimini, D., Borgeaud, M., Hoekman, D.H., Vissers, M.A.M., 2003. Crop classification using multiconfiguration C-band SAR data. IEEE Trans. Geosci. Remote Sens. 41, 1611–1619. https://doi.org/10.1109/TGRS.2003.813530

Dela Torre, D.M.G., Gao, J., Macinnis-Ng, C., Shi, Y., 2021. Phenology-based delineation of irrigated and rain-fed paddy fields with Sentinel-2 imagery in Google Earth Engine. Geo-Spatial Inf. Sci. 00, 1–16. https://doi.org/10.1080/10095020.2021.1984183

Dey, S., Mandal, D., Robertson, L.D., Banerjee, B., Kumar, V., McNairn, H., Bhattacharya, A., Rao, Y.S., 2020. In-season crop classification using elements of the Kennaugh matrix derived from polarimetric RADARSAT-2 SAR data. Int. J. Appl. Earth Obs. Geoinf. 88, 102059. https://doi.org/10.1016/j.jag.2020.102059

Dikitanan, R., Grosjean, G., Leyte, J., Nowak, A., 2017. Climate-Resilient Agriculture (CRA) in Philippines. CSA Ctry. Profiles Asia Ser. 24p.

Dingle Robertson, L., Davidson, A., McNairn, H., Hosseini, M., Mitchell, S., De Abelleyra, D., Verón, S., Cosh, M.H., 2020. Synthetic Aperture Radar (SAR) image processing for operational space-based agriculture mapping. Int. J. Remote Sens. 41, 7112–7144. https://doi.org/10.1080/01431161.2020.1754494

FAO, 2017. The future of food and agriculture: trends and challenges, The future of food and agriculture: trends and challenges. Rome.

FAO, 2016. Crop Yield Forecasting: Methodological and Institutional Aspects 241.

FAO, IFAD, UNICEF, WFP, WHO, 2021. The State of Food Security and Nutrition in the World 2021: Transforming food systems for food security, improved nutrition and affordable healthy diets for all., Fao.

FAO, IFAD, UNICEF, WFP, WHO, 2018. Food Security and Nutrition in the World the State of Building Climate Resilience for Food Security and Nutrition.

FAO, IFAD, UNICEF, WHO, WEP, 2020. The State of Food Security and Nutrition in the World 2020, The State of Food Security and Nutrition in the World 2020. Transformaing food systems for affordable healthy diets. FAO, Rome. https://doi.org/10.4060/ca9692en

Fikriyah, V.N., Darvishzadeh, R., Laborte, A., Khan, N.I., Nelson, A., 2019. Discriminating transplanted and direct seeded rice using Sentinel-1 intensity data. Int. J. Appl. Earth Obs. Geoinf. 76, 143–153. https://doi.org/10.1016/j.jag.2018.11.007

Fisette, T., Rollin, P., Aly, Z., Campbell, L., Daneshfar, B., Filyer, P., Smith, A., Davidson, A., Shang, J.,

Jarvis, I., 2013. AAFC annual crop inventory, in: 2013 Second International Conference on Agro-Geoinformatics (Agro-Geoinformatics). IEEE, pp. 270–274. https://doi.org/10.1109/Argo-Geoinformatics.2013.6621920
Foody, G.M., Mathur, A., 2004. A relative evaluation of multiclass image classification by support vector machines. IEEE Trans. Geosci. Remote Sens. 42, 1335–1343. https://doi.org/10.1109/TGRS.2004.827257
Forkuor, G., Conrad, C., Thiel, M., Ullmann, T., Zoungrana, E., 2014. Integration of optical and synthetic aperture radar imagery for improving crop mapping in northwestern Benin, West Africa. Remote Sens. 6, 6472–6499. https://doi.org/10.3390/rs6076472
Gao, S., Niu, Z., Huang, N., Hou, X., 2013. Estimating the Leaf Area Index, height and biomass of maize using HJ-1 and RADARSAT-2. Int. J. Appl. Earth Obs. Geoinf. 24, 1–8. https://doi.org/10.1016/j.jag.2013.02.002
Gardener, M., 2012. Statistics for ecologists using R and Excel. Pelagic Publishing, Exeter.
Gareth, J., Daniela, W., Trevor, H., Robert., T., 2013. An Introduction to Statistical Learning: with applications in R, Current Medicinal Chemistry, Springer Texts in Statistics. Springer New York, New York, NY. https://doi.org/10.1007/978-1-4614-7138-7
Gella, G.W., Bijker, W., Belgiu, M., 2021. Mapping crop types in complex farming areas using SAR imagery with dynamic time warping. ISPRS J. Photogramm. Remote Sens. 175, 171–183. https://doi.org/10.1016/j.isprsjprs.2021.03.004
Gillespie, T.W., Foody, G.M., Rocchini, D., Giorgi, A.P., Saatchi, S., 2008. Measuring and modelling biodiversity from space. Prog. Phys. Geogr. 32, 203–221. https://doi.org/10.1177/0309133308093606
Godfray, H.C.J., Beddington, J.R., Crute, I.R., Haddad, L., Lawrence, D., Muir, J.F., Pretty, J., Robinson, S., Thomas, S.M., Toulmin, C., 2010. Food security: The challenge of feeding 9 billion people. Science (80-.). https://doi.org/10.1126/science.1185383
Guarini, R., Bruzzone, L., Santoni, M., Vuolo, F., Dini, L., 2016. Analysis of the potentiality of multi-temporal COSMO-SkyMed ® data for classifying summer crops, in: 2016 IEEE International Geoscience and Remote Sensing Symposium (IGARSS). IEEE, pp. 3170–3173. https://doi.org/10.1109/IGARSS.2016.7729820
Hua, L., Wang, H., Sui, H., Wardlow, B., Hayes, M.J., Wang, J., 2019. Mapping the spatial-temporal dynamics of vegetation response lag to drought in a semi-arid region. Remote Sens. 11. https://doi.org/10.3390/rs11161873
Huang, C., Davis, L.S., Townshend, J.R.G., 2002. An assessment of support vector machines for land cover classification. Int. J. Remote Sens. 23, 725–749. https://doi.org/10.1080/01431160110040323
Inglada, J., Arias, M., Tardy, B., Hagolle, O., Valero, S., Morin, D., Dedieu, G., Sepulcre, G., Bontemps, S., Defourny, P., Koetz, B., 2015. Assessment of an operational system for crop type map production using high temporal and spatial resolution satellite optical imagery. Remote Sens. 7, 12356–12379. https://doi.org/10.3390/rs70912356
Jia, K., Li, Q., Tian, Y., Wu, B., Zhang, F., Meng, J., 2012. Crop classification using multi-configuration SAR data in the North China Plain. Int. J. Remote Sens. 33, 170–183. https://doi.org/10.1080/01431161.2011.587844
Karthikeyan, L., Chawla, I., Mishra, A.K., 2020. A review of Remote Sensing applications in agriculture for food security: Crop growth and yield, irrigation, and crop losses. J. Hydrol. 586, 124905. https://doi.org/10.1016/j.jhydrol.2020.124905
Kearns, M., Ron, D., 1999. Algorithmic Stability and Sanity-Check Bounds for Leave-One-Out Cross-Validation. Neural Comput. 11, 1427–1453. https://doi.org/10.1162/089976699300016304
Khabbazan, S., Vermunt, P., Steele-Dunne, S., Arntz, L.R., Marinetti, C., van der Valk, D., Iannini, L., Molijn, R., Westerdijk, K., van der Sande, C., 2019. Crop monitoring using Sentinel-1 data: A case study from The Netherlands. Remote Sens. 11, 1–24. https://doi.org/10.3390/rs11161887
Khan, M.R., de Bie, C.A.J.M., van Keulen, H., Smaling, E.M.A., Real, R., 2010. Disaggregating and mapping crop statistics using hypertemporal Remote Sensing. Int. J. Appl. Earth Obs. Geoinf. 12, 36–46. https://doi.org/10.1016/j.jag.2009.09.010
Khosravi, I., Alavipanah, S.K., 2019. A random forest-based framework for crop mapping using temporal, spectral, textural and polarimetric observations. Int. J. Remote Sens. 40, 7221–7251. https://doi.org/10.1080/01431161.2019.1601285

Kobayashi, N., Tani, H., Wang, X., Sonobe, R., 2020. Crop classification using spectral indices derived from Sentinel-2A imagery. J. Inf. Telecommun. 4, 67–90. https://doi.org/10.1080/24751839.2019.1694765

Koide, N., Robertson, A.W., Ines, A.V.M., Qian, J.H., Dewitt, D.G., Lucero, A., 2013. Prediction of rice production in the Philippines using seasonal climate forecasts. J. Appl. Meteorol. Climatol. 52, 552–569. https://doi.org/10.1175/JAMC-D-11-0254.1

Kushwaha, A., Dave, R., Kumar, G., Saha, K., Khan, A., 2022. Assessment of rice crop biophysical parameters using Sentinel-1 C-band SAR data. Adv. Sp. Res. https://doi.org/10.1016/j.asr.2022.02.021

Legaspi, R.M.B., Toribio, E.C.B., Yohanon, E.P.L., Predo, C.D., Vergara, D.G.K., 2021. Assessing the profitability and sustainability of upland farming systems in Cambantoc subwatershed, Philippines. IOP Conf. Ser. Earth Environ. Sci. 892, 012066. https://doi.org/10.1088/1755-1315/892/1/012066

Li, H., Zhang, C., Zhang, S., Atkinson, P.M., 2020. Crop classification from full-year fully-polarimetric L-band UAVSAR time-series using the Random Forest algorithm. Int. J. Appl. Earth Obs. Geoinf. 87, 102032. https://doi.org/10.1016/j.jag.2019.102032

Liu, C. an, Chen, Z. xin, Shao, Y., Chen, J. song, Hasi, T., PAN, H. zhu, 2019. Research advances of SAR Remote Sensing for agriculture applications: A review. J. Integr. Agric. 18, 506–525. https://doi.org/10.1016/S2095-3119(18)62016-7

Lloyd, D., 1990. A phenological classification of terrestrial vegetation cover using shortwave vegetation index imagery. Int. J. Remote Sens. 11, 2269–2279. https://doi.org/10.1080/01431169008955174

López-Lozano, R., Duveiller, G., Seguini, L., Meroni, M., García-Condado, S., Hooker, J., Leo, O., Baruth, B., 2015. Towards regional grain yield forecasting with 1km-resolution EO biophysical products: Strengths and limitations at pan-European level. Agric. For. Meteorol. 206, 12–32. https://doi.org/10.1016/j.agrformet.2015.02.021

Löw, F., Michel, U., Dech, S., Conrad, C., 2013. Impact of feature selection on the accuracy and spatial uncertainty of per-field crop classification using Support Vector Machines. ISPRS J. Photogramm. Remote Sens. 85, 102–119. https://doi.org/10.1016/j.isprsjprs.2013.08.007

Lu, D., Weng, Q., 2007. A survey of image classification methods and techniques for improving classification performance. Int. J. Remote Sens. 28, 823–870. https://doi.org/10.1080/01431160600746456

Ma, T., Han, L., Liu, Q., 2021. Retrieving the Soil Moisture in Bare Farmland Areas Using a Modified Dubois Model. Front. Earth Sci. 9, 1–14. https://doi.org/10.3389/feart.2021.735958

Mansaray, L.R., Kabba, V.T.S., Zhang, L., Bebeley, H.A., 2021. Optimal multi-temporal Sentinel-1A SAR imagery for paddy rice field discrimination; a recommendation for operational mapping initiatives. Remote Sens. Appl. Soc. Environ. 22, 100533. https://doi.org/10.1016/j.rsase.2021.100533

Mantovani, R.G., Rossi, A.L.D., Vanschoren, J., Bischl, B., De Carvalho, A.C.P.L.F., 2015. Effectiveness of Random Search in SVM hyper-parameter tuning. Proc. Int. Jt. Conf. Neural Networks 2015-Septe. https://doi.org/10.1109/IJCNN.2015.7280664

Mascolo, L., Lopez-Sanchez, J.M., Vicente-Guijalba, F., Nunziata, F., Migliaccio, M., Mazzarella, G., 2016. A Complete Procedure for Crop Phenology Estimation with PolSAR Data Based on the Complex Wishart Classifier. IEEE Trans. Geosci. Remote Sens. 54, 6505–6515. https://doi.org/10.1109/TGRS.2016.2585744

Mashaba-Munghemezulu, Z., Chirima, G.J., Munghemezulu, C., 2021. Delineating smallholder maize farms from sentinel-1 coupled with sentinel-2 data using machine learning. Sustain. 13. https://doi.org/10.3390/su13094728

Mather, P., Tso, B., 2016. Classification Methods for Remotely Sensed Data, Paper Knowledge . Toward a Media History of Documents. CRC Press. https://doi.org/10.1201/9781420090741

Maxwell, A.E., Warner, T.A., Fang, F., 2018. Implementation of machine-learning classification in Remote Sensing: An applied review. Int. J. Remote Sens. 39, 2784–2817. https://doi.org/10.1080/01431161.2018.1433343

McNairn, H., Shang, J., 2016. A Review of Multitemporal Synthetic Aperture Radar (SAR) for Crop Monitoring. Multitemporal Remote Sensing, Remote Sens. Digit. Image Process. 20. https://doi.org/10.1007/978-3-319-47037-5_15

Meier, U., Bleiholder, H., Buhr, L., Feller, C., Hack, H., Heß, M., Lancashire, P., Schnock, U., Stauß, R., Van den Boom, T., Weber, E., Zwerger, P., 2009. The BBCH system to coding the phenological growth stages of plants-history and publications. J. für Kult. 61, 41–52. https://doi.org/10.5073/JfK.2009.02.01

Meroni, M., d'Andrimont, R., Vrieling, A., Fasbender, D., Lemoine, G., Rembold, F., Seguini, L., Verhegghen, A., 2021b. Comparing land surface phenology of major European crops as derived from SAR and multispectral data of Sentinel-1 and -2. Remote Sens. Environ. 253. https://doi.org/10.1016/j.rse.2020.112232

Mingwei, Z., Qingbo, Z., Zhongxin, C., Jia, L., Yong, Z., Chongfa, C., 2008. Crop discrimination in Northern China with double cropping systems using Fourier analysis of time-series MODIS data. Int. J. Appl. Earth Obs. Geoinf. 10, 476–485. https://doi.org/10.1016/j.jag.2007.11.002

Mondal, S., Jeganathan, C., 2018. Mountain agriculture extraction from time-series MODIS NDVI using dynamic time warping technique. Int. J. Remote Sens. 39, 3679–3704. https://doi.org/10.1080/01431161.2018.1444289

Moron, V., Lucero, A., Hilario, F., Lyon, B., Robertson, A.W., DeWitt, D., 2009. Spatio-temporal variability and predictability of summer monsoon onset over the Philippines. Clim. Dyn. 33, 1159–1177. https://doi.org/10.1007/s00382-008-0520-5

Mountrakis, G., Im, J., Ogole, C., 2011. Support vector machines in Remote Sensing: A review. ISPRS J. Photogramm. Remote Sens. 66, 247–259. https://doi.org/10.1016/j.isprsjprs.2010.11.001

Nasirzadehdizaji, R., Sanli, F.B., Abdikan, S., Cakir, Z., Sekertekin, A., Ustuner, M., 2019. Sensitivity analysis of multi-temporal Sentinel-1 SAR parameters to crop height and canopy coverage. Appl. Sci. 9. https://doi.org/10.3390/app9040655

Nelson, A., Setiyono, T., Rala, A., Quicho, E., Raviz, J., Abonete, P., Maunahan, A., Garcia, C., Bhatti, H., Villano, L., Thongbai, P., Holecz, F., Barbieri, M., Collivignarelli, F., Gatti, L., Quilang, E., Mabalay, M., Mabalot, P., Barroga, M., Bacong, A., Detoito, N., Berja, G., Varquez, F., Wahyunto, Kuntjoro, D., Murdiyati, S., Pazhanivelan, S., Kannan, P., Mary, P., Subramanian, E., Rakwatin, P., Intrman, A., Setapayak, T., Lertna, S., Minh, V., Tuan, V., Duong, T., Quyen, N., Van Kham, D., Hin, S., Veasna, T., Yadav, M., Chin, C., Ninh, N., 2014. Towards an Operational SAR-Based Rice Monitoring System in Asia: Examples from 13 Demonstration Sites across Asia in the RIICE Project. Remote Sens. 6, 10773–10812. https://doi.org/10.3390/rs61110773

Nelson, A., Wassmann, R., Sander, B.O., Palao, L.K., 2015. Climate-Determined Suitability of the Water Saving Technology "alternate Wetting and Drying" in Rice Systems: A Scalable Methodology demonstrated for a Province in the Philippines. PLoS One 10, 1–19. https://doi.org/10.1371/journal.pone.0145268

Ngo, K.D., Lechner, A.M., Vu, T.T., 2020. Land cover mapping of the Mekong Delta to support natural resource management with multi-temporal Sentinel-1A synthetic aperture radar imagery. Remote Sens. Appl. Soc. Environ. 17, 100272. https://doi.org/10.1016/j.rsase.2019.100272

Nguyen, D.B., Gruber, A., Wagner, W., 2016. Mapping rice extent and cropping scheme in the Mekong Delta using Sentinel-1A data. Remote Sens. Lett. 7, 1209–1218. https://doi.org/10.1080/2150704X.2016.1225172

Ouzemou, J.E., El Harti, A., Lhissou, R., El Moujahid, A., Bouch, N., El Ouazzani, R., Bachaoui, E.M., El Ghmari, A., 2018. Crop type mapping from pansharpened Landsat 8 NDVI data: A case of a highly fragmented and intensive agricultural system. Remote Sens. Appl. Soc. Environ. 11, 94–103. https://doi.org/10.1016/j.rsase.2018.05.002

Pal, M., Mather, P.M., 2005. Support vector machines for classification in Remote Sensing. Int. J. Remote Sens. 26, 1007–1011. https://doi.org/10.1080/01431160512331314083

Pandžić, M., Ljubii, N., Mimić, G., Pandži, J., Pejak, B., Crnojević, V., 2020. A case study of monitoring maize dynamics in serbia by utilizing sentinel-1 data and growing degree days. ISPRS Ann. Photogramm. Remote Sens. Spat. Inf. Sci. 5, 117–124. https://doi.org/10.5194/isprs-Annals-V-3-2020-117-2020

Pfeil, I., Reub, F., Vreugdenhil, M., Navacchi, C., Wagner, W., 2020. Classification of Wheat and Barley Fields Using Sentinel-1 Backscatter. Int. Geosci. Remote Sens. Symp. 140–143. https://doi.org/10.1109/IGARSS39084.2020.9323560

Phan, H., Le Toan, T., Bouvet, A., 2021. Understanding Dense Time Series of Sentinel-1 Backscatter from Rice Fields: Case Study in a Province of the Mekong Delta, Vietnam. Remote Sens. 13, 921. https://doi.org/10.3390/rs13050921

Ramezan, C., Warner, T., Maxwell, A., 2019. Evaluation of Sampling and Cross-Validation Tuning Strategies for Regional-Scale Machine Learning Classification. Remote Sens. 11, 185. https://doi.org/10.3390/rs11020185

Ramos, M.D., Tendencia, E., Espana, K., Sabido, J., Bagtasa, G., 2016. Assessment of satellite precipitation products in the philippine archipelago. Int. Arch. Photogramm. Remote Sens. Spat. Inf. Sci. - ISPRS Arch. 2016-Janua, 423–427. https://doi.org/10.5194/isprsarchives-XLI-B1-423-2016

Rembold, F., Meroni, M., Urbano, F., Csak, G., Kerdiles, H., Perez-Hoyos, A., Lemoine, G., Leo, O., Negre, T., 2019. ASAP: A new global early warning system to detect anomaly hot spots of agricultural production for food security analysis. Agric. Syst. 168, 247–257. https://doi.org/10.1016/j.agsy.2018.07.002

Sakamoto, T., Gitelson, A.A., Arkebauer, T.J., 2013. MODIS-based corn grain yield estimation model incorporating crop phenology information. Remote Sens. Environ. 131, 215–231. https://doi.org/10.1016/j.rse.2012.12.017

Salehi, B., Daneshfar, B., Davidson, A.M., 2017. Accurate crop-type classification using multi-temporal optical and multi-polarization SAR data in an object-based image analysis framework. Int. J. Remote Sens. 38, 4130–4155. https://doi.org/10.1080/01431161.2017.1317933

Selvaraj, S., Haldar, D., Danodia, A., 2019. Time Series Sentinel-1A Profile Analysis for Heterogeneous Kharif Crops Discrimination in North India. Ursi Ap-Rasc 2019 1–4.

Santoro, M., Wegmüller, U., 2014. Multi-temporal synthetic aperture radar metrics applied to map open water bodies. IEEE J. Sel. Top. Appl. Earth Obs. Remote Sens. 7, 3225–3238. https://doi.org/10.1109/JSTARS.2013.2289301

Schlund, M., Erasmi, S., 2020. Sentinel-1 time series data for monitoring the phenology of winter wheat. Remote Sens. Environ. 246, 111814. https://doi.org/10.1016/j.rse.2020.111814

Schlund, M., Scipal, K., Davidson, M.W.J., 2017. Forest classification and impact of BIOMASS resolution on forest area and aboveground biomass estimation. Int. J. Appl. Earth Obs. Geoinf. 56, 65–76. https://doi.org/10.1016/j.jag.2016.12.001

Sheykhmousa, M., Mahdianpari, M., Ghanbari, H., Mohammadimanesh, F., Ghamisi, P., Homayouni, S., 2020. Support Vector Machine Versus Random Forest for Remote Sensing Image Classification: A Meta-Analysis and Systematic Review. IEEE J. Sel. Top. Appl. Earth Obs. Remote Sens. 13, 6308–6325. https://doi.org/10.1109/JSTARS.2020.3026724

Sibhatu, K.T., Qaim, M., 2017. Rural food security, subsistence agriculture, and seasonality. PLoS One 12, 1–15. https://doi.org/10.1371/journal.pone.0186406

Son, N.T., Chen, C.F., Chen, C.R., Minh, V.Q., 2018. Assessment of Sentinel-1A data for rice crop classification using random forests and support vector machines. Geocarto Int. 33, 587–601. https://doi.org/10.1080/10106049.2017.1289555

Song, P., Mansaray, L.R., Huang, J., Huang, W., 2018. Mapping paddy rice agriculture over China using AMSR-E time series data. ISPRS J. Photogramm. Remote Sens. 144, 469–482. https://doi.org/10.1016/j.isprsjprs.2018.08.015

Song, X.-P., Huang, W., Hansen, M.C., Potapov, P., 2021. An evaluation of Landsat, Sentinel-2, Sentinel-1 and MODIS data for crop type mapping. Sci. Remote Sens. 3, 100018. https://doi.org/10.1016/j.srs.2021.100018

Sonobe, R., Tani, H., Wang, X., Kobayashi, N., Shimamura, H., 2014. Random forest classification of crop type using multioral TerraSAR-X dual-polarimetric data. Remote Sens. Lett. 5, 157–164. https://doi.org/10.1080/2150704X.2014.889863

Stuecker, M.F., Tigchelaar, M., Kantar, M.B., 2018. Climate variability impacts on rice production in the Philippines. PLoS One 13, 1–17. https://doi.org/10.1371/journal.pone.0201426

Tolpekin, V., Stein, A., 2013. The core of GIScience: a system based approach. Faculty of Geo-Information Science and Earth Observation (ITC), University of Twente, Enschede.

Tufail, R., Ahmad, A., Javed, M.A., Ahmad, S.R., 2021. A machine learning approach for accurate crop type mapping using combined SAR and optical time series data. Adv. Sp. Res. https://doi.org/10.1016/j.asr.2021.09.019

Tuvdendorj, B., Zeng, H., Wu, B., Elnashar, A., Zhang, M., Tian, F., Nabil, M., Nanzad, L., Bulkhbai, A., Natsagdorj, N., 2022. Performance and the Optimal Integration of Sentinel-1/2 Time-Series Features for Crop Classification in Northern Mongolia. Remote Sens. 14, 1830. https://doi.org/10.3390/rs14081830

Umutoniwase, N., Lee, S.K., 2021. The Potential of Sentinel-1 SAR Parameters in Monitoring Rice Paddy Phenological Stages in Gimhae, South Korea. Korean J. Remote Sens. 37, 789–802. https://doi.org/10.7780/kjrs.2021.37.4.9

USDA, 2018. Commodity intelligence report. United States Dep. Agric. Foreign Agric. Serv. Rep. 1–9.

Van Tricht, K., Gobin, A., Gilliams, S., Piccard, I., 2018. Synergistic use of radar sentinel-1 and optical sentinel-2 imagery for crop mapping: A case study for Belgium. Remote Sens. 10, 1–22. https://doi.org/10.3390/rs10101642

Varela, R.P., Fernandez, E.V., Degamo, J.R.S., 2013. Agricultural development and habitat change in the Agusan River Basin in Mindanao, Philippines. Int. J. Dev. Sustain. 2, 2020–2030.

Veloso, A., Mermoz, S., Bouvet, A., Le Toan, T., Planells, M., Dejoux, J., Ceschia, E., 2017a. Understanding the temporal behavior of crops using Sentinel-1 and Sentinel-2-like data for agricultural applications. Remote Sens. Environ. 199, 415–426. https://doi.org/10.1016/j.rse.2017.07.015

Veloso, A., Mermoz, S., Bouvet, A., Le Toan, T., Planells, M., Dejoux, J.F., Ceschia, E., 2017b. Understanding the temporal behavior of crops using Sentinel-1 and Sentinel-2-like data for agricultural applications. Remote Sens. Environ. 199, 415–426. https://doi.org/10.1016/j.rse.2017.07.015

Wang, D., Su, Y., Zhou, Q., Chen, Z., 2015a. Advances in research on crop identification using SAR. 2015 4th Int. Conf. Agro-Geoinformatics, Agro-Geoinformatics 2015 312–317. https://doi.org/10.1109/Agro-Geoinformatics.2015.7248111

Wang, D., Zhou, Q., Su, Y., Chen, Z., 2015b. Advances in research on crop identification using SAR, in: 2015 Fourth International Conference on Agro-Geoinformatics (Agro-Geoinformatics). IEEE, pp. 312–317. https://doi.org/10.1109/Agro-Geoinformatics.2015.7248111

Wang, H., Magagi, R., Goïta, K., Trudel, M., McNairn, H., Powers, J., 2019. Crop phenology retrieval via polarimetric SAR decomposition and Random Forest algorithm. Remote Sens. Environ. 231, 111234. https://doi.org/10.1016/j.rse.2019.111234

Wang, Y., Fang, S., Zhao, L., Huang, X., Jiang, X., 2022. Parcel-based summer maize mapping and phenology estimation combined using Sentinel-2 and time series Sentinel-1 data. Int. J. Appl. Earth Obs. Geoinf. 108. https://doi.org/10.1016/j.jag.2022.102720

Wardlow, B.D., Egbert, S.L., 2008. Large-area crop mapping using time-series MODIS 250 m NDVI data: An assessment for the U.S. Central Great Plains. Remote Sens. Environ. 112, 1096–1116. https://doi.org/10.1016/j.rse.2007.07.019

Wei, S., Zhang, H., Wang, C., Wang, Y., Xu, L., 2019. Multi-temporal SAR data large-scale crop mapping based on U-net model. Remote Sens. 11. https://doi.org/10.3390/rs11010068

Weiss, M., Jacob, F., Duveiller, G., 2020. Remote Sensing for agricultural applications: A meta-review. Remote Sens. Environ. 236, 111402. https://doi.org/10.1016/j.rse.2019.111402

World Food Programme, 2021. WFP Philippines Country Achievements Based on the Annual Country Report 2020 1–44.

WorldBank, 2020. Transforming Philippine Agriculture During Covid-19 and Beyond. WorldBank 1–128.

Yang, H., Pan, B., Li, N., Wang, W., Zhang, J., Zhang, X., 2021. A systematic method for spatio-temporal phenology estimation of paddy rice using time series Sentinel-1 images. Remote Sens. Environ. 259, 112394. https://doi.org/10.1016/j.rse.2021.112394

Zeng, L., Wardlow, B.D., Xiang, D., Hu, S., Li, D., 2020. A review of vegetation phenological metrics extraction using time-series, multispectral satellite data. Remote Sens. Environ. 237, 111511. https://doi.org/10.1016/j.rse.2019.111511

Zhang, X., Friedl, M.A., Schaaf, C.B., Strahler, A.H., Hodges, J.C.F., Gao, F., Reed, B.C., Huete, A., 2003. Monitoring vegetation phenology using MODIS. Remote Sens. Environ. 84, 471–475. https://doi.org/10.1016/S0034-4257(02)00135-9

Zhang, X., Zhang, M., Zheng, Y., Wu, B., 2016. Crop mapping using PROBA-V time series data at the Yucheng and hongxing farm in China. Remote Sens. 8, 1–18. https://doi.org/10.3390/rs8110915

APPENDICES

Appendix I: Discrimination accuracy of the proposed SAR metrics. The P.A, U.A. and O.A. represent the producer accuracy, user accuracy and the overall accuracy, respectively

No.	Stage/Approach	Features	Rice		Maize		O.A. (%)	Kappa
			P.A. (%)	U.A. (%)	P.A. (%)	U.A. (%)		
1.	Significant features only	FloweringVV FloweringCR HarvDateVV HarvDateCR BackDiffCR	89	85	75	82	83.9	0.66
2.	All features	LandPrepVH LandPrepVV LandPrepCR CropEDateVH CropEDateVV CropEDateCR FloweringVH FloweringVV FloweringCR HarvDateVH HarvDateVV HarvDateCR BackDiffVH BackDiffVV BackDiffCR Maturity_days	84	84	75	75	80.6	0.59
3.	Crop Establishment Date	CropEDateVH CropEDateVV CropEDateCR	89	81	67	80	80.6	0.58
4.	Flowering	FloweringVH FloweringVV FloweringCR	89	74	50	75	74.2	0.42
5.	Harvest Date	HarvDateVH HarvDateVV HarvDateCR	84	70	42	63	67.7	0.28

Appendix II: Map showing the field observation of crop types in Pangasinan (left) and SVM classification results (right) using the features from Harvest Date (in VH, VV and VV/VH ratio).

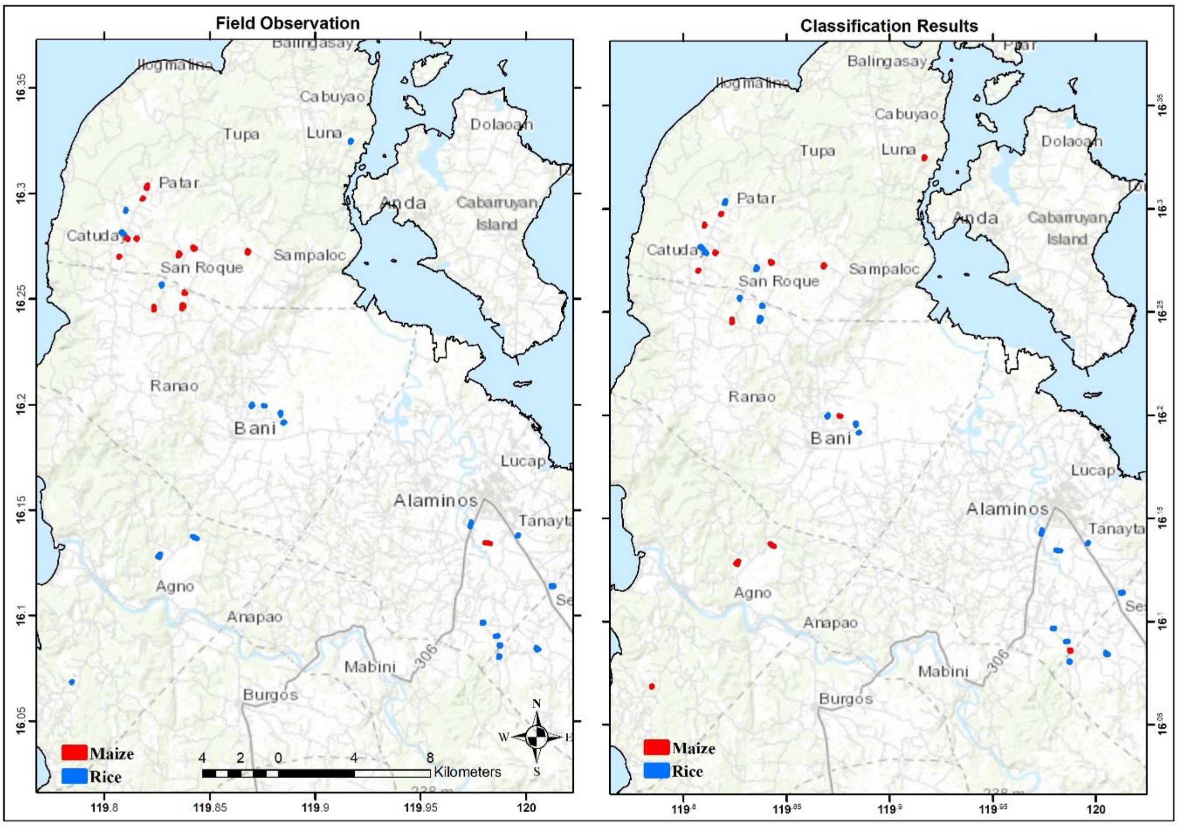

Appendix III: Error Matrix of SVM model when using CropEDate (in VH only)

	Reference classes				
Predicted (Classification Results)	Maize	Rice	Total	Error of Commission (%)	User Accuracy (%)
Maize	11	8	19	42	58
Rice	1	11	12	8	92
Total	12	19	31		
Error of Omission	8	42			
Producer Accuracy	92	58			

Overall Accuracy 74.2%, Kappa 44.8% (Moderate)

Appendix IV: Code used for the SVM model at different growth stages

```
### Using SVM with Leave-One-Out Cross-Validation (LOOCV) in R
rm(list = ls(all.names = TRUE)) # will clear all objects, including hidden objects
gc() # free up memory and report memory usage
# set working directory. This will be the directory where all the files are located
setwd("C:/Analysis")
# load required libraries (Note: if these packages are not installed, then install them first and then load)
# rgdal: a comprehansive repository for handling spatial data
# raster: for the manipulation of raster data
# caret: for the machine learning algorithms
# sp: for the manipulation of spatial objects
# nnet: Artificial Neural Network
# randomForest: Random Forest
# kernlab: Support Vector Machines
# e1071: provides miscellaneous functions requiered by the caret package
install.packages("pacman"); pacman::p_load(rgdal,raster,caret,sp,nnet,randomForest,kernlab,e1071,readr)
# Read the data
training_set <- read.csv("samples_final_april.csv")
str(training_set) # check the structure of data frame with the function str():
head(training_set)
#Land Preparation (LandPrep), Crop Est. Date (CropEDate), Flowering and Harvest Date (HarvestDate) in VH, VV and VV/VH Ratio (CR)
#plot the data
qplot(CropEDateVH, FloweringVH,data = training_set, color=Croptype, main="Scatterplot CropEDate vs Flowering in VH", xlab="Crop Est. Date (dB) in VH", ylab="FLW (dB) in VH")
qplot(CropEDateVV, FloweringVV,data = training_set, color=Croptype, main="Scatterplot CropEDate vs Flowering in VV", xlab="Crop Est. Date (dB) in VV", ylab="FLW (dB) in VV")
qplot(CropEDateCR, FloweringCR,data = training_set, color=Croptype, main="Scatterplot CropEDate vs Flowering in VV/VH", xlab="Crop Est. Date (dB) in VV/VH", ylab="FLW (dB) in VV/VH")
#Backscatter at FID (field-level) at CropEDate
qplot(CropEDateVH, FID,data = training_set, color=Croptype, main="Scatterplot CropEDate vs FID in VH", xlab="Crop Est. Date (dB) in VH", ylab="Farm ID")
#Re-label the class variable to have meaningful values (1=Rice, 2= Maize)
training_set$class[training_set$class==1] <- "Rice"
training_set$class[training_set$class==2] <- "Maize" # Do the same for the test dataset
head(training_set)
View(training_set)
#Convert the class variable to type factor
training_set$class <- as.factor(training_set$class) # converting to a factor
class(training_set$class) # confirm if its a factor
#cross-validation is applied for tuning hyperparameters c and sigma for the svmRadialsigma approach
# and for training and validating the model when the sample size is small
# k-Fold with k=10 is mostly used as opposed to LOOCV due to computation cost
#However, our sample size = 31 is ok for LOOCV
```

First approach is to do a random search first
set.seed (123)
fitControl <- trainControl (method = "cv", #cross-validation of the training data
number = 10, search = 'random',
savePredictions = TRUE,
allowParallel = TRUE, # allow use of multiple cores if specified in training
verboseIter = TRUE)
model_svm <- caret::train(class ~ **HarvDateVH + HarvDateVV + HarvDateCR** , #Note only features at Harvest Date (HarvestDate) in VH, VV and VV/VH ratio are included in the model here
data=training_set, method = "svmRadialSigma", metric="Accuracy", trainControl = fitControl, tuneLength = 20)
#using all features in the model (15)
SVM.rbf.model <- caret::train(class ~ LandPrepVH + LandPrepVV+ LandPrepCR + #Land preparation stage
CropEDateVH + CropEDateVV+ CropEDateCR + #Crop Establishment Stage
FloweringVH + FloweringVV + FloweringCR + # Flowering stage
HarvDateVH + HarvDateVV + HarvDateCR + #Harvest stage
BackDiffVH + BackDiffVV + BackDiffCR, # Backscatter difference at FLW and CE
data=training_set, method = "svmRadialSigma", metric="Accuracy", trainControl = fitControl, tuneLength = 20)
model_svm # to view the details of the model
model_svm$bestTune # to view the best accuracy and sigm and c
SVM.rbf.model
SVM.rbf.model$bestTune
#Now do grid search with values of **c** and **sigma** from the model
# Set up a resampling method in the model training process
set.seed(41)
fitControl_a <- trainControl(method = "cv", # repeated cross-validation of the training data
number = 10, # number of folds #note the serach = 'random' has been removed
#repeats = 5, # number of repeats
savePredictions = TRUE,
allowParallel = TRUE, # allow use of multiple cores if specified in training
verboseIter = TRUE) # view the training iterations

# Generate a grid search of candidate hyper-parameter values for inclusion into the models training
# The hyper-parameter values should be based on values from the results of random search to achieve high accuracies
# For example, the parameters should be a range but include a combinations which gives you the highest accuracy.
svm.grid_a <- expand.grid(sigma=seq(from = 0.1, to = 0.4, by = 0.1), # controls for non-linearity in the hyperplane
C=seq(from = 0.2, to = 2.2, by = 0.1)) # controls the influence of each support vector # range made based on random serach values
# Train the support vector machines model
model_svm_1 <- caret::train(class ~ HarvDateVH + HarvDateVV + HarvDateCR, #Note only features at Crop Establishment Date (CropEDate) in VH, VV and VV/VH ratio are included in the model

```
                        data=training_set, method = "svmRadialSigma", metric="Accuracy", trainControl = fitControl_a, tuneGrid = svm.grid_a)

model_svm_1 # to view the details of the model
model_svm_1$bestTune # to view the best accuracy and sigma and c
### Having understanding of the accuracy we perform cross validation now with k = 10
###k-Fold cross-validation
#Appllying k-fold Cross Validation
#set.seed(42)
#define training set
#load the required package :lattice
#load the required package:ggplot2
# in creating the folds we specify the target feature (dependent variable) and # of folds
#folds = createFolds(training_set$class, k = 31) #requires the caret package
#Randomly shuffle the data
training_set<-training_set[sample(nrow(training_set)),]
#Create 31 equally size folds
folds <- cut(seq(1,nrow(training_set)),breaks=31,labels=FALSE)
#Perform Leave-one-out cross validation
for(i in 1:31){
  #Segement your data by fold using the which() function
  testIndexes <- which(folds==i,arr.ind=TRUE)
  testData <- training_set[testIndexes, ]
  trainData <- training_set[-testIndexes, ]
  #Use the test and train data partitions however you desire...
}
View(testData)
# now apply (train) the classifer on the training_fold #takes 10 seconds average
svm_model <- caret::train(class ~ HarvDateVH +  HarvDateVV + HarvDateCR, #Note only features at Crop Establishment Date (CropEDate) in VH, VV and VV/VH ratio are included in the model
                        data=trainData,
                        method = "svmRadialSigma", metric="Accuracy", trainControl = fitControl_a, tuneGrid = svm.grid_a)
svm_pred = predict(svm_model, newdata = testData) # ok model
svm_pred # ok
print(svm_model) #ok
#summary(svm_model)
#create a confusion matrix
#cm = table(testData$class, svm_pred) #ok
#cm #ok
svm_errorMat = table(svm_pred,testData$class) # Take note of the reference classes (true) and the predicted (classified)
svm_errorMat # Final matrix shows only one obs. classified 100% accurate or not (misclassified)
#cm <- confusionMatrix(table(trainData$class, svm_pred))
accuracy = sum(diag(cm))/sum(cm)
accuracy
```

```
O.Accuracy<- sum(diag(cm))/sum(cm)
O.Accuracy
### END ###
#kappa cutoffs - as rules of thumb for interpretation
# .81 - 1.00 Almost perfect
# .61 - .80 substantial
# .41 - 60 Moderate
# .21 - .40 Fair
# .00 - .20 Slight
# <.00 Poor
#summary(svm_model) # see that all predicator are statistically signficant
#displaying the svm_model
########################END HERE################################
#FIXED COST AND SIGMA
svm.model <- caret::train(class ~ HarvDateVH +  HarvDateVV + HarvDateCR, #Note only features at Crop Establishment Date (CropEDate) in VH, VV and VV/VH ratio are included in the model
                    data=trainData,
                    method = "svmRadialSigma", metric="Accuracy", cost = 32, sigma = 0.2496192)
svm.pred = predict(svm.model, newdata = testData) # ok model
svm.pred
print(svm.model)
#using svm (e1071)
svm.model2 <- svm(class ~ HarvDateVH +  HarvDateVV + HarvDateCR, #Note only features at Crop Establishment Date (CropEDate) in VH, VV and VV/VH ratio are included in the model
                    data=trainData,
                    method = "svmRadialSigma", metric="Accuracy", cost = 1.3, sigma = 0.1)
svm.pred2 = predict(svm.model2, newdata = testData) # ok model
svm.pred2
print(svm.model2)
summary(svm.model2)
pred2.cm = table(testData$class, svm.pred2)
pred2.cm2 = table(svm.pred2,testData$class) # ok Reference is rice, classifed maize
pred2.cm2
# Radial Basis Function (RBF) Kernel
SVM.rbf.model <- svm(class ~ HarvDateVH +  HarvDateVV + HarvDateCR,
                data=trainData, type="C-classification", kernel = "radial", cost = 100, gamma=0.102,  scale = FALSE)
ypred=predict(SVM.rbf.model, newdata = testData)
ypred
CM=table(prediction=ypred,truth=testData$class)
OA=sum(diag(CM))/length(testData$class)
CM
OA
summary(SVM.rbf.model)

# Radial Basis Function (RBF) Kernel using ALL features (15 features)
```

```
SVM.rbf.model <- svm(class ~ LandPrepVH + LandPrepVV+ LandPrepCR + #Land preparation stage
                 CropEDateVH + CropEDateVV+ CropEDateCR + #Crop Establishment Stage
                 FloweringVH + FloweringVV + FloweringCR + # Flowering stage
                 HarvDateVH +  HarvDateVV + HarvDateCR + #Harvest stage
                 BackDiffVH + BackDiffVV + BackDiffCR, # Backscatter difference at FLW and CE
                data=trainData, type="C-classification", kernel = "radial", cost = 100, gamma=0.102,  scale
= FALSE)
ypred=predict(SVM.rbf.model, newdata = testData)
ypred
CM=table(prediction=ypred,truth=testData$class)
OA=sum(diag(CM))/length(testData$class)
CM
OA
summary(SVM.rbf.model)
```

Appendix V: Training samples in VH polarization

FID	X_coord	Y_coord	Attributes	CropEstMethod	LandPrepVH	CropEDateVH	FloweringVH	HarvDateVH	Maturity_days	class	Croptype
105	179597.10	1780574.00	Irrigated Rice	Direct seeded rice	-16.556	-18.577	-15.113	-16.384	113	1	Rice
121	165295.70	1793559.00	Irrigated Rice	Direct seeded rice	-14.750	-16.708	-16.975	-15.210	99	1	Rice
123	165927.70	1793542.00	Irrigated Rice	Direct seeded rice	-18.434	-19.192	-15.567	-16.909	120	1	Rice
125	166904.30	1792646.00	Irrigated Rice	Direct seeded rice	-17.087	-18.943	-15.763	-15.640	85	1	Rice
127	166756.40	1793130.00	Irrigated Rice	Direct seeded rice	-16.773	-16.773	-15.948	-15.777	99	1	Rice
103	177535.80	1781271.00	Irrigated Rice	Direct seeded rice	-16.960	-18.516	-15.035	-16.884	105	1	Rice
102	176311.60	1787156.00	Irrigated Rice	Direct seeded rice	-14.457	-15.173	-15.334	-15.054	99	1	Rice
101	176855.40	1781983.00	Irrigated Rice	Transplanted rice	-17.394	-16.859	-15.755	-16.683	84	1	Rice
107	177706.00	1780775.00	Irrigated Rice	Transplanted rice	-14.932	-18.146	-15.164	-15.647	92	1	Rice
115	178706.40	1786535.00	Rainfed Rice	Transplanted rice	-15.085	-16.893	-15.444	-14.555	92	1	Rice
117	180426.10	1783849.00	Rainfed Rice	Transplanted rice	-14.496	-16.832	-15.716	-15.598	62	1	Rice
134	160831.60	1799965.00	Rainfed Rice	Transplanted rice	-14.544	-15.313	-14.896	-15.474	84	1	Rice
149	160486.20	1785740.00	Irrigated Rice	Transplanted rice	-14.568	-17.745	-16.362	-17.753	90	1	Rice
150	162318.60	1786664.00	Rainfed Rice	Transplanted rice	-15.036	-14.813	-16.191	-18.611	101	1	Rice
155	155939.50	1779181.00	Irrigated Rice	Transplanted rice	-15.770	-17.837	-15.119	-15.105	83	1	Rice
171	170529.60	1807353.00	Irrigated Rice	Transplanted rice	-16.513	-18.688	-15.272	-15.737	90	1	Rice
177	158871.20	1802716.00	Irrigated Rice	Transplanted rice	-16.895	-16.221	-16.019	-17.021	83	1	Rice
109	177659.60	1780193.00	Irrigated Rice	Transplanted rice	-17.646	-17.903	-15.288	-15.431	84	1	Rice
170	159107.00	1803877.00	Rainfed Rice	Transplanted rice	-15.398	-16.622	-16.214	-16.576	98	1	Rice
136	158714.60	1801441.00	Maize	Direct seeded maize	-16.097	-16.630	-16.174	-17.443	120	2	Maize
138	159097.00	1802431.00	Maize	Direct seeded maize	-15.447	-16.911	-16.378	-16.486	59	2	Maize
164	160151.30	1805123.00	Maize	Direct seeded maize	-14.782	-15.725	-15.008	-15.931	120	2	Maize
166	159936.00	1804500.00	Maize	Direct seeded maize	-16.396	-16.881	-16.042	-16.061	59	2	Maize
167	161723.20	1801539.00	Maize	Direct seeded maize	-14.786	-16.370	-15.038	-17.002	121	2	Maize
169	162489.80	1801865.00	Maize	Direct seeded maize	-15.695	-15.450	-14.217	-17.560	144	2	Maize
135	160411.60	1798745.00	Maize	Direct seeded maize	-14.811	-16.447	-15.622	-17.509	121	2	Maize
104	177158.40	1786161.00	Maize	Direct seeded maize	-16.309	-16.943	-17.721	-17.928	143	2	Maize
130	161976.60	1799525.00	Maize	Direct seeded maize	-14.514	-16.454	-15.698	-15.221	100	2	Maize
163	165221.00	1801621.00	Maize	Direct seeded maize	-16.423	-17.008	-15.568	-15.351	90	2	Maize
176	159587.30	1802419.00	Maize	Direct seeded maize	-15.264	-16.632	-14.834	-16.632	136	2	Maize
132	161868.00	1798818.00	Maize	Direct seeded maize	-15.500	-17.009	-14.469	-15.448	106	2	Maize

Appendix VI: Training samples in VV polarization

FID	X_coord	Y_coord	Attributes	CropEstMethod	LandPrepVV	CropEDateVV	FloweringVV	HarvDateVV	Maturity_days	class	Croptype
105	179597.10	1780574.00	Irrigated Rice	Direct seeded rice	-10.022	-10.021	-10.612	-10.973	113	1	Rice
121	165295.70	1793559.00	Irrigated Rice	Direct seeded rice	-9.009	-8.661	-11.940	-11.094	99	1	Rice
123	165927.70	1793542.00	Irrigated Rice	Direct seeded rice	-12.186	-9.235	-10.869	-11.164	120	1	Rice
125	166904.30	1792646.00	Irrigated Rice	Direct seeded rice	-9.628	-13.557	-11.484	-11.191	85	1	Rice
127	166756.40	1793130.00	Irrigated Rice	Direct seeded rice	-8.663	-8.663	-9.201	-11.682	99	1	Rice
103	177535.80	1781271.00	Irrigated Rice	Direct seeded rice	-10.548	-11.945	-12.022	-12.583	105	1	Rice
102	176311.60	1787156.00	Irrigated Rice	Direct seeded rice	-8.662	-7.633	-10.523	-10.676	99	1	Rice
101	176855.40	1781983.00	Irrigated Rice	Transplanted rice	-11.125	-10.789	-10.868	-11.239	84	1	Rice
107	177706.00	1780775.00	Irrigated Rice	Transplanted rice	-10.174	-9.588	-10.211	-9.623	92	1	Rice
115	178706.40	1786535.00	Rainfed Rice	Transplanted rice	-8.828	-9.346	-9.322	-9.675	92	1	Rice
117	180426.10	1783849.00	Rainfed Rice	Transplanted rice	-9.482	-10.721	-10.059	-10.994	62	1	Rice
134	160831.60	1799965.00	Rainfed Rice	Transplanted rice	-9.282	-9.184	-9.554	-9.931	84	1	Rice
149	160486.20	1785740.00	Irrigated Rice	Transplanted rice	-8.835	-10.396	-10.935	-11.667	90	1	Rice
150	162318.60	1786664.00	Rainfed Rice	Transplanted rice	-10.340	-9.813	-10.444	-10.884	101	1	Rice
155	155939.50	1779181.00	Irrigated Rice	Transplanted rice	-8.204	-9.015	-8.805	-9.598	83	1	Rice
171	170529.60	1807353.00	Irrigated Rice	Transplanted rice	-9.047	-9.084	-9.703	-9.888	90	1	Rice
177	158871.20	1802716.00	Irrigated Rice	Transplanted rice	-10.838	-10.008	-11.260	-11.574	83	1	Rice
109	177659.60	1780193.00	Irrigated Rice	Transplanted rice	-11.352	-10.151	-10.020	-10.429	84	1	Rice
170	159107.00	1803877.00	Rainfed Rice	Transplanted rice	-10.203	-10.635	-10.386	-10.213	98	1	Rice
136	158714.60	1801441.00	Maize	Direct seeded maize	-9.732	-9.160	-9.423	-9.948	120	2	Maize
138	159097.00	1802431.00	Maize	Direct seeded maize	-10.074	-10.252	-9.437	-10.247	59	2	Maize
164	160151.30	1805123.00	Maize	Direct seeded maize	-9.552	-9.285	-9.409	-10.146	120	2	Maize
166	159936.00	1804500.00	Maize	Direct seeded maize	-8.903	-9.676	-9.104	-9.141	59	2	Maize
167	161723.20	1801539.00	Maize	Direct seeded maize	-9.786	-10.194	-10.164	-11.232	121	2	Maize
169	162489.80	1801865.00	Maize	Direct seeded maize	-10.696	-10.425	-9.082	-11.340	144	2	Maize
135	160411.60	1798745.00	Maize	Direct seeded maize	-9.160	-9.460	-10.001	-11.272	121	2	Maize
104	177158.40	1786161.00	Maize	Direct seeded maize	-9.948	-10.242	-11.619	-8.170	143	2	Maize
130	161976.60	1799525.00	Maize	Direct seeded maize	-9.474	-10.162	-9.137	-9.433	100	2	Maize
163	165221.00	1801621.00	Maize	Direct seeded maize	-9.987	-10.041	-10.090	-9.068	90	2	Maize
176	159587.30	1802419.00	Maize	Direct seeded maize	-9.641	-9.804	-9.940	-9.826	136	2	Maize
132	161868.00	1798818.00	Maize	Direct seeded maize	-10.213	-10.196	-8.856	-9.463	106	2	Maize

Appendix VII: Training samples in VV/VH ratio polarization

FID	X_coord	Y_coord	Attributes	CropEstMethod	LandPrepVV	CropEDateVV	FloweringVV	HarvDateVV	Maturity_days	class	Croptype
105	179597.10	1780574.00	Irrigated Rice	Direct seeded rice	-10.022	-10.021	-10.612	-10.973	113	1	Rice
121	165295.70	1793559.00	Irrigated Rice	Direct seeded rice	-9.009	-8.661	-11.940	-11.094	99	1	Rice
123	165927.70	1793542.00	Irrigated Rice	Direct seeded rice	-12.186	-9.235	-10.869	-11.164	120	1	Rice
125	166904.30	1792646.00	Irrigated Rice	Direct seeded rice	-9.628	-13.557	-11.484	-11.191	85	1	Rice
127	166756.40	1793130.00	Irrigated Rice	Direct seeded rice	-8.663	-8.663	-9.201	-11.682	99	1	Rice
103	177535.80	1781271.00	Irrigated Rice	Direct seeded rice	-10.548	-11.945	-12.022	-12.583	105	1	Rice
102	176311.60	1787156.00	Irrigated Rice	Direct seeded rice	-8.662	-7.633	-10.523	-10.676	99	1	Rice
101	176855.40	1781983.00	Irrigated Rice	Transplanted rice	-11.125	-10.789	-10.868	-11.239	84	1	Rice
107	177706.00	1780775.00	Irrigated Rice	Transplanted rice	-10.174	-9.588	-10.211	-9.623	92	1	Rice
115	178706.40	1786535.00	Rainfed Rice	Transplanted rice	-8.828	-9.346	-9.322	-9.675	92	1	Rice
117	180426.10	1783849.00	Rainfed Rice	Transplanted rice	-9.482	-10.721	-10.059	-10.994	62	1	Rice
134	160831.60	1799965.00	Rainfed Rice	Transplanted rice	-9.282	-9.184	-9.554	-9.931	84	1	Rice
149	160486.20	1785740.00	Irrigated Rice	Transplanted rice	-8.835	-10.396	-10.935	-11.667	90	1	Rice
150	162318.60	1786664.00	Rainfed Rice	Transplanted rice	-10.340	-9.813	-10.444	-10.884	101	1	Rice
155	155939.50	1779181.00	Irrigated Rice	Transplanted rice	-8.204	-9.015	-8.805	-9.598	83	1	Rice
171	170529.60	1807353.00	Irrigated Rice	Transplanted rice	-9.047	-9.084	-9.703	-9.888	90	1	Rice
177	158871.20	1802716.00	Irrigated Rice	Transplanted rice	-10.838	-10.008	-11.260	-11.574	83	1	Rice
109	177659.60	1780193.00	Irrigated Rice	Transplanted rice	-11.352	-10.151	-10.020	-10.429	84	1	Rice
170	159107.00	1803877.00	Rainfed Rice	Transplanted rice	-10.203	-10.635	-10.386	-10.213	98	1	Rice
136	158714.60	1801441.00	Maize	Direct seeded maize	-9.732	-9.160	-9.423	-9.948	120	2	Maize
138	159097.00	1802431.00	Maize	Direct seeded maize	-10.074	-10.252	-9.437	-10.247	59	2	Maize
164	160151.30	1805123.00	Maize	Direct seeded maize	-9.552	-9.285	-9.409	-10.146	120	2	Maize
166	159936.00	1804500.00	Maize	Direct seeded maize	-8.903	-9.676	-9.104	-9.141	59	2	Maize
167	161723.20	1801539.00	Maize	Direct seeded maize	-9.786	-10.194	-10.164	-11.232	121	2	Maize
169	162489.80	1801865.00	Maize	Direct seeded maize	-10.696	-10.425	-9.082	-11.340	144	2	Maize
135	160411.60	1798745.00	Maize	Direct seeded maize	-9.160	-9.460	-10.001	-11.272	121	2	Maize
104	177158.40	1786161.00	Maize	Direct seeded maize	-9.948	-10.242	-11.619	-8.170	143	2	Maize
130	161976.60	1799525.00	Maize	Direct seeded maize	-9.474	-10.162	-9.137	-9.433	100	2	Maize
163	165221.00	1801621.00	Maize	Direct seeded maize	-9.987	-10.041	-10.090	-9.068	90	2	Maize
176	159587.30	1802419.00	Maize	Direct seeded maize	-9.641	-9.804	-9.940	-9.826	136	2	Maize
132	161868.00	1798818.00	Maize	Direct seeded maize	-10.213	-10.196	-8.856	-9.463	106	2	Maize

Appendix VIII: Training samples showing the Backsactter Difference and Maturity in days

FID	X_coord	Y_coord	Attributes	CropEstMethod	BackDiffVH	BackDiffVV	BackDiffCR	Maturity_days	class	Croptype
105	179597.10	1780574.00	Irrigated Rice	Direct seeded rice	3.464	-0.591	-4.054	113	1	Rice
121	165295.70	1793559.00	Irrigated Rice	Direct seeded rice	-0.267	-3.279	-3.012	99	1	Rice
123	165927.70	1793542.00	Irrigated Rice	Direct seeded rice	3.625	-1.634	-5.259	120	1	Rice
125	166904.30	1792646.00	Irrigated Rice	Direct seeded rice	3.180	2.073	-1.107	85	1	Rice
127	166756.40	1793130.00	Irrigated Rice	Direct seeded rice	0.825	-0.537	-1.362	99	1	Rice
103	177535.80	1781271.00	Irrigated Rice	Direct seeded rice	3.481	-0.077	-3.558	105	1	Rice
102	176311.60	1787156.00	Irrigated Rice	Direct seeded rice	-0.160	-2.889	-2.729	99	1	Rice
101	176855.40	1781983.00	Irrigated Rice	Transplanted rice	1.103	-0.079	-1.182	84	1	Rice
107	177706.00	1780775.00	Irrigated Rice	Transplanted rice	2.982	-0.623	-3.605	92	1	Rice
115	178706.40	1786535.00	Rainfed Rice	Transplanted rice	1.449	0.024	-1.425	92	1	Rice
117	180426.10	1783849.00	Rainfed Rice	Transplanted rice	1.116	0.662	-0.454	62	1	Rice
134	160831.60	1799965.00	Rainfed Rice	Transplanted rice	0.417	-0.370	-0.787	84	1	Rice
149	160486.20	1785740.00	Irrigated Rice	Transplanted rice	1.383	-0.539	-1.922	90	1	Rice
150	162318.60	1786664.00	Rainfed Rice	Transplanted rice	-1.377	-0.631	0.747	101	1	Rice
155	155939.50	1779181.00	Irrigated Rice	Transplanted rice	2.718	0.210	-2.508	83	1	Rice
171	170529.60	1807353.00	Irrigated Rice	Transplanted rice	3.415	-0.619	-4.034	90	1	Rice
177	158871.20	1802716.00	Irrigated Rice	Transplanted rice	0.202	-1.251	-1.454	83	1	Rice
109	177659.60	1780193.00	Irrigated Rice	Transplanted rice	2.615	0.131	-2.484	84	1	Rice
170	159107.00	1803877.00	Rainfed Rice	Transplanted rice	0.408	0.248	-0.160	98	1	Rice
136	158714.60	1801441.00	Maize	Direct seeded maize	0.456	-0.263	-0.719	120	2	Maize
138	159097.00	1802431.00	Maize	Direct seeded maize	0.533	0.815	0.282	59	2	Maize
164	160151.30	1805123.00	Maize	Direct seeded maize	0.717	-0.124	-0.841	120	2	Maize
166	159936.00	1804500.00	Maize	Direct seeded maize	0.839	0.572	-0.266	59	2	Maize
167	161723.20	1801539.00	Maize	Direct seeded maize	1.333	0.030	-1.303	121	2	Maize
169	162489.80	1801865.00	Maize	Direct seeded maize	1.233	1.343	0.110	144	2	Maize
135	160411.60	1798745.00	Maize	Direct seeded maize	0.825	-0.541	-1.366	121	2	Maize
104	177158.40	1786161.00	Maize	Direct seeded maize	-0.778	-1.377	-0.599	143	2	Maize
130	161976.60	1799525.00	Maize	Direct seeded maize	0.756	1.025	0.269	100	2	Maize
163	165221.00	1801621.00	Maize	Direct seeded maize	1.440	-0.049	-1.489	90	2	Maize
176	159587.30	1802419.00	Maize	Direct seeded maize	1.798	-0.136	-1.934	136	2	Maize
132	161868.00	1798818.00	Maize	Direct seeded maize	2.540	1.339	-1.201	106	2	Maize